PORCINE MODEL OF XENOBIOTIC METABOLISM

BY

ARUN KUMAR DE

DISSERTATION

Submitted in partial fulfillment of the requirements
for the degree of Doctor of Philosophy in Animal Sciences
in the Graduate College of the
University of Illinois at Urbana-Champaign, 2016

Urbana, Illinois

Doctoral Committee:

Professor Lawrence B. Schook, Chair, Director of Research
Professor Bryan White
Associate Professor Alfred L. Roca
Assistant Professor Dipanjan Pan

Abstract

A xenobiotic is a foreign chemical substance found in the environment. The body removes xenobiotics by xenobiotic metabolism. Drug metabolizing enzymes (DMEs) play central roles in the metabolism, elimination, and detoxification of xenobiotics introduced into the body. Orphan nuclear receptors play crucial role in regulation of the expression of DMEs. The pig has quickly grown into an important biomedical research tool over the past few decades. The pig is an appropriate animal model for the investigation of xenobiotic disposition, as the transporters and CYP enzymes are very similar to those in humans. The characterization of porcine drug metabolism genes and the genes involved in regulating drug metabolism can provide insights into human drug metabolic diseases and individual variability of responses toward a drug. The tissue- and stage-specific expression of the nuclear receptors in pigs and their comparison to humans will be of great interest. Consequently, the goal of the proposal is to validate pig as a model of xenobiotic metabolism in order to get a better understanding of the pharmacokinetic properties of the xenobiotics. Expression of orphan nuclear receptors were screened across various porcine organs (liver, kidney, lung, small intestine, spleen, pancreas, heart, brain and skeletal muscle). Analysis of the mRNA expression levels of porcine orphan nuclear receptors in total RNA from various porcine organs was also performed by real time reverse transcriptase PCR. Expression of all the porcine nuclear receptors studied except (PPARγ) was detected in the liver and kidney. Most of the nuclear receptors showed higher expression in the liver. The tissue distribution and the expression profiles of the porcine nuclear receptors were consistent with those of human. To evaluate the effect of xenobiotic

exposure on the expression pattern of the nuclear receptors, expression pattern of nuclear receptors were evaluated in three different developmental stages i.e; three month old fetus, one month old piglet and one year old adult pig. The expression levels of the nuclear receptors in adult tissues were higher than that of one month old piglets which in turn were higher than those of a three month old fetal piglet. Porcine orphan nuclear receptors liver X receptor alpha (LXRα), liver X receptor beta (LXRβ) and constitutive androstane receptor (CAR) were cloned and the sequence analysis revealed eight novel transcript variants for LXRα and LXRβ each and five novel transcript variants for CAR. The expression profiles and the physiochemical properties of the novel identified transcript variants were analyzed. Further, we developed and characterized a porcine hepatocyte cell line representative of human primary hepatocytes to support drug toxicity and metabolism assessments. Three independent hepatocyte cell lines were developed from three different Oncopigs and all of them expressed hepatocyte specific and most important drug metabolism and regulation genes comparable to those porcine primary hepatocytes. We evaluated the effect of selective CYP modulators on three porcine hepatocyte cell lines. All the three independent porcine hepatocyte cell lines behaved the same way and the gene regulation pattern in hepatocyte cell lines was similar to that of primary hepatocytes and human models. These findings indicate that this porcine hepatocyte cell line represents a useful and predictive model for high throughput screening of new drugs as well as studies on metabolism and hepatotoxicity of chemicals.

To my wife Kriti De, for her love and encouragement

Acknowledgements

I would like to thank my advisor Lawrence B. Schook for giving me the opportunity to work in his lab. He has given me enough freedom to pursue my research interest and has also shaped the way I think and write as a scientist.

I also want to thank my committee member Alfred L. Roca for his guidance and helpful feedback on my written documents. I thank my committee member Dipanjan Pan for helpful discussions in different phases of my PhD work and allowing me to work in his lab. I owe thanks to Bryan A. White for accepting to be on my thesis committee and for giving suggestions to improve my research work.

I also thank Laurie Rund of the Schook lab for her useful comments during lab meetings and her support in ensuring a good working environment. I am also grateful to all my lab mates for creating a good environment for research.

I would like to thank Indian Council of Agricultural Research (ICAR) for providing fellowship during my PhD period. I take this opportunity to record my grateful thanks and gratitude to my parents for their constant help and encouragement. I would like to thank my wife Kriti De for her love, kindness and constant encouragement.

I take this opportunity in offering my humble prayers to the Almighty God for His richest blessings which enable me to complete the Ph.D. work successfully.

Table of Contents

Chapter 1: General Introduction

A xenobiotic is a chemical substance found in the environment. Thus, it includes pesticides, occupational chemicals, environmental contaminants, clinical drugs, deployment-related chemicals and foreign chemicals created by other organisms [1]. The body removes xenobiotics by xenobiotic metabolism. Many of the chemical reactions involved in the biotransformation of xenobiotics have now been traced to particular enzymes. Drug metabolizing enzymes (DMEs) play central roles in the metabolism, elimination, and detoxification of xenobiotics introduced into the body [2]. DMEs protect the body from the potential harmful effects of the xenobiotics by enzymatic modification of the xenobiotics and subsequent disposal. Dozens of enzymes responsible for xenobiotic biotransformation and transporters responsible for excretion of the xenobiotics have been identified. Analysis of the pig genome has revealed high similarity between porcine and human genes, including genes associated with xenobiotic metabolism [3]. The characterization of porcine drug metabolism genes and the genes involved in regulating xenobiotic metabolism can provide insights into human drug metabolic diseases and individual variability of responses toward a drug or xenobiotic.

Major factors that contribute to the failure of a new drug in preclinical and clinical studies are toxicity and lack of efficacy. The adverse effects of new drugs are often not discovered until preclinical animal safety studies or even clinical trials; 40% of drugs fail in preclinical animal studies and 89% of those that reach clinical trials fail [4]. There is a critical need for more predictive and reliable *in vitro* testing methods. A

good model can identify issues related to toxicity early in the discovery process thereby saving millions of dollars.

Pig in Biomedical Research

Pigs are increasingly being used as the major non-rodent animal species of choice in biomedical research especially in preclinical toxicological testing of pharmaceuticals. The popularity of pig specially minipig in pharmacology, pharmacokinetic, and toxicological safety evaluation experiments has increased very rapidly over recent years [5]. The pig was first used in research in ancient Greece and has quickly grown into an important biomedical research tool over the past few decades [3]. The pig is considered to be a good model in biomedical research due to its anatomical, physiological and biochemical similarity to humans. Many organs and systems including liver, heart, kidneys, brain, reproductive and gastrointestinal system show similarities with humans [6]. Similarity in size and physiology to humans allows pigs to be used for many experimental approaches not feasible in mice.

The pig is a true omnivore like human and because of this, the physiology of digestion and metabolic processes in the liver are also similar to humans. Similarities between pigs and humans in the way they metabolize xenobiotics both *in vitro* and *in vivo* have been reported by several researchers [7–9]. The Cytochrome P450 enzyme system (P450), which is mainly responsible for the biotransformation of xenobiotics has been studied in pig and porcine metabolic pathways have been found to be relatively similar to human [10]. Pig can be used as a laboratory model for human xenobiotic metabolism without the requirement to induce biotransformation enzymes

[11]. Analysis of the pig genome has revealed high similarity between porcine and human genes, including genes associated with drug metabolism [3]. Metabolism of several compounds by pig liver microsomes has been studied [12,13]; a study on pharmacokinetics of two model drugs atenolol and 5-aminosalicylate indicates that pig may give estimate of pharmacokinetic parameters comparable to those obtained in human [14].

Overview of Xenobiotic Metabolism

Xenobiotic metabolism, which occurs primarily in the liver and small intestine, refers to the enzymatic modification of chemical compounds. Upon conversion to hydrophilic compounds, xenobiotics are eliminated from the body through renal or biliary routes. Drug metabolizing enzymes (DMEs) play central roles in the metabolism, elimination, and detoxification of xenobiotics introduced into the body. Drug biotransformation (metabolism) is traditionally classified as phase I and phase II metabolism and phase III transport. An overview of xenobiotic metabolism has been presented in Figure 1.1. Most of the tissues and organs express diverse and various DMEs, including phase I and phase II metabolizing enzymes and phase III transporters. These DMEs can be present in abundance at the basal level, or expression can be induced after exposure to xenobiotics [15].

Phase I metabolism includes oxidation, reduction, hydrolysis, and hydration. Enzymes catalyzing these reactions are found in virtually all tissues, especially in the hepato-intestinal axis [16]. There are a large number of phase I xenobiotic metabolizing enzymes and most prominent is cytochrome P450 (CYP) superfamily.

CYP isoforms are found abundantly in the liver, GI tract, lung, and kidney [17]. The CYPs detoxify or bio-activate a vast number of xenobiotic chemicals and are involved in functionalization reactions that include hydroxylation, N- and O- dealkylation, hydroxylation, oxidation and deamination [18]. In humans, five CYP gene families, CYP1, CYP2, CYP3, CYP4, and CYP7, are believed to play crucial roles in hepatic and extrahepatic metabolism and elimination of xenobiotics and drugs [19]. The products of phase I metabolism are generally more polar and more readily excreted than the parent compounds and are often substrates for phase II enzymes [16].

The pig is an appropriate animal model for the investigation of drug disposition, because the transporters and CYP enzymes are very similar to those in humans [20]. The CYPs constitute the major enzyme family capable of catalyzing the oxidative biotransformation of most drugs and other lipophilic xenobiotics and are of particular relevance for clinical pharmacology. Several of these CYP subfamilies have been characterized in the pig and minipig [21] and enzymes equivalent to human P450s (like CYP1A, CYP2A6, CYP2E1 and CYP3A4) has been identified in pig [11,22]. Figure 1.2 shows the relative abundance of the porcine liver P450 enzymes and Table 1.1 shows their sequence similarity with human equivalent proteins. Moreover, the main liver enzyme of drug metabolism (CYP3A) has been reported in pig in comparable amounts and activity levels to humans [20]. Minipig cytochrome P450 3A, 2A and 2C enzymes were found to have similar properties to human analogs [23]. In addition, the porcine pregnane X receptor protein which regulates CYP3A has higher sequence similarity to that of humans than the mouse gene [24]. That makes the pig a better model than the mouse to determine whether a compound is toxic to humans.

For these reasons, pigs are considered an ideal model for evaluating the safety of pharmaceuticals and biopharmaceuticals [25].

Phase II metabolism involves conjugation with endogenous hydrophilic compounds to increase polarity and water solubility, thereby increasing excretion in the bile and urine, resulting in a detoxification effect. The phase II metabolizing or conjugating enzymes, consisting of many superfamily of enzymes including sulfotransferases (SULT) and UDP-glucuronosyl transferases (UGT), DT-diaphorase or NAD(P)H:quinone oxidoreductase (NQO) or NAD(P)H: menadione reductase (NMO), epoxide hydrolases (EPH), glutathione S-transferases (GST) and N-acetyltransferases (NAT) [15]. Each superfamily of phase II DMEs consists of families and subfamilies of genes encoding the various isoforms with different substrate specificity, tissue and developmental expression. The liver microsomal system plays the principle role in phase II metabolism and is known for its high metabolic capacity [26]. In general, conjugation with phase II DMEs generally increases hydrophilicity, and thereby enhances excretion in the bile (Figure 1.1).

Phase III biotransformation refers to active membrane transporters that function to transport xenobiotics across membranes. These transporters are classified as primary, secondary and tertiary. Primary transporters derive energy from ATP hydrolysis, whereas secondary and tertiary transporters derive energy by an exchange of intracellular ions [27]. Phase III transporters play crucial roles in drug absorption, distribution, and excretion. They include P-glycoprotein, multidrug resistance–associated protein, organic anion transporting polypeptide 2, and ABC

transporters. They are expressed in many tissues, including liver, intestine, kidney, and brain [15].

Regulation of xenobiotic metabolism by nuclear receptors

Regulating the expression of various drug metabolism enzymes can affect metabolism, pharmacokinetics, drug-drug interactions, and their ability to protect the human body against exposure to environmental xenobiotics [16]. Several classes of xenobiotics induce the transcription of genes encoding biotransformation enzymes and transporters. Different nuclear receptors, including orphan nuclear receptors, play a crucial role in regulation of the metabolism and clearance of drugs and xenobiotics introduced into the body [28]. These receptors are master regulators of the three phases of biotransformation [29]. Figure 1.3 represents a schematic diagram how nuclear receptors regulate the metabolism of xenobiotics.

Orphan nuclear receptors comprise a gene superfamily encoding the transcription factors that sense endogenous, such as small lipophilic hormones, and exogenous, such as drugs, xenobiotics and transfer into cellular responses by regulating the expression of their target genes. Regulation of gene expression at the transcriptional level by orphan nuclear receptors plays a crucial role in the metabolism and clearance of drugs and xenobiotics that are introduced into the body for the purpose of protection the body from the environmental insults.

Important nuclear receptors (NRs) involved in the regulation of phase I, phase II metabolizing enzymes and phase III transporters are liver X receptors (LXRα and

LXRβ), constitutive androstane receptor (CAR), peroxisome proliferator activated receptors (PPARα, PPARβ and PPARγ), retinoid X receptors (RXRα, RXRβ and RXRγ), pregnane X receptor (PXR) and farnesoid X receptor (FXR).

Structural and functional organization of nuclear receptor superfamily

Regarding the xenobiotic nuclear receptors, the organizational structure of most nuclear receptors is quite similar. All NR proteins exhibit a characteristic modular structure that consists of five to six domains (designated A to F, from the N-terminal to the C-terminal end) on the basis of regions of conserved sequence and function (Figure 1.4). The DNA-binding domain (DBD, region C) of the receptor is responsible for recognition of the response element in the promoter region of the target gene and the ligand binding domain (LBD; region E) of the receptor is where endogenous or exogenous ligands bind to the receptor [30]. DBD and LBD domain are the most highly conserved domains. These two regions are the most important and can function independently. The variable N-terminal A/B domain (AF2) and AF2 (Activation function 2) region are less conserved and are involved in the binding of the co-regulatory proteins and activation of the receptors. The C-terminal F region, which is contiguous with the E domain, is not present in all receptors, and its function is poorly understood.

Liver X Receptors (LXRs)

Liver X receptors are transcription factors commonly known as cholesterol sensors [31]. The two related LXRs; LXRα (NR1H3) and LXRβ (NR1H2) are among the emerging significant newer drug targets within the NR family. LXRs are probably

best known as nuclear oxysterol receptors and physiological master regulators of lipid and cholesterol metabolism and have attracted recent attention because they also display anti-inflammatory activities [32]. LXRs generally function as heterodimers with retinoid X receptor (RXR) [15]. LXRα and LXRβ bind to a specific DNA sequence, called the LXR response element (LXRE), that consists of direct repeats of the consensus half-site sequence 5'-AGGTCA-3' in which the half-sites are spaced by four nucleotides (DR4 motif) [15]. Human LXRα (447 amino acids) and LXRβ (460 amino acids) share 77% sequence similarity in their DBD and LBD. Although LXRs were initially discovered as orphan receptors, the search for natural ligands resulted in the identification of various oxysterols as strong candidates for endogenous LXR agonists. In human, LXRα is predominantly expressed in liver, kidney, spleen and intestine, whereas LXRβ is expressed ubiquitously [33].

Constitutive Androstane Receptor (CAR, NR1I3)

The orphan nuclear receptor CAR was identified in 1994 [34] . It was originally defined as constitutively activated receptor, because it does not require a ligand for its activation. It forms a heterodimer with RXR, which binds to retinoic acid response element of the promoter region of its target gene and trans-actives target gene [35]. In human, CAR is mainly expressed in liver and less abundantly in intestine [28]. CAR is located in the cytoplasm of hepatocytes in the absence of ligands and it is trans-located into the nucleus after treatment with ligands.

Peroxisome Proliferator Activated Receptors (PPARs)

Currently three members of this nuclear receptor family have been identified as: PPARα (NR1C1), PPARβ (NR1C2) and PPARγ (NR1C3) [36]. PPARs have been cloned in several species, including humans, rodents, amphibians, teleosts, and cyclostome [37]. In human, PPARα is highly expressed in organs involved in fatty acid oxidation including the liver, heart, kidney, intestine and adipose tissue. PPARβ is mostly expressed in brain, kidney and intestine. PPARγ is expressed in spleen, intestine and fat cells. PPARs play a crucial role in regulation of lipoprotein and fatty acid metabolism [15].

Retinoid X Receptors (RXRs)

There are three members of the family, RXRα, RXRβ and RXRγ. RXR can form heterodimers with other orphan nuclear receptors as a common partner and the formation of heterodimer with RXR is a critical step for facilitating the specific binding and activation of most of the nuclear receptors [15].

Pregnane X Receptor (PXR, NR1I2)

PXR is now recognized as another key xenosensor of the NR1I nuclear receptor subfamily [38]. PXR forms a heterodimer with RXRα and, following ligand activation, interacts with a set of core gene promoter elements within xenobiotic-responsive enhancer modules that consist typically of DR-3 or ER6 motifs [39]. PXR was first cloned from mouse liver four years after discovery of CAR [40]. PXR received its name due because the receptor was activated by pregnane (21-carbon) steroids such as

pregnenolone 16acarbonitrile (PCN), a synthetic inducer of the CYP3A family of steroid hydroxylases [41]. In human, PXR is expressed in liver and intestine at high level and in kidney and lung to a lower level [42].

Farnesoid X Receptor (FXR, NR1H4)

Farnesoid X receptor (FXR) is a nuclear receptor that is identified in 1995 and encoded by the *NR1H4* gene in humans [43]. Chenodeoxycholic acid and other bile acids are natural ligands for FXR. FXR also forms heterodimer with RXR and binds to FXR response element (FXRE) in the promoter region of its target genes. In human, FXR is expressed at high levels in the liver and intestine [15].

***In vitro* Model of Drug metabolism**

Metabolism of a drug or xenobiotics is critical for its pharmacokinetic properties, and the liver is the main organ of drug or xenobiotics biotransformation [44,45]. *In vitro* models generate many ADME (absorption, distribution, metabolism and excretion) parameters including metabolic stability, drug-drug interaction potential, cell proliferation and cytotoxicity [46]. These assays provide a simple and fast way to test the potency and toxicity of the new chemical entities. The liver plays a central role in drug metabolism and disposition through its phase I and phase II drug metabolism enzymes and phase III transporters. Therefore, primary human hepatocytes are generally used for drug metabolism and toxicity studies as they provide a complete picture of the metabolic fate of xenobiotics *in vitro* [44,47]. However, their widespread use is greatly hindered by the scarcity of suitable human liver samples. Moreover, *in*

vitro phenotypic instability of hepatocytes, the irregular availability of fresh human liver for cell harvesting purposes, and the high batch-to-batch functional variability of hepatocyte preparations obtained from different human liver donors complicate their use in routine testing [48]. Most of the human liver cell lines have poor or fractional CYP expression [49]. To date, the lack of a reliable animal model for assessment of drug toxicity and metabolism is a major limitation in early high throughput screening of xenobiotics. Immunological and physiological differences between rodents and humans represent major constraints for the use of rodent-based models in drug screening. Therefore, a large animal model surrogate for human hepatocytes is a very important improvement over the current methods for early screening of novel drugs and xenobiotics.

Over the years, the pig has gained increasing importance as a biomedical model due to similarities in size, anatomy and physiology with humans [50]. Similarities between pigs and humans in the way they metabolize xenobiotics have been reported by several researchers [7–9]. CYP enzymes have been extensively studied in pigs and enzymes equivalent to human P450 (eg. CYP1A, 2A6, 2E1, 3A4) have been identified in pig liver [11,22,51]. The sequence identity between human and porcine P450 enzymes is striking, ranging from 72 to 95 % [51]. Biotransformation data indicate that the CYP1A, 2A and 3A enzyme systems seem to be functionally very similar between pigs and humans [52,53]. Therefore, the pig may be a good animal model to study xenobiotic metabolism.

Approach:

Assessing Xenobiotic Metabolism in a Porcine Model

In order to properly assess xenobiotic metabolism in a porcine model, expression of drug metabolism genes across different porcine organs was determined. The selected genes are then cloned and sequenced. Splice variants are identified, followed by assessment of tissue specific expression profiles of splice variants. *In vitro* drug testing is then performed, followed ultimately by development of the pig model (Figure 1.5).

Thesis outline

Chapter 1 of this thesis, described early on is a general introduction covering overview of xenobiotic metabolism, orphan nuclear receptors and their role in regulation of xenobiotic metabolism. Also reviewed is the importance of pig in biomedical research. In chapter 2, the expression profiles of porcine orphan nuclear receptors across different organs were investigated. The expression pattern of the orphan nuclear receptors in different organs in three developmental stages (Three month old fetal piglet, one month old piglet and one year old adult pig) were analyzed and the following questions were addressed: 1) whether the expression patterns of the orphan nuclear receptors was consistent with those of human 2) what is the effect of xenobiotic exposure on the expression pattern of the porcine orphan nuclear receptors. Chapter 3 describes the identification and characterization of novel transcript variants (splice variants) of porcine liver X receptors (LXRα and LXRβ). Moreover the role of porcine LXRs in xenobiotic metabolism regulation was analyzed

in an *in vitro* model. Chapter 4 describes the identification and characterization of novel splice variants of porcine CAR. The role of CAR in porcine xenobiotic metabolism regulation was analyzed in an *in vitro* model. Chapter 5 describes the development of an *in vitro* porcine model of drug metabolism and toxicity testing. In chapter 5, the following questions were addressed: 1) whether the expression values of the most important drug metabolism enzymes in porcine primary hepatocytes are consistent with that of human. 2) Whether transformed porcine hepatocyte cell line can be used as representative of primary hepatocytes in assessment of xenobiotic metabolism and toxicity.

Figures

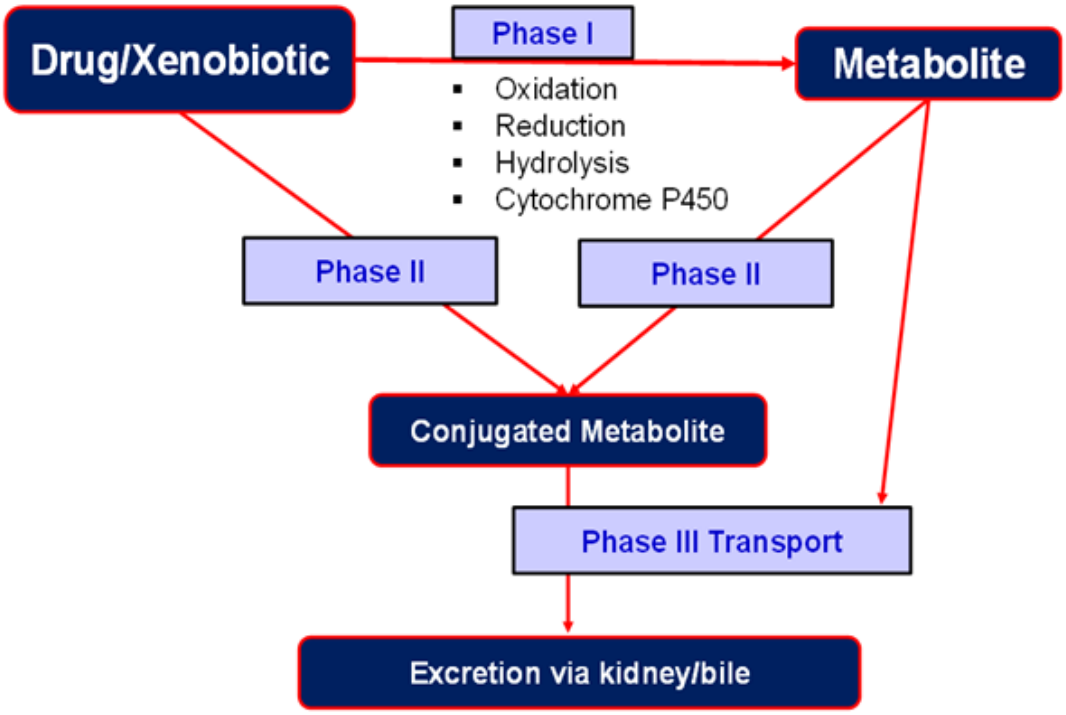

Figure 1.1. Schematic diagram of overview of xenobiotic metabolism.

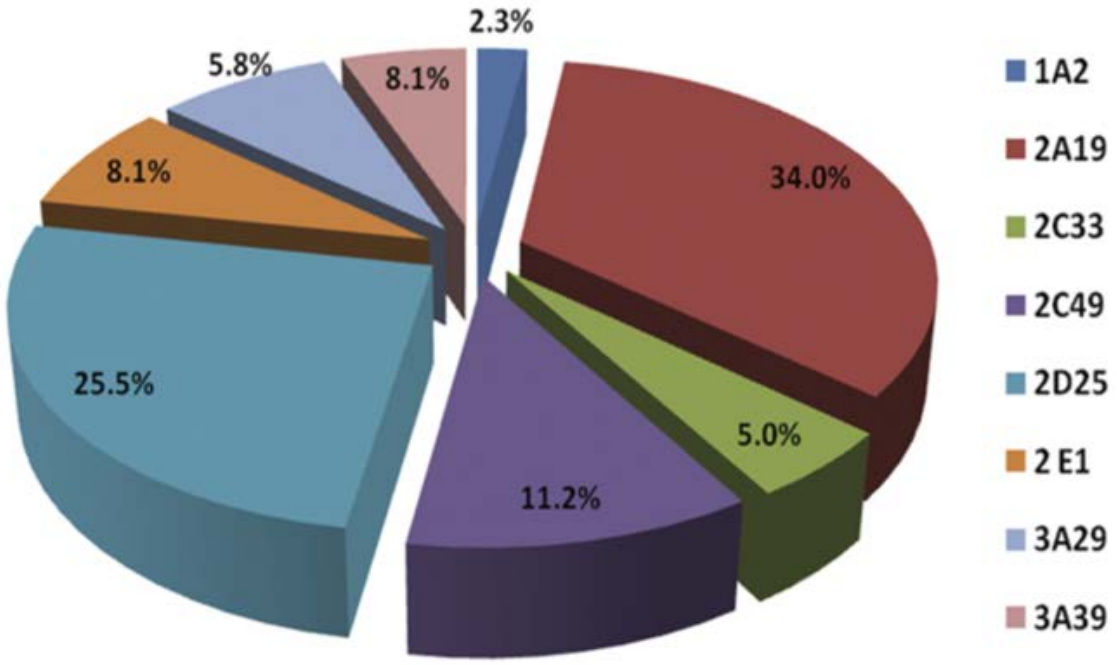

Figure 1.2. Relative abundance of porcine liver P450 enzymes (adapted from [51]).

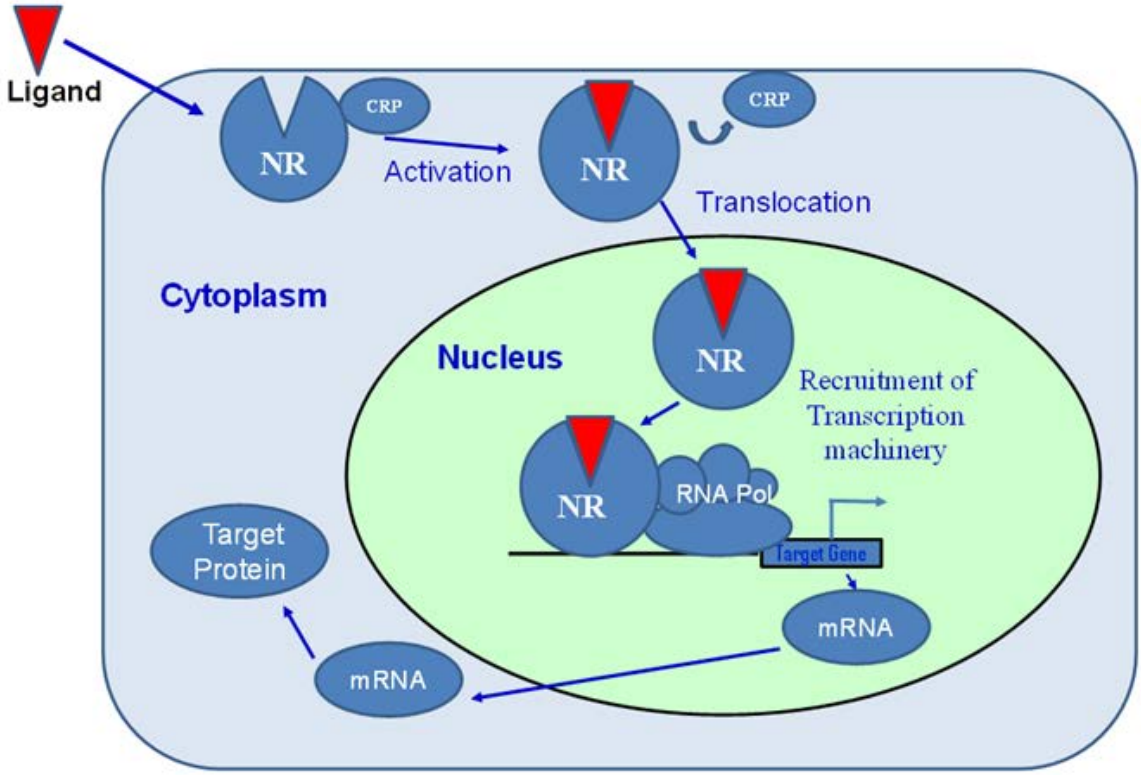

Figure 1.3. Overview of regulation of xenobiotic metabolism by nuclear receptors (NRs).

Upon ligand activation, NRs detach from cytoplasmic retention protein (CRP). Then NRs translocate to nucleus and induce the transcription of target gene (drug metabolism enzyme genes).

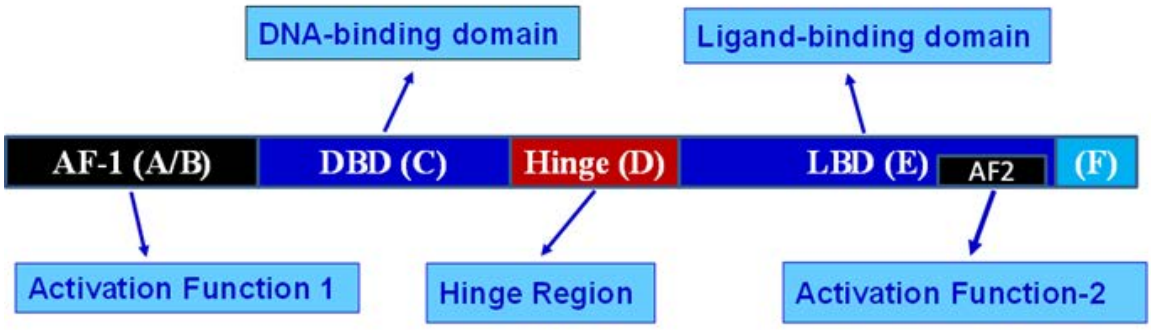

Figure 1.4. Structural organization of nuclear receptors.

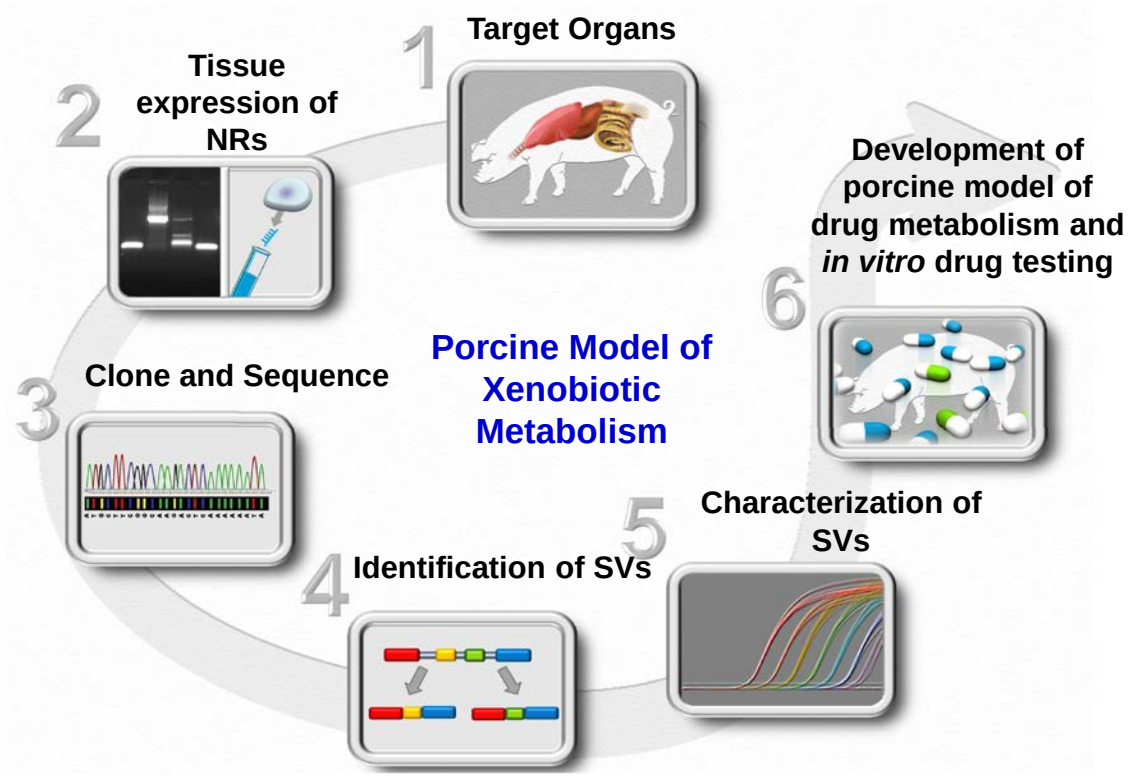

Figure 1.5. Overview of research approach.

References

1. Croom E. Metabolism of xenobiotics of human environments. Prog Mol Biol Transl Sci. 2012;112: 31–88. doi:10.1016/B978-0-12-415813-9.00003-9

2. Meyer UA. Overview of enzymes of drug metabolism. J Pharmacokinet Biopharm. 1996;24: 449–59. Available: http://www.ncbi.nlm.nih.gov/pubmed/9131484

3. Schook LB, Collares TV, Darfour-Oduro KA, De AK, Rund LA, Schachtschneider KM, et al. Unraveling the swine genome: implications for human health. Annu Rev Anim Biosci. Annual Reviews; 2015;3: 219–44. doi:10.1146/annurev-animal-022114-110815

4. McKim JM. Building a tiered approach to in vitro predictive toxicity screening: a focus on assays with in vivo relevance. Comb Chem High Throughput Screen. 2010;13: 188–206. Available: http://www.pubmedcentral.nih.gov/articlerender.fcgi?artid=2908937&tool=pmcentrez&rendertype=abstract

5. Forster R, Bode G, Ellegaard L, van der Laan JW. The RETHINK project--minipigs as models for the toxicity testing of new medicines and chemicals: an impact assessment. J Pharmacol Toxicol Methods. Elsevier Inc.; 2010;62: 158–9. doi:10.1016/j.vascn.2010.05.003

6. Bode G, Clausing P, Gervais F, Loegsted J, Luft J, Nogues V, et al. The utility of the minipig as an animal model in regulatory toxicology. J Pharmacol Toxicol Methods. 2010;62: 196–220. doi:10.1016/j.vascn.2010.05.009

7. Skaanild MT, Friis C. Cytochrome P450 sex differences in minipigs and conventional pigs. Pharmacol Toxicol. 1999;85: 174–80. Available: http://www.ncbi.nlm.nih.gov/pubmed/10563516

8. Skaanild MT, Friis C. Porcine CYP2A polymorphisms and activity. Basic Clin Pharmacol Toxicol. 2005;97: 115–21. doi:10.1111/j.1742-7843.2005.pto_148.x

9. Skaanild MT. Porcine cytochrome P450 and metabolism. Curr Pharm Des. 2006;12: 1421–7. Available: http://www.ncbi.nlm.nih.gov/pubmed/16611125

10. Murayama N, Kaneko N, Horiuchi K, Ohyama K, Shimizu M, Ito K, et al. Cytochrome P450-dependent drug oxidation activity of liver microsomes from Microminipigs, a possible new animal model for humans in non-clinical studies. Drug Metab Pharmacokinet. 2009;24: 404–8. Available: http://www.ncbi.nlm.nih.gov/pubmed/19745566

11. Soucek P, Zuber R, Anzenbacherová E, Anzenbacher P, Guengerich FP. BMC Pharmacology. 2001;450: 2–6.

12. Monshouwer M, Van't Klooster GA, Nijmeijer SM, Witkamp RF, van Miert AS. Characterization of cytochrome P450 isoenzymes in primary cultures of pig hepatocytes. Toxicol In Vitro. 1998;12: 715–23. Available: http://www.ncbi.nlm.nih.gov/pubmed/20654461

13. Anzenbacher P, Soucek P, Anzenbacherová E, Gut I, Hrubý K, Svoboda Z, et al. Presence and activity of cytochrome P450 isoforms in minipig liver microsomes. Comparison with human liver samples. Drug Metab Dispos. 1998;26: 56–9. Available: http://www.ncbi.nlm.nih.gov/pubmed/9443853

14. Kvetina J, Svoboda Z, Nobilis M, Pastera J, Anzenbacher P. Experimental Goettingen minipig and beagle dog as two species used in bioequivalence studies for clinical pharmacology (5-aminosalicylic acid and atenolol as model drugs). Gen Physiol Biophys. 1999;18 Spec No: 80–5. Available: http://www.ncbi.nlm.nih.gov/pubmed/10703724

15. Xu C, Li CY-T, Kong A-NT. Induction of phase I, II and III drug metabolism/transport by xenobiotics. Arch Pharm Res. 2005;28: 249–68. Available: http://www.ncbi.nlm.nih.gov/pubmed/15832810

16. Xie W, Uppal H, Saini SPS, Mu Y, Little JM, Radominska-Pandya A, et al. Orphan nuclear receptor-mediated xenobiotic regulation in drug metabolism. Drug Discov Today. 2004;9: 442–9. doi:10.1016/S1359-6446(04)03061-2

17. Nelson DR, Zeldin DC, Hoffman SMG, Maltais LJ, Wain HM, Nebert DW. Comparison of cytochrome P450 (CYP) genes from the mouse and human genomes , including nomenclature recommendations for genes , pseudogenes and alternative-splice variants. 2003;450: 1–18. doi:10.1097/01.fpc.0000054151.92680.31

18. Omiecinski CJ, Vanden Heuvel JP, Perdew GH, Peters JM. Xenobiotic metabolism, disposition, and regulation by receptors: from biochemical phenomenon to predictors of major toxicities. Toxicol Sci. 2011;120 Suppl : S49–75. doi:10.1093/toxsci/kfq338

19. Lewis DF V. Human cytochromes P450 associated with the phase 1 metabolism of drugs and other xenobiotics: a compilation of substrates and inhibitors of the

CYP1, CYP2 and CYP3 families. Curr Med Chem. 2003;10: 1955–72. Available: http://www.ncbi.nlm.nih.gov/pubmed/12871098

20. Anzenbacher P, Soucek P, Anzenbacherova E, Gut I, Hruby K, Svoboda Z, et al. Presence and Activity of Cytochrome P450 Isoforms in Minipig Liver Microsomes. Comparison with Human Liver Samples. Drug Metab Dispos. 1998;26: 56–59. Available: http://dmd.aspetjournals.org/content/26/1/56.short

21. Bode G, Clausing P, Gervais F, Loegsted J, Luft J, Nogues V, et al. The utility of the minipig as an animal model in regulatory toxicology. J Pharmacol Toxicol Methods. 2010;62: 196–220. doi:10.1016/j.vascn.2010.05.009

22. Szotáková B, Baliharová V, Lamka J, Nozinová E, Wsól V, Velík J, et al. Comparison of in vitro activities of biotransformation enzymes in pig, cattle, goat and sheep. Res Vet Sci. 2004;76: 43–51. Available: http://www.ncbi.nlm.nih.gov/pubmed/14659728

23. Soucek P, Zuber R, Anzenbacherová E, Anzenbacher P, Guengerich FP. Minipig cytochrome P450 3A, 2A and 2C enzymes have similar properties to human analogs. BMC Pharmacol. 2001;1: 11. Available: http://www.pubmedcentral.nih.gov/articlerender.fcgi?artid=60991&tool=pmcentrez&rendertype=abstract

24. Gray MA, Pollock CB, Schook LB, Squires EJ. Characterization of porcine pregnane X receptor, farnesoid X receptor and their splice variants. Exp Biol Med (Maywood). 2010;235: 718–36. doi:10.1258/ebm.2010.009339

25. Forster R, Ancian P, Fredholm M, Simianer H, Whitelaw B, Project SG of the R.

The minipig as a platform for new technologies in toxicology. J Pharmacol Toxicol Methods. 2010;62: 227–35. doi:10.1016/j.vascn.2010.05.007

26. Negishi M, Pedersen LG, Petrotchenko E, Shevtsov S, Gorokhov A, Kakuta Y, et al. Structure and function of sulfotransferases. Arch Biochem Biophys. 2001;390: 149–57. doi:10.1006/abbi.2001.2368

27. Xie W, Uppal H, Saini SPS, Mu Y, Little JM, Radominska-Pandya A, et al. Orphan nuclear receptor-mediated xenobiotic regulation in drug metabolism. Drug Discov Today. 2004;9: 442–9. doi:10.1016/S1359-6446(04)03061-2

28. Willson TM, Kliewer SA. PXR, CAR and drug metabolism. Nat Rev Drug Discov. 2002;1: 259–66. doi:10.1038/nrd753

29. Köhle C, Bock KW. Coordinate regulation of human drug-metabolizing enzymes, and conjugate transporters by the Ah receptor, pregnane X receptor and constitutive androstane receptor. Biochem Pharmacol. 2009;77: 689–99. doi:10.1016/j.bcp.2008.05.020

30. Prakash C, Zuniga B, Seog Song C, Jiang S, Cropper J, Park S, et al. Nuclear Receptors in Drug Metabolism, Drug Response and Drug Interactions. Nucl Recept Res. AgiAl Pubkishing House; 2015;2. doi:10.11131/2015/101178

31. Zhao C, Dahlman-Wright K. Liver X receptor in cholesterol metabolism. J Endocrinol. 2010;204: 233–40. doi:10.1677/JOE-09-0271

32. Huang N, Shaik-Dasthagirisaheb YB, LaValley MP, Gibson FC. Liver X receptors contribute to periodontal pathogen-elicited inflammation and oral bone

loss. Mol Oral Microbiol. 2015;30: 438–50. doi:10.1111/omi.12103

33. Hong C, Tontonoz P. Liver X receptors in lipid metabolism: opportunities for drug discovery. Nat Rev Drug Discov. Nature Publishing Group, a division of Macmillan Publishers Limited. All Rights Reserved.; 2014;13: 433–44. doi:10.1038/nrd4280

34. Baes M, Gulick T, Choi HS, Martinoli MG, Simha D, Moore DD. A new orphan member of the nuclear hormone receptor superfamily that interacts with a subset of retinoic acid response elements. Mol Cell Biol. 1994;14: 1544–52. Available: http://www.pubmedcentral.nih.gov/articlerender.fcgi?artid=358513&tool=pmcentrez&rendertype=abstract

35. Sueyoshi T, Negishi M. Phenobarbital response elements of cytochrome P450 genes and nuclear receptors. Annu Rev Pharmacol Toxicol. 2001;41: 123–43. doi:10.1146/annurev.pharmtox.41.1.123

36. Gilde AJ, van der Lee KAJM, Willemsen PHM, Chinetti G, van der Leij FR, van der Vusse GJ, et al. Peroxisome proliferator-activated receptor (PPAR) alpha and PPARbeta/delta, but not PPARgamma, modulate the expression of genes involved in cardiac lipid metabolism. Circ Res. 2003;92: 518–24. doi:10.1161/01.RES.0000060700.55247.7C

37. Omiecinski CJ, Vanden Heuvel JP, Perdew GH, Peters JM. Xenobiotic metabolism, disposition, and regulation by receptors: from biochemical phenomenon to predictors of major toxicities. Toxicol Sci. 2011;120 Suppl : S49–75. doi:10.1093/toxsci/kfq338

38. Reschly EJ, Krasowski MD. Evolution and function of the NR1I nuclear hormone

receptor subfamily (VDR, PXR, and CAR) with respect to metabolism of xenobiotics and endogenous compounds. Curr Drug Metab. 2006;7: 349–65. Available: http://www.pubmedcentral.nih.gov/articlerender.fcgi?artid=2231810&tool=pmcentrez&rendertype=abstract

39. Reschly EJ, Krasowski MD. Evolution and function of the NR1I nuclear hormone receptor subfamily (VDR, PXR, and CAR) with respect to metabolism of xenobiotics and endogenous compounds. Curr Drug Metab. 2006;7: 349–65.

40. Kliewer SA, Moore JT, Wade L, Staudinger JL, Watson MA, Jones SA, et al. An Orphan Nuclear Receptor Activated by Pregnanes Defines a Novel Steroid Signaling Pathway. Cell. Elsevier; 1998;92: 73–82. doi:10.1016/S0092-8674(00)80900-9

41. Kliewer SA, Moore JT, Wade L, Staudinger JL, Watson MA, Jones SA, et al. An Orphan Nuclear Receptor Activated by Pregnanes Defines a Novel Steroid Signaling Pathway. Cell. Elsevier; 1998;92: 73–82. doi:10.1016/S0092-8674(00)80900-9

42. Coumoul X, Diry M, Barouki R. PXR-dependent induction of human CYP3A4 gene expression by organochlorine pesticides. Biochem Pharmacol. 2002;64: 1513–9. Available: http://www.ncbi.nlm.nih.gov/pubmed/12417264

43. Forman BM, Goode E, Chen J, Oro AE, Bradley DJ, Perlmann T, et al. Identification of a nuclear receptor that is activated by farnesol metabolites. Cell. Elsevier; 1995;81: 687–693. doi:10.1016/0092-8674(95)90530-8

44. Lübberstedt M, Müller-Vieira U, Mayer M, Biemel KM, Knöspel F, Knobeloch D, et al. HepaRG human hepatic cell line utility as a surrogate for primary human hepatocytes in drug metabolism assessment in vitro. J Pharmacol Toxicol Methods.

63: 59–68. doi:10.1016/j.vascn.2010.04.013

45. Tuschl G, Hrach J, Walter Y, Hewitt PG, Mueller SO. Serum-free collagen sandwich cultures of adult rat hepatocytes maintain liver-like properties long term: a valuable model for in vitro toxicity and drug-drug interaction studies. Chem Biol Interact. 2009;181: 124–37. doi:10.1016/j.cbi.2009.05.015

46. Zhang D, Luo G, Ding X, Lu C. Preclinical experimental models of drug metabolism and disposition in drug discovery and development. Acta Pharm Sin B. 2012;2: 549–561. doi:10.1016/j.apsb.2012.10.004

47. Brandon EFA, Raap CD, Meijerman I, Beijnen JH, Schellens JHM. An update on in vitro test methods in human hepatic drug biotransformation research: pros and cons. Toxicol Appl Pharmacol. 2003;189: 233–46. Available: http://www.ncbi.nlm.nih.gov/pubmed/12791308

48. Guillouzo A, Corlu A, Aninat C, Glaise D, Morel F, Guguen-Guillouzo C. The human hepatoma HepaRG cells: a highly differentiated model for studies of liver metabolism and toxicity of xenobiotics. Chem Biol Interact. 2007;168: 66–73. doi:10.1016/j.cbi.2006.12.003

49. Gómez-Lechón MJ, Donato T, Jover R, Rodriguez C, Ponsoda X, Glaise D, et al. Expression and induction of a large set of drug-metabolizing enzymes by the highly differentiated human hepatoma cell line BC2. Eur J Biochem. 2001;268: 1448–59. Available: http://www.ncbi.nlm.nih.gov/pubmed/11231298

50. Schook LB, Collares TV, Hu W, Liang Y, Rodrigues FM, Rund LA, et al. A Genetic Porcine Model of Cancer. PLoS One. 2015;10: e0128864.

doi:10.1371/journal.pone.0128864

51. Achour B, Barber J, Rostami-Hodjegan A. Cytochrome P450 Pig Liver Pie: Determination of Individual Cytochrome P450 Isoform Contents in Microsomes from Two Pig Livers Using Liquid Chromatography in Conjunction with Mass Spectrometry. Drug Metab Dispos. 2011;39: 2130–2134. doi:10.1124/dmd.111.040618

52. Bogaards JJ, Bertrand M, Jackson P, Oudshoorn MJ, Weaver RJ, van Bladeren PJ, et al. Determining the best animal model for human cytochrome P450 activities: a comparison of mouse, rat, rabbit, dog, micropig, monkey and man. Xenobiotica. 2000;30: 1131–52. doi:10.1080/00498250010021684

53. Nebbia C, Dacasto M, Rossetto Giaccherino A, Giuliano Albo A, Carletti M. Comparative expression of liver cytochrome P450-dependent monooxygenases in the horse and in other agricultural and laboratory species. Vet J. 2003;165: 53–64. Available: http://www.ncbi.nlm.nih.gov/pubmed/12618071

Chapter 2: Tissue specific mRNA expression profiles of porcine orphan nuclear receptors that regulate xenobiotic metabolism and transport

Abstract

Orphan nuclear receptors (NRs) are master regulators for a wide variety of physiological processes and metabolism of endogenous compounds and exogenous xenobiotics. In the present study, expression of orphan nuclear receptors was screened across various porcine organs (liver, kidney, lung, small intestine, spleen, pancreas, heart, brain and skeletal muscle). Analysis of the mRNA expression levels of porcine orphan nuclear receptors in total RNA from various porcine organs was also performed by real time reverse transcriptase PCR. Expression of all the porcine nuclear receptors studied except (PPARγ) was detected in the liver and kidney. Most of the nuclear receptors showed higher expression in the liver. To evaluate the effect of xenobiotic exposure on the expression pattern of the nuclear receptors, expression pattern of nuclear receptors were evaluated in three different developmental stages i.e. 3 month old fetus, 1 month old piglet and 1 year old adult pig. The expression levels of the nuclear receptors in adult tissues were higher than that of 1 month old piglets which in turn were higher than those of 3 month old fetal piglet. As the animals get older, they get more exposure to the xenobiotics, which induce the expression of the DMEs and nuclear receptors.

Introduction

Orphan nuclear receptors (NRs) are transcription factors that play important roles in a wide variety of physiological processes, such as cell growth, cell differentiation and metabolic homeostasis [1–3]. They also regulate the expression of phase I and phase II drug metabolism enzymes (DME) and phase III transporters. Regulation of gene expression of DMEs and transporters plays a crucial role in the metabolism and clearance of drugs and xenobiotics introduced into the body. Most NRs share two functional domains; N-terminal DNA-binding domain (DBD) and C-terminal ligand binding domain (LBD)[4].

The number of NR genes varies considerably from species to species; in human, 48 receptors were found, 49 in mouse, 21 in *Drosophila*, 33 in sea urchin, and more than 270 in *Caenorhabditis elegans* [5–7]). Of the nuclear receptors, pregnane X receptor (PXR, NR1I2), constitutive androstane receptor (CAR, NR1I3), farnesoid X receptor (FXR, NR1H4), liver X receptor alpha (LXRα, NR1H3), liver X receptor beta (LXRβ, NR1H2) and peroxisome proliferator activated receptor alpha (PPARα, NR1C1) are primary transcriptional regulators of the genes involved in the metabolism and elimination of drugs and xenobiotics [8–11]. Nuclear receptors LXR, CAR, FXR, PPAR and PXR regulate gene expression by forming heterodimers with the retinoid X receptor [12]. NRs activate or repress target gene transcription through interaction with transcriptional co-regulators like co-activators or co-repressors, which leads to chromatin modification [13].

A considerable degree of cross talk between nuclear receptors and drug metabolism enzymes and receptors exists [14]. mRNA expression profiles of nuclear

receptors are important for understanding the regulation mechanism of drug metabolizing enzymes and transporters. Detailed understanding of transcription profiles of nuclear receptors has major implication for screening of new chemicals or drugs. The tissue distribution of the important nuclear receptors has been reported in human [14]. However, the tissue specific expression pattern of the porcine nuclear receptors has been poorly documented. The present study was therefore undertaken to study the tissue distribution of mRNA expression of most important nuclear receptors linked to xenobiotic metabolism. The expression patterns of the orphan nuclear receptors in three developmental stages (3 month old fetal piglet, 1 month old piglet and 1 year old adult pig) were also analyzed.

Materials and Methods

Animals

Tissue samples (liver, kidney, lung, small intestine, spleen, pancreas, heart, brain and skeletal muscle) were collected from cross pigs (Minnesota Minipig sire X Large White Yorkshire dam) maintained in Animal Science Department, UIUC farm. Animals were euthanized and the above tissue samples were collected. All tissue samples were snap frozen in dry ice and stored at – 80 °C before RNA isolation.

RNA Isolation

Total RNA was isolated from porcine tissues (liver, kidney, lung, small intestine, spleen, pancreas, heart, brain and skeletal muscle) using RNeasy Mini Kit (Qiagen) as per the manufacturer's protocol. RNA pellets were dissolved in nuclease-free water and stored at -80°C until analysis. Quality of the RNA was determined using

NanoDrop spectrophotometer and analyzed by an Agilent 2100 Bioanalyzer to determine RNA integrity as well as the presence/absence of gDNA by the Carver High-Throughput DNA Sequencing and Genotyping Unit (HTS lab, University of Illinois, Urbana, IL, USA). The concentration of the RNA was determined by Qubit® RNA HS Assay Kit (Thermo Fisher Scientific, Life Technologies) as per manufacturer's protocol.

Reverse Transcription PCR (RT-PCR)

Tissue distribution of the nuclear receptors was detected by reverse transcription PCR. Reverse transcription of RNA was performed from 1 µg total RNA in the presence of RNase inhibitor, random hexamer primers (50 ng/µL), deoxynucleotides (dNTPs, 10 mM), SuperScript III reverse transcriptase (200 U/µL) and reverse transcriptase buffer in a 20 µL final reaction volume using SuperScript III First-Strand Synthesis System for RT-PCR kit (Invitrogen,Life Technologies, IN, USA).

PCR reactions were performed in a 25 µl reaction volume containing 50 ng cDNA as the template, 0.5 M of each primer, 2X PCR buffer (including 1.5 mM $MgCl_2$), 200 mM dNTPs, and 0.625 units of Taq DNA polymerase. Information on PCR primers and thermocycler conditions used are listed in table 2.1.

Quantitative RT-PCR

Relative quantification of the genes was analyzed quantitative real time PCR (qPCR). qPCR was performed by using Power SYBR green PCR Master Mix (2X) (Applied Biosystems) in a Taqman ABI 7900 Real-Time PCR system (Applied

Biosystems). Information on primer used is listed in table 2.2. The thermal cycling conditions for real-time PCR were one cycle of 50 °C for 2 min (AmpErase uracil-N-glycosylase activation) and 95°C for 10 min (AmpliTaq Gold activation), followed by 40 cycles of 95°C for 15 sec (denaturation) and 60°C for 1 min (annealing and extension). The housekeeping gene GAPDH was used as endogenous control to normalize for RNA loading or differences in reverse transcription efficiency. For preparation of nuclear receptor calibration curves, the total RNA obtained from liver was used except for PPARγ, for which total RNA from spleen was used.

Data Analysis

The relative expression of each mRNA was calculated by the ΔCt method (where ΔCt is the value obtained by subtracting the Ct value of the GAPDH mRNA from the Ct value of the target mRNA). The amount of target relative to GAPDH mRNA was expressed as $2^{-(\Delta Ct)}$. Data are expressed as the ratio of target mRNA to GAPDH mRNA. Studies were conducted in triplicate and data are shown as mean values.

Results

Screening of mRNA expression of porcine orphan nuclear receptors

The mRNA expression of the porcine orphan nuclear receptors was screened across different porcine tissues and the result is presented in table 2.3. Whereas, LXRβ transcript was detected in all the organs, expression of LXRα transcript was detected in liver, kidney, lung, small intestine and spleen. Expression of CAR was detected in liver, kidney, small intestine and spleen. Among the PPAR isoforms,

PPARβ was detected in all the tissues screened whereas PPARα was detected in liver, kidney, small intestine and heart and PPARγ was detected in small intestine and spleen. PXR was detected in liver, kidney, lung and small intestine. FXR was detected in liver, kidney and small intestine. Among RXR isoforms, RXRβ was detected in all the tissue screened except small intestine; whereas RXRα was detected in liver, kidney, lung, spleen, heart and skeletal muscle and RXRγ was detected in liver, heart, brain and skeletal muscle.

Differential mRNA expression of porcine orphan nuclear receptors

The differential expression of the porcine orphan nuclear receptor mRNAs in different tissues was analyzed by quantitative real time PCR. The result of tissue specific differential expression profiles of LXRα and LXRβ mRNAs is presented in Figure 2.1. Liver and lung showed higher expression of LXRα compared to spleen, kidney and small intestine. In case of LXRβ, high expression was detected in liver and small intestine. Figure 2.2 shows the relative CAR mRNA expression in various porcine tissues. CAR mRNA was expressed at high level at liver and small intestine and a relatively lower level at kidney and spleen. The tissue specific differential mRNA expression for PPAR isoforms is presented in Figure 2.3. PPARα mRNA was expressed at highest in the liver. Highest level of PPARβ and PPARγ mRNAs expression was detected in lung and small intestine respectively. PXR and FXR mRNAs were expressed at high levels in liver and small intestine, with a very weak or no expression in kidney and lung (Figure 2.4 & Figure 2.5). Figure 2.6 shows the differential mRNA expression of three RXR isoforms across different porcine tissues.

Both RXRα and RXRβ mRNAs were expressed at high levels in the liver. RXRγ mRNA was expressed at high levels in skeletal muscle and liver.

To evaluate the effect of xenobiotic exposure on the expression pattern of xenosensors, expression pattern of nuclear receptors were evaluated in three different developmental stages i.e. 3-month-old fetus, 1-month-old piglet and 1-year-old adult pig. The results are depicted in Figure 2.1 to Figure 2.6. It was found that the mRNA expressions of all the orphan nuclear receptors increased gradually with increase in age of pig. The mRNA expression levels of the nuclear receptors in fetal tissues were very low. The expression levels of the nuclear receptors in adult tissues were higher than those of 1 month old piglets which in turn were higher than those of 3 month old piglets. As the animals get older, they get more exposure of the xenobiotics which may induce the expression of the nuclear receptors.

Discussion

Prediction of drug interactions and *in vivo* clearance of new chemicals and drugs are generally done by the ability of the chemicals to induce drug metabolizing enzymes and transporters [15]. Nuclear receptors are the master regulators of the expression of phase I and phase II drug metabolizing enzymes and phase III transporters [16]. Therefore, the tissue distribution and expression profiles of the nuclear receptors are crucial to understand the control mechanism of these enzymes and transporters. In that context, the present study was designed to investigate the tissue-specific mRNA expression profiles of porcine orphan nuclear receptors involved in regulation of xenobiotic metabolism. Although rodents are generally used as animal models for assessment of drug metabolism and toxicity, they are not

reliable predictors of human CYP enzyme inducibility because of divergence of amino acid sequences in the ligand binding domain of nuclear receptors leading to variation in xenobiotic response [12]. The sequence identity between human and porcine P450 enzymes and nuclear receptors is striking, ranging from 72 to 95 % [17] making them good large animal model to drug metabolism and toxicity.

As expected, expression of all the porcine nuclear receptors except (PPARγ) was detected in liver and kidney. As the hepato-intestinal axis and kidney play the major role in the metabolism and disposition of xenobiotics, the expression of most of the nuclear receptors involved in the regulation of xenobiotic metabolism was detected. The expression profile of the porcine nuclear receptors was consistent with that of human[16,18]. Expression of LXRα and LXRβ was reported in different tissues of mouse embryos from 14.5 days postcoitum like liver, lung and small intestine [19]. LXRα and LXRβ transcripts were also detected in mouse and human placenta [20]. CAR mRNA was expressed at high levels in liver and small intestine (Figure 2.2) and PXR mRNA was expressed at high levels in liver and small intestine and lower levels at kidney and lung (Figure 2.4). This is consistent with the findings of human [14,21–23] and rat [24]. PPARα mRNA was expressed at high level in the liver, small intestine and kidney (Figure 2.3). Similar findings were reported in case of human PPARα expression [14]. In mice and rat also, PPARα is expressed at high levels in the liver, kidney and heart [25,26]. High levels of PPARβ expression was found in lung and skeletal muscle (Figure 2.3) which is consistent with those of human [14]. The mRNA expression of three isoforms of RXR is consistent with the expression pattern in human tissues [14].

To evaluate the effect of xenobiotic exposure on the expression pattern of xenosensors, expression pattern of nuclear receptors were evaluated in three different developmental stages i.e. 3-month-old fetus, 1-month-old piglet and 1-year-old adult pig. The expression of the orphan nuclear receptors was found very low or basal level in fetal tissues and expression values increased with increase in age of pig. This demonstrate that increasing exposure of xenobiotics may induce increased expression of nuclear receptors.

Figures and Tables

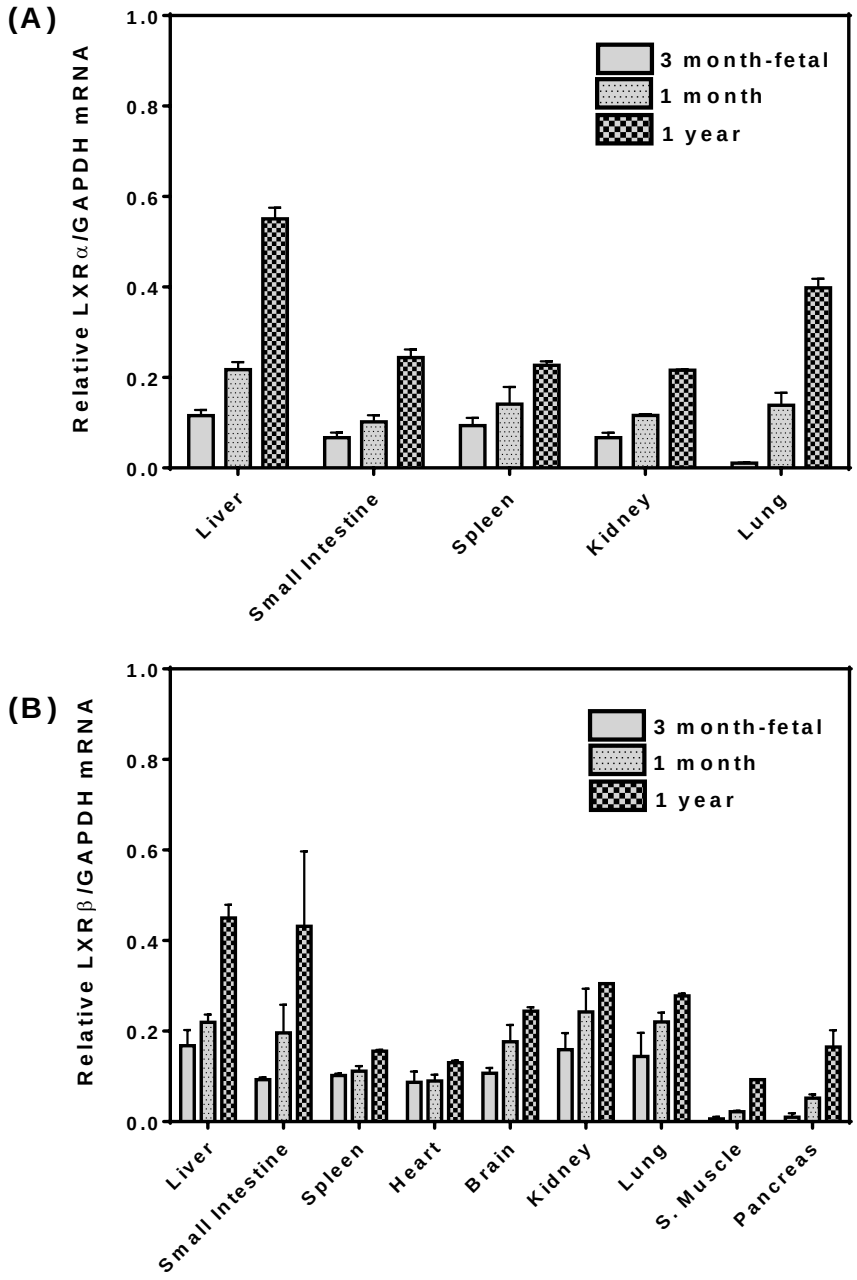

Figure 2.1. Stage and tissue specific differential expression of porcine LXRα (A) and LXRβ (B)

Real time RT-PCR was performed to analyze the stage and tissue specific expression profiles of LXRα and LXRβ. Relative expression values of LXRs were calculated based on the assumption that average expression level of housekeeping gene GAPDH is 1.

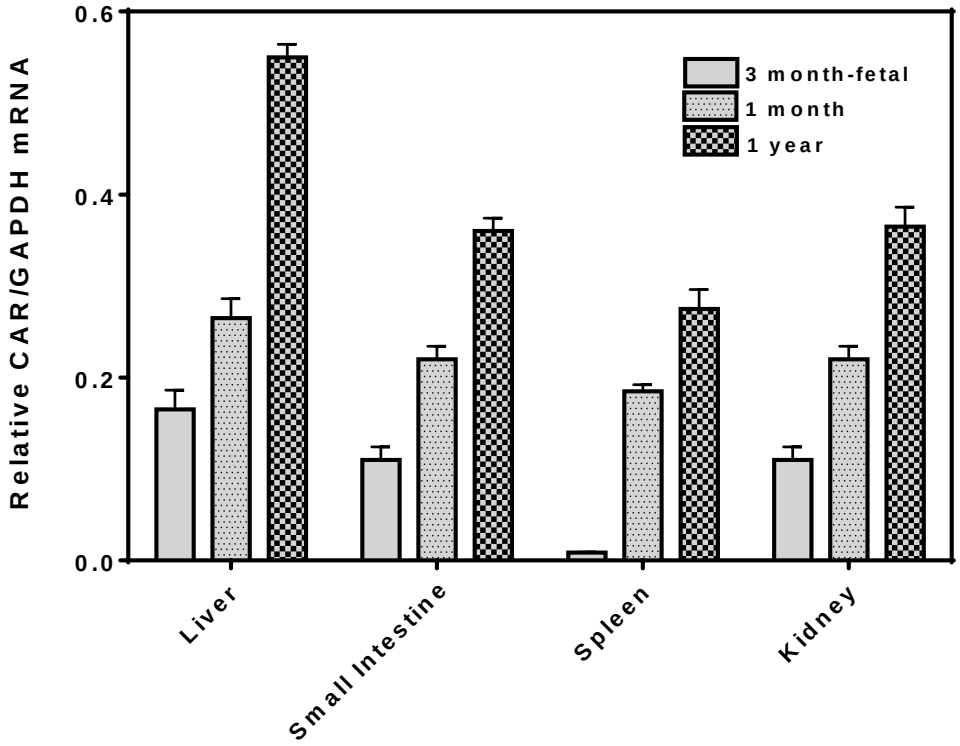

Figure 2.2. Stage and tissue specific differential expression of porcine CAR

Real time RT-PCR was performed to analyze the stage and tissue specific expression profiles of CAR. Relative expression values of CAR were calculated based on the assumption that average expression level of housekeeping gene GAPDH is 1.

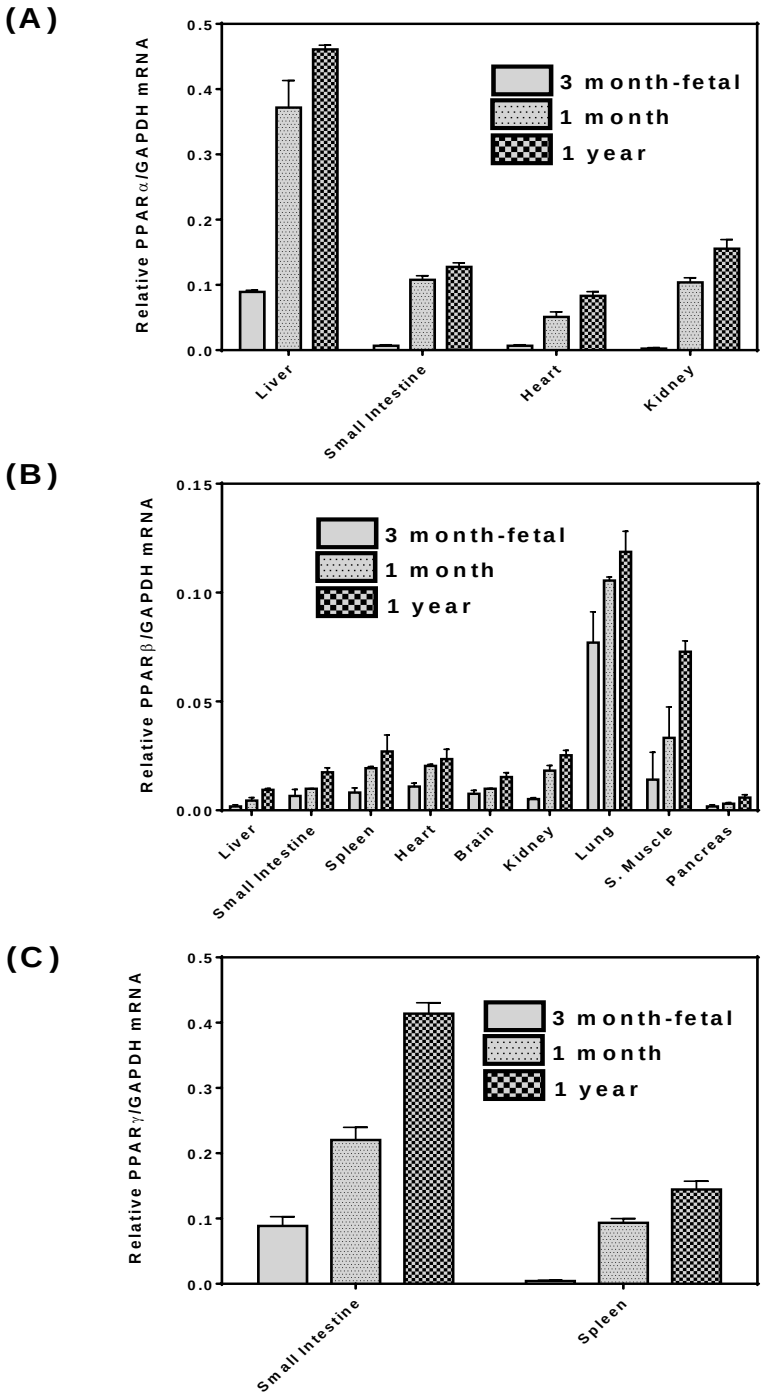

Figure 2.3. Stage and tissue specific differential expression of porcine PPARα (A), PPARβ (B) and PPARγ (C)

Real time RT-PCR was performed to analyze the stage and tissue specific expression profiles of PPARs. Relative expression values of PPARs were calculated based on the assumption that average expression level of housekeeping gene GAPDH is 1.

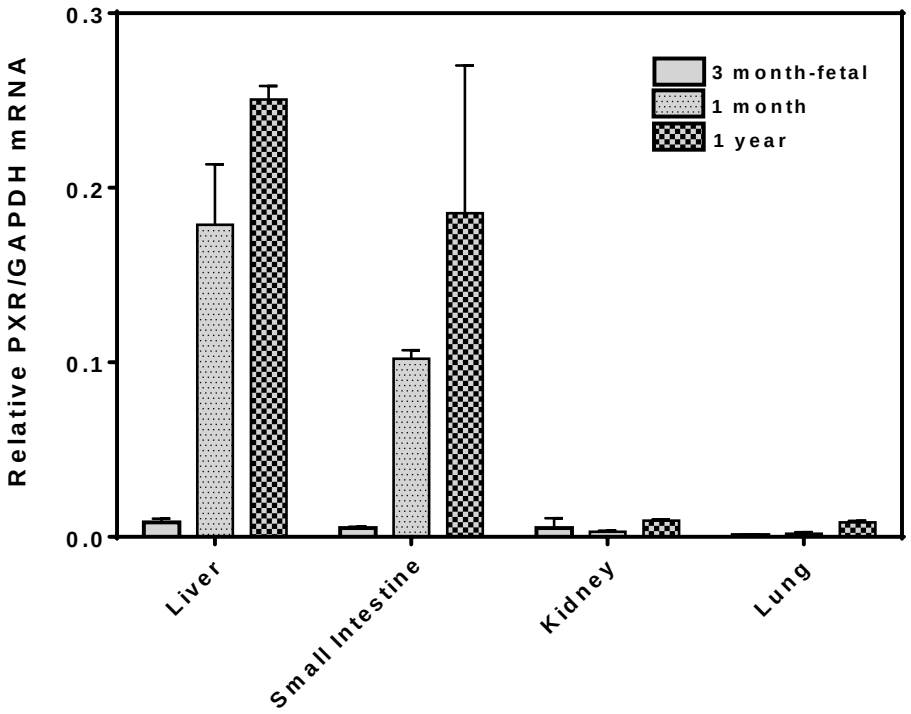

Figure 2.4. Stage and tissue specific differential expression of porcine PXR

Real time RT-PCR was performed to analyze the stage and tissue specific expression profiles of PXR. Relative expression values of PXR were calculated based on the assumption that average expression level of housekeeping gene GAPDH is 1.

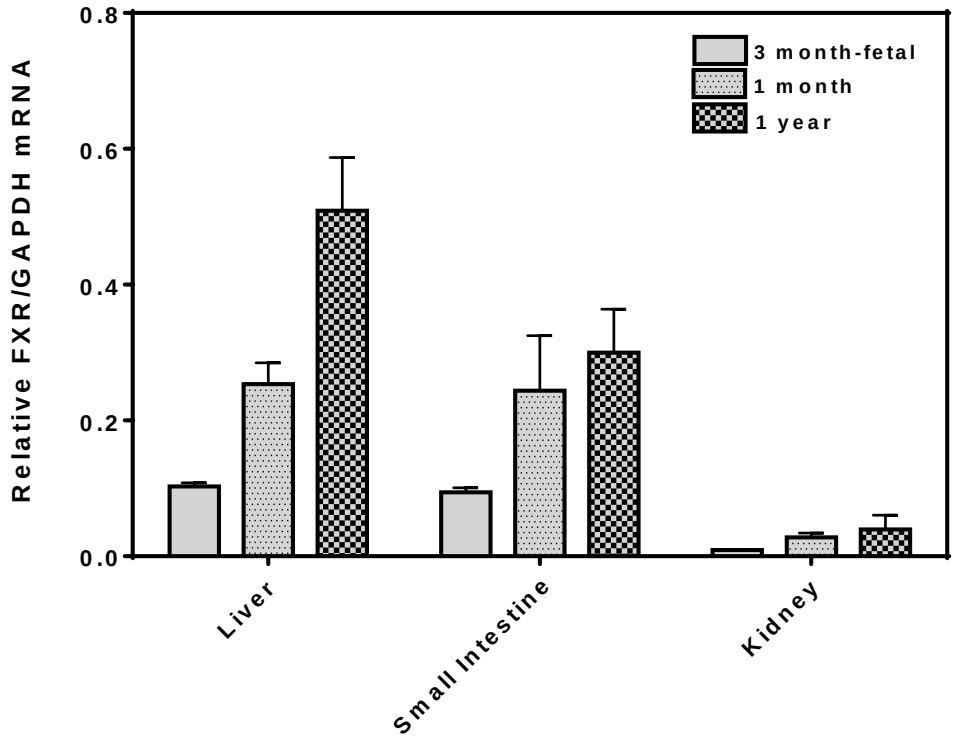

Figure 2.5. Stage and tissue specific differential expression of porcine FXR

Real time RT-PCR was performed to analyze the stage and tissue specific expression profiles of FXR. Relative expression values of FXR were calculated based on the assumption that average expression level of housekeeping gene GAPDH is 1.

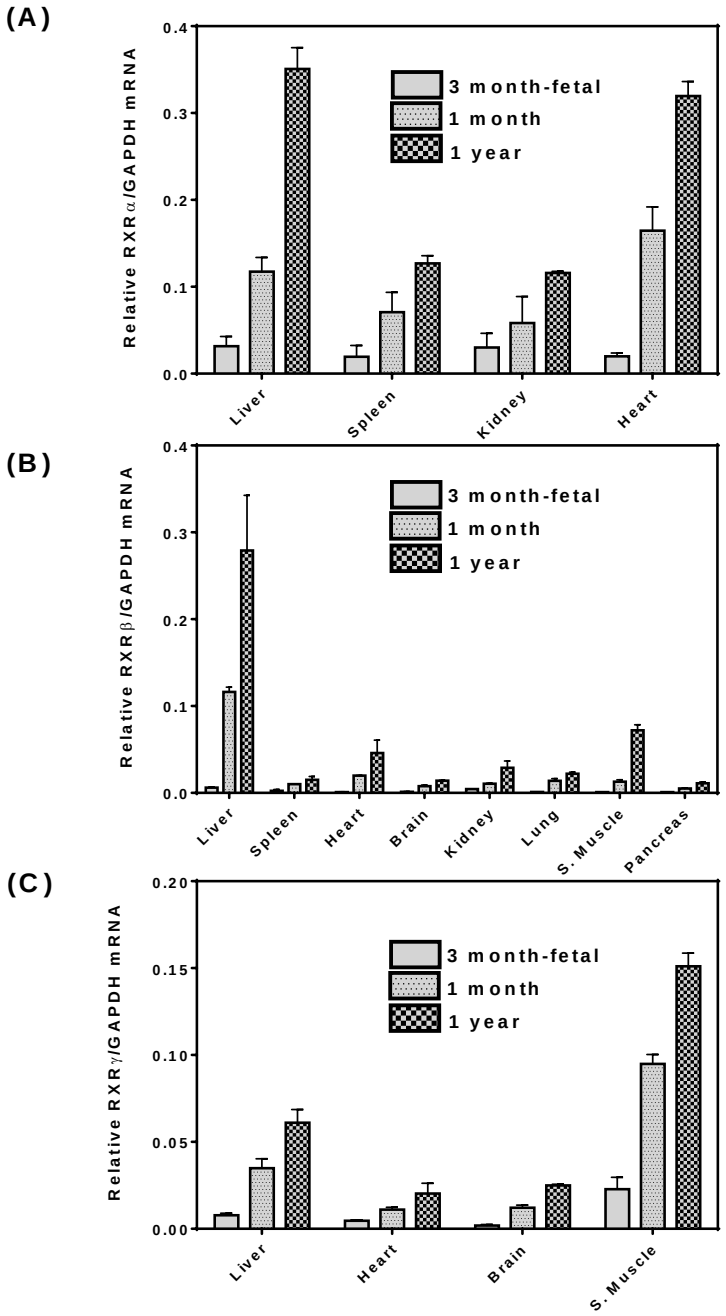

Figure 2.6. Stage and tissue specific differential expression of porcine RXRα (A), RXRβ (B) and RXRγ (C)

Real time RT-PCR was performed to analyze the stage and tissue specific expression profiles of RXRs. Relative expression values of RXRs were calculated based on the assumption that average expression level of housekeeping gene GAPDH is 1.

Table 2.1

Genes	Primers	Sequences (5'-3')	Ta[1] (°C)
PXR	Forward	CTCCCAGAGGACGGTTTGAA	57
	Reverse	AATTCCAGGGTGGTGTAGGC	
FXR	Forward	TCAGTCCTTGTCACAGCCAC	57
	Reverse	CGCAAACGACACAAAGCTCA	
CAR	Forward	AGAAGATGGAGCGCATGTGG	58
	Reverse	GGATGCCGTACACAGTCCAT	
LXRα	Forward	TAGGAATGGGGTCCAGGCAC	57
	Reverse	TCCACTGCAGAGTCAGGAGA	
LXRβ	Forward	CAAGGGGACGAAAGCAGCTC	59
	Reverse	AGCTGAGCACGTTGTAGTGG	
PPARα	Forward	GGGCTTCTTTCGGAGAACCA	61
	Reverse	GACGAAAGGCGGGTTATTGC	
PPARβ	Forward	TGTGGAAGCAGCTGGTGAAT	58
	Reverse	GAAGGGCTTTCGGAGGTCG	
PPARγ	Forward	AACATTTCACAAGAGGTGACCA	57
	Reverse	GAACCCCGAGGCTTTATCCC	
RXRα	Forward	ATGACCCCGTCACCAACATC	61
	Reverse	GAGTCCGGGTTGAAGAGGAC	
RXRβ	Forward	AGCCATCTTTGACCGGGTG	57
	Reverse	CTCAAGCGTGAGGAACACCA	
RXRγ	Forward	CGTTCCCCAAACGTGATGCT	60
	Reverse	TTCGTTCACTGGCTTTCCAAG	

Table 2.1. Primer sequences for reverse transcription PCR

[1]Ta denotes annealing temperature

PXR indicates pregnane X receptor, FXR indicates farnesoid X receptor, CAR indicates constitutive androstane receptor, LXR indicates liver X receptor, PPAR indicates peroxisome proliferator activated receptor and RXR indicates retinoid X receptor

Table 2.2

Genes	Primers	Sequences (5'-3')
PXR	Forward	GACAACAGTGGGAAAGAGAT
	Reverse	CCCTGAAGTAGGAGATGACT
FXR	Forward	CATTCAACCATCACCACGCAGAGA
	Reverse	GCACATCCCAGACTTCACAGAGA
CAR	Forward	GAAAGCAGGGTTACAGTGGGAGTA
	Reverse	CTTCAGGTGTTGGGATGGTGGTC
LXRα	Forward	TCCAGGTAGAGAGGCTGCAACATA
	Reverse	AGTTTCATTAGCATCCGTGGGAAC
LXRβ	Forward	GAGTCTTCCTGAGAGGGGCAGATA
	Reverse	CGTGGTAGGCTTGAGGTGTAAGC
PPARα	Forward	AATAACCCGCCTTTCGTCATACAC
	Reverse	GACCTCCGCCTCCTTGTTCT
PPARβ	Forward	CCATGCTGTCATGGGTGAAACTCT
	Reverse	GTCAACCATGGTCACCTCTTGTGA
PPARγ	Forward	CTTATTGACCCAGAAAGCGATGCC
	Reverse	TGTCAACCATGGTCACCTCTTGT
RXRα	Forward	CCTTCTCGCACCGCTCCATA
	Reverse	CGTCAGCACCCTGTCAAAGATG
RXRβ	Forward	GGAGCCATCTTTGACCGGGTG
	Reverse	CTCAGGCAGCCAAGTTCTGTCTT
RXRγ	Forward	CTTCCCGTTCCCCAAACGTGAT
	Reverse	CTTCCAGAAAAGATCCCCAGTCCC

Table 2.2. Primer sequences for real-time PCR

PXR indicates pregnane X receptor, FXR indicates farnesoid X receptor, CAR indicates constitutive androstane receptor, LXR indicates liver X receptor, PPAR indicates peroxisome proliferator activated receptor and RXR indicates retinoid X receptor

Table 2.3

Genes	Tissues								
	L	K	Lu	S. I	Sp	Pan	Hrt	B	S. Mus
LXRα	+	+	+	+	+	-	-	-	-
LXRβ	+	+	+	+	+	+	+	+	+
CAR	+	+	-	+	+	-	-	-	-
PPARα	+	+	-	+	-	-	+	-	-
PPARβ	+	+	+	+	+	+	+	+	+
PPARγ	-	-	-	+	+	-	-	-	-
PXR	+	+	+	+	-	-	-	-	-
FXR	+	+	-	+	-	-	-	-	-
RXRα	+	+	+	-	+	-	+	-	+
RXRβ	+	+	+	-	+	+	+	+	+
RXRγ	+	-	-	-	-	-	+	+	+

Table 2. 3. Tissue specific expression of porcine nuclear receptors

+ denotes detected; - denotes Non-detected; Qualitative reverse transcriptase PCR was done to screen the detection of the nuclear receptors in different porcine tissues.

L indicates liver, K indicates kidney, Lu indicates lung, S.I indicates small intestine, Pan indicates pancreas, Hrt indicates heart, B indicates brain, S. Mus indicates skeletal muscle, PXR indicates pregnane X receptor, FXR indicates farnesoid X receptor, CAR indicates constitutive androstane receptor, LXR indicates liver X receptor, PPAR indicates peroxisome proliferator activated receptor and RXR indicates retinoid X receptor

References:

1. Mangelsdorf DJ, Thummel C, Beato M, Herrlich P, Schütz G, Umesono K, et al. The nuclear receptor superfamily: the second decade. Cell. 1995;83: 835–9. Available: http://www.ncbi.nlm.nih.gov/pubmed/8521507

2. Glass CK, Rosenfeld MG. The coregulator exchange in transcriptional functions of nuclear receptors. Genes Dev. 2000;14: 121–41. Available: http://www.ncbi.nlm.nih.gov/pubmed/10652267

3. Mukherjee S, Mani S. Orphan nuclear receptors as targets for drug development. Pharm Res. 2010;27: 1439–68. doi:10.1007/s11095-010-0117-7

4. Mangelsdorf DJ, Evans RM. The RXR heterodimers and orphan receptors. Cell. 1995;83: 841–50. Available: http://www.ncbi.nlm.nih.gov/pubmed/8521508

5. Bertrand S, Brunet FG, Escriva H, Parmentier G, Laudet V, Robinson-Rechavi M. Evolutionary genomics of nuclear receptors: from twenty-five ancestral genes to derived endocrine systems. Mol Biol Evol. 2004;21: 1923–37. doi:10.1093/molbev/msh200

6. Maglich JM, Sluder A, Guan X, Shi Y, McKee DD, Carrick K, et al. Comparison of complete nuclear receptor sets from the human, Caenorhabditis elegans and Drosophila genomes. Genome Biol. 2001;2: RESEARCH0029. Available: http://www.pubmedcentral.nih.gov/articlerender.fcgi?artid=55326&tool=pmcentrez&rendertype=abstract

7. Robinson-Rechavi M, Carpentier AS, Duffraisse M, Laudet V. How many

nuclear hormone receptors are there in the human genome? Trends Genet. 2001;17: 554–6. Available: http://www.ncbi.nlm.nih.gov/pubmed/11585645

8. Evans RM, Mangelsdorf DJ. Nuclear Receptors, RXR, and the Big Bang. Cell. 2014;157: 255–66. doi:10.1016/j.cell.2014.03.012

9. Tzameli I, Moore DD. Role reversal: new insights from new ligands for the xenobiotic receptor CAR. Trends Endocrinol Metab. Elsevier; 2001;12: 7–10. doi:10.1016/S1043-2760(00)00332-5

10. Xie W, Evans RM. Orphan nuclear receptors: the exotics of xenobiotics. J Biol Chem. 2001;276: 37739–42. doi:10.1074/jbc.R100033200

11. Xie W, Chiang JYL. Nuclear receptors in drug metabolism and beyond. Drug Metab Rev. Taylor & Francis; 2013;45: 1–2. doi:10.3109/03602532.2013.754577

12. Xie W, Uppal H, Saini SPS, Mu Y, Little JM, Radominska-Pandya A, et al. Orphan nuclear receptor-mediated xenobiotic regulation in drug metabolism. Drug Discov Today. 2004;9: 442–9. doi:10.1016/S1359-6446(04)03061-2

13. McKenna NJ, O'Malley BW. Minireview: nuclear receptor coactivators--an update. Endocrinology. 2002;143: 2461–5. doi:10.1210/endo.143.7.8892

14. Nishimura M, Naito S, Yokoi T. Tissue-specific mRNA expression profiles of human nuclear receptor subfamilies. Drug Metab Pharmacokinet. 2004;19: 135–49. Available: http://www.ncbi.nlm.nih.gov/pubmed/15499180

15. Omiecinski CJ, Vanden Heuvel JP, Perdew GH, Peters JM. Xenobiotic metabolism, disposition, and regulation by receptors: from biochemical phenomenon

to predictors of major toxicities. Toxicol Sci. 2011;120 Suppl : S49–75. doi:10.1093/toxsci/kfq338

16. Xu C, Li CY-T, Kong A-NT. Induction of phase I, II and III drug metabolism/transport by xenobiotics. Arch Pharm Res. 2005;28: 249–68. Available: http://www.ncbi.nlm.nih.gov/pubmed/15832810

17. Achour B, Barber J, Rostami-Hodjegan A. Cytochrome P450 Pig Liver Pie: Determination of Individual Cytochrome P450 Isoform Contents in Microsomes from Two Pig Livers Using Liquid Chromatography in Conjunction with Mass Spectrometry. Drug Metab Dispos. 2011;39: 2130–2134. doi:10.1124/dmd.111.040618

18. Takegoshi S, Jiang S, Ohashi R, Savchenko AS, Iwanari H, Tanaka T, et al. Protein expression of nuclear receptors in human and murine tissues. Pathol Int. 2009;59: 61–72. doi:10.1111/j.1440-1827.2008.02330.x

19. Annicotte J-S, Schoonjans K, Auwerx J. Expression of the liver X receptor alpha and beta in embryonic and adult mice. Anat Rec A Discov Mol Cell Evol Biol. 2004;277: 312–6. doi:10.1002/ar.a.20015

20. Marceau G, Volle DH, Gallot D, Mangelsdorf DJ, Sapin V, Lobaccaro J-MA. Placental expression of the nuclear receptors for oxysterols LXRalpha and LXRbeta during mouse and human development. Anat Rec A Discov Mol Cell Evol Biol. 2005;283: 175–81. doi:10.1002/ar.a.20157

21. Lehmann JM, Kliewer SA, Moore LB, Smith-Oliver TA, Oliver BB, Su JL, et al. Activation of the nuclear receptor LXR by oxysterols defines a new hormone

response pathway. J Biol Chem. 1997;272: 3137–40. Available: http://www.ncbi.nlm.nih.gov/pubmed/9013544

22. Choi HS, Chung M, Tzameli I, Simha D, Lee YK, Seol W, et al. Differential transactivation by two isoforms of the orphan nuclear hormone receptor CAR. J Biol Chem. 1997;272: 23565–71. Available: http://www.ncbi.nlm.nih.gov/pubmed/9295294

23. Baes M, Gulick T, Choi HS, Martinoli MG, Simha D, Moore DD. A new orphan member of the nuclear hormone receptor superfamily that interacts with a subset of retinoic acid response elements. Mol Cell Biol. 1994;14: 1544–52.

24. Zhang H, LeCulyse E, Liu L, Hu M, Matoney L, Zhu W, et al. Rat pregnane X receptor: molecular cloning, tissue distribution, and xenobiotic regulation. Arch Biochem Biophys. 1999;368: 14–22. doi:10.1006/abbi.1999.1307

25. Issemann I, Green S. Activation of a member of the steroid hormone receptor superfamily by peroxisome proliferators. Nature. 1990;347: 645–50. doi:10.1038/347645a0

26. Braissant O, Foufelle F, Scotto C, Dauça M, Wahli W. Differential expression of peroxisome proliferator-activated receptors (PPARs): tissue distribution of PPAR-alpha, -beta, and -gamma in the adult rat. Endocrinology. 1996;137: 354–66. doi:10.1210/endo.137.1.8536636

Chapter 3: Porcine Liver X receptor: Identification of splice variants and its role in regulation of xenobiotic metabolism in an *in vitro* porcine model

Abstract

Liver X receptors LXRα (NR1H3) and LXRβ (NR1H2) are members of the nuclear hormone receptor superfamily of ligand-activated transcription factors. Both LXRs regulate different metabolic pathways and are involved in the regulation of different endogenous metabolites and xenobiotics. In the present study, eight novel transcript variants of both LXRα and LXRβ were detected. Molecular modeling studies with a synthetic ligand indicate a reduction of the binding affinity of the splice variants compared to the wild type proteins. The role of LXRs in xenobiotic metabolism in an *in vitro* porcine model was investigated and it was found that LXR modulate expression of a number of cytochrome P450 enzymes to regulate the metabolism of xenobiotics.

Introduction

Nuclear receptors are transcription factors that are involved in regulation of metabolism of a wide variety of endogenous and exogenous compounds [1]. A total of 49 members of this family of transcription factor have been identified in human [2]. The transcription factors regulate the expression of the target genes by binding to response elements in the promoters of the target genes [3,4]. The binding of ligand which varies from metabolic intermediate to xenobiotics triggers either gene activation or gene silencing [3]. Nuclear receptors share a common structural motif, composed of functionally distinct domains; the N-terminal activation function 1 domain, the much conserved DNA binding domain (DBD) and the C-terminal ligand-binding domain (LBD)[4]. Between the DBD and LBD is the hinge domain that provides flexibility between these two domains. Activation function 2 is part of LBD and is recognized by either coactivators or corepressors [5].

Liver X receptors LXRα (NR1H3) and LXRβ (NR1H2) are members of the nuclear hormone receptor superfamily of ligand-activated transcription factors. LXRs form heterodimer with the retinoid X receptor (RXR) to regulate target gene expression [6]. Heterodimers of both LXRs with retinoid X receptor (RXR) bind to hormone response elements of the DR-4 type, direct repeats of two similar hexanucleotide half-sites spaced by four nucleotides [7]. In human, the two LXR subtypes are encoded by separate genes and share about 78% amino acid identity in the DNA-binding and ligand binding domains [8]. In human, whereas LXRβ is broadly expressed, the expression of LXRα is restricted to certain tissues, such as liver, small intestine, spleen, kidney, adrenal gland, adipose, and macrophages [7,9–

11]. The natural ligands of LXRs are thought to be oxidized derivatives of cholesterol such as 22(R)-hydroxycholesterol, 24(S), 25-epoxycholesterol and 27-hydroxycholesterol [9,12]. Both LXRs are key regulators of multiple pathways including metabolic, inflammatory and proliferative disease pathways making them highly interesting pharmaceutical targets for novel therapies [13,14].

Alternative pre-mRNA splicing is responsible for the production of multiple mature mRNAs from a single gene, which explains in part how mammalian complexity arises from a surprisingly small number of genes [15]. This process is essential for the generation of protein diversity at the transcriptional, translational and post-translational level [15]. Multiple isoforms have been identified for many members of the nuclear hormone receptor family. In several cases, different receptor isoforms have been found to have distinct activities and to play distinct biological roles [16,17]. Analysis of the pig genome has revealed high similarity between porcine and human genes, including genes associated with drug metabolism [18]. For these reasons, pigs are considered an ideal model for evaluating the safety of pharmaceuticals and biopharmaceuticals [19]. However no information of the transcript variants of LXR in pig is available. Role of LXR in xenobiotic metabolism in porcine is not well understood. The objective of the present study was to identify and characterize transcript variants of porcine LXR and investigate the role of LXR in regulation of xenobiotic metabolism in porcine model. In this study we identified 8 novel LXRα and LXRβ transcript variants each and investigated the properties of the transcript variants by molecular modeling studies.

Materials and Methods

Reagents

All chemicals were purchased from Sigma-Aldrich (USA) unless stated otherwise. Cell culture plastics were from Midsci, USA.

RNA Isolation and cDNA synthesis

Total RNA was isolated from porcine tissues using RNeasy Mini Kit (Qiagen) as per manufacturer's protocol. RNA pellets were dissolved in nuclease-free water and stored at -80°C until analysis. Quality of the RNA was determined by using Nano Drop spectrophotometer. The concentration of the RNA was determined by Qubit® RNA HS Assay Kit (Thermo Fisher Scientific, Life Technologies) as per manufacturer's protocol.

Reverse transcription of RNA was performed from 1 µg total RNA in the presence of RNase inhibitor, random hexamer primers (50 ng/µl), deoxynucleotides (dNTPs, 10mM), SuperScript III reverse transcriptase (200 U/µl) and reverse transcriptase buffer in a 20 µl final reaction volume using SuperScript III First-Strand Synthesis System for RT-PCR kit (Invitrogen, Life Technologies, IN, USA).

Cloning and sequencing of LXRα and LXRβ genes

Based on the exonic regions of the porcine LXRα (NR1H3) and LXRβ (NR1H2) genes, cDNAs that together encode the complete ORF of both the genes were amplified using the primer sets (Table 3.1). PCR reactions were performed in a 25 µl reaction volume containing 50 ng cDNA as the template, 0.5 M of each primer, 2X

PCR buffer (including 1.5 mM $MgCl_2$), 200 mM dNTPs, and 0.625 units of Taq DNA polymerase. PCR reaction conditions were as follows: denaturation at 95 °C for 5 min, followed by 35 cycles of 95 °C for 30 s, 57°C for LXRα and 60 °C LXRβ for 30 s, and 72 °C for 2 min, with a final extension at 72 °C for 20 min. Then, the 5′ and 3′ untranslated regions of LXRα and LXRβ transcripts from various tissues were amplified using total RNA and the FirstChoiceTM RNA ligase-mediated (RLM)-RACE kit (Ambion, Austin, TX). This procedure used primers supplied with the kit and the nested gene-specific primers listed in Table 3.1. These products were cloned into pCRTOPO2.1 vector and sequenced. The cDNAs and deduced amino acid sequences were analyzed using the Biology Workbench (http://workbench.sdsc.edu/).

Generation of 3-D structure of LXRα and LXRβ and their splice variants through homology modeling

In the absence of crystal structures of porcine LXRα and LXRβ, we opted to develop homology models. The deduced amino acid sequences of LXRα and LXRβ were analyzed by the Geneious R6 software (www.geneious.com). The query sequence was submitted in protein-protein BLAST (Basic Local Alignment Search Tool) programme to find out the related protein structure with maximum sequence identity, highest score and least *E*-value to be used as a template (http://www.ncbi.nlm.nih.gov/BLAST). The proteins (PDB ID: 1UHL) and (PDB ID: 1P8) were used as templates for LXRα and LXRβ homology modeling respectively. The sequences of the template proteins were retrieved from the protein data bank (www.rcsb.org).

LXRα and LXRβ transcript variant sequences were aligned and trimmed by Bioedit v7.2.5 software (http://www.mbio.ncsu.edu/bioedit/bioedit.html). The short sequences as well as ambiguous alignments were removed. Further, the entropy values were predicted. The entropy of each amino acid positions reflects the variability of that position along all sequences. Lower entropy indicates high predictability of an amino acid at a position whereas high entropy reflects high uncertainly.

All deduced protein sequences of LXRα, LXRβ and their identified transcript variants were modeled using MODELLER v9.1 (http://salilab.org/modeller) program [20,21]. The sequence-structure matches were established using a variety of fold assignment methods, including sequence-sequence, profile sequence, and alignments. Each model was evaluated using a multiple scoring algorithm that includes length of modeled sequence, identity of structure-sequence alignment, gap of alignment, compactness of model, and potential Z-scores. Representative models were ranked based on statistical potential value of Discrete Optimizes Potential Energy (DOPE) and the best one was selected.

Evaluation and validation of the3-D structures

The final modeled structures were validated by Procheck [22] (http://services.mbi.ucla.edu/PROCHECK/). Procheck was used to perform full geometric analysis as well as stereochemical quality of protein structures. Ramachandran plot statistics was used to evaluate the stability of the models.

Molecular docking analysis to investigate the interaction of LXRα, LXRβ and their splice variants with a synthetic ligand

T0901317 is a well-known synthetic ligand of both isoform of LXR [23] . To gain an understanding of the molecular interactions during ligand binding, molecular docking analysis of LXRα, LXRβ and their splice variants with a synthetic ligand T0901317 was done. The chemical properties of T0901317 are presented in Table 3.3.

Protein and Ligand preparation

Each modeled proteins were prepared using protein preparation wizard of Schrodinger LLC., Portland, USA (http://www.schrodinger.com). This adds hydrogen atoms charges, and does energy minimization of the structures using Impact Refinement module using OPLS (2005) force field. The minimization was terminated when the energy converged or Root Mean Square Deviation (RMSD) reached a maximum cutoff of 0.03Å.

The ligand T0901317 (CID 447912) (Figure 3.1) was obtained from Pubchem database (http://www.pubchem.com). This ligand was built with Chemsketch v12.0 (ACD Labs, USA; http://www.acdlabs.com), and the 3D structure was further energy minimized by LigPrep program (Schrodinger suite LLC., Portland, USA) using the OPLS 2005 force field at pH 7.0 and keeping rest of the parameter values as default.

The pharmacophore model was developed using PHASE 3D-QSAR software [24] which utilizes conformational sampling and other scoring parameters to identify the common 3D pharmacophore. The pharmacophore model provides a standard set of

six pharmacophore features, hydrogen bond acceptor (A), hydrogen bond donor (D), hydrophobic group(H), negatively ionizable (N), positively ionizable (P) and aromatic ring (R). Phase analysis predicted 13 sites of hydrogen bond acceptor (A), 1 site of hydrogen bond donor (D), 5 sites of hydrophobic group (H), and two aromatic ring (R) for the ligand T0901317 (Figure 3.1).

Molecular docking

The molecular docking was carried out using Glide program [25] of Schrodinger suite. Glide is designed to assist in high-throughput screening of potential ligand based on binding mode and affinity for a given receptor molecule. Glide provides three different level of docking precisions (HTVS, High-Throughput Virtual Screening; SP, Standard Precision; XP, Xtra Precision). The entire Glide program was run using default mode. Minimization cycle for conjugate gradient and steepest descent minimization were used with default value of 0.05 Å for initial step size and 1.0 Å for maximum step size. In the coincide criteria for minimization, both the energy change criteria and gradient criteria were used with default value of 10^{-7} and 0.001 kcal/mol respectively. All conformations were considered for docking and in the docking process the Glide score was used to select the best conformation for the ligand.

Effects of T0901317 and GW3965 on transcript expression LXRα, LXRβ, SREBP1, FASN and genes involved in phase I, Phase II drug metabolism, phase II transport and nuclear receptors

T0901317 and GW3965 are well documented potent synthetic agonists of both LXR α and LXRβ [23,26]. To gain insight into the role of LXRs in porcine xenobiotic metabolism, the effect of the two synthetic ligands on the expressions of the most important drug metabolism and regulation genes in porcine primary hepatocytes were investigated.

Cell culture and treatments

Primary hepatocytes were isolated by using a simplified manual perfusion method. Immediately after the animal was euthanized, a single liver lobe was resected, washed 2-3 times with ice cold phosphate buffer saline and transported to the laboratory in ice cold Krebs Ringer Solution. Then the liver sample was cannulated with suitable pipette into visible blood vessels on the cut surface and was flushed with 500 ml of buffer A containing 8.3 g/l NaCl, 0.5 g/l KCl, 2.4 g/l HEPES and 0.19 g/l EGTA at pH 7.4 and 37°C. This was followed by perfusion of 500 ml buffer B containing 8.3 g/l NaCl, 0.5 g/l KCl and 2.4 g/l HEPES. Continuous recirculating perfusion was then carried out on the tissue using a pre-warmed digestion buffer (Buffer C) solution containing 3.9 g/l NaCl, 0.5 g/l KCl, 2.4 g/l HEPES, 0.7 g/l $CaCl_2$ X $2H_2O$ and 0.1 % Collagenase (type IV). Following sufficient digestion, the liver capsule was removed and dissolved cells were liberated by gentle shaking of the liver specimen in ice cold buffer D containing 9.91 g/l Hanks buffered salt without calcium and magnesium, 2.4 g/l HEPES and 2.0 g/l bovine serum

albumin. A scalpel was used to cut through the regions which were not well perfused to release cells contained within. The resulting cell suspension was filtered through a nylon mesh with 100 µm pore size and centrifuged at 50 g for 3 min at 4°C. After, we employed a cell incubation step for 10 min with DNase1 containing buffer at 4°C during which cell clumps were broken and damaged cells digested. Then the resulting suspension was filtered through 70 µm nylon mesh and cells were harvested by 50 g for 3 min. This was followed by three washing in ice cold buffer D. The resulting cell clumps were finally re-suspended in culture medium (William's E supplemented with 100 mU/ml penicillin, 100 µg/ml streptomycin, 2mM glutamate and 10% Fetal bovine serum). Viability of hepatocytes was determined by trypan blue dye exclusion test [27].

Freshly isolated hepatocytes were cultured in William's E medium supplemented with 100 mU/ml penicillin, 100 µg/ml streptomycin, 2 mM glutamate and 10% fetal bovine serum. Prior to experiments, cells were washed twice with PBS followed by incubation in medium containing different concentrations of T0901317 and GW3965.

Real time PCR

Total RNA isolation and cDNA synthesis have been done as described previously. Relative quantification of the genes involved in phase-I, phase-II drug metabolism, phase III transport and nuclear receptors was performed by using Power SYBR green PCR Master Mix (2X) (Applied Biosystems) in Taqman ABI 7900 Real-Time PCR system (Applied Biosystems). The thermal cycling conditions for real-time PCR were one cycle of 50 °C for 2 min (AmpErase uracil-N-glycosylase

activation) and 95°C for 10 min (AmpliTaq Gold activation), followed by 40 cycles of 95°C for 15 sec (denaturation) and 60°C for 1 min (annealing and extension). The housekeeping genes GAPDH and ACTB were used as endogenous control to normalize for RNA loading or differences in reverse transcription efficiency. The information on the primers are presented in table 3.2. The relative expression levels were calculated with respect to the normalized expression of the controls by delta delta Ct (ΔΔCt) method.

Results:

Identification of novel transcript variants of porcine LXRα and LXRβ

Total eight novel LXRα transcript variants (LXRα-2-9) were detected in different porcine tissues (Figure 3.2). LXRα-1 (wild type) transcript consists of 10 exons which code for 447 amino acids. In most of the identified novel transcript variants, one or more than one exons were missing leading to truncated amino acids (Figure 3.2, Figure 3.3 and Table 3.4). LXRα-2 had a shorter 5' UTR. LXRα-3 had deleted exon 6 during splicing. LXRα-4 had missing exons 5, 6 and 7. LXRα-5 deleted a part of exon 6. Exons 3 and 4 were missing in LXRα-6, whereas exon 4 was missing in LXRα-7. LXRα-8 had deleted exon 9. LXRα-9 used an alternative promoter, so N-terminal 141 amino acids were deleted. The expression profiles of the different variants are indicated in Figure 3.2. LXRα-1 and LXRα-5 were detected in all the tissues screened. LXRα-2 and LXRα-3 were detected in liver, kidney, small intestine and spleen. LXRα-4 was detected in liver and kidney, LXRα-6 was detected in kidney and lung, LXRα-8 was detected in liver and small intestine. LXRα-6 was detected in only kidney and LXRα-9 was detected in only lung. The physiochemical

properties of the deduced amino acids of the transcript variants of LXRα are presented in Table 3.4.

Similarly, eight novel transcript variants of LXRβ (LXRβ-2-9) were detected (Figure 3.4). LXRβ-1 (wild type) consists of 10 exons which codes for 458 amino acids. The identified splice variants code for truncated amino acids except LXRβ-3 which codes for 468 amino acids (Table 3.5). LXRβ-2 had a shorter 3' UTR. LXRβ-3 had a 30 nucleotide insert between exon 4 and 5. LXRβ-4 had deleted exon 4, whereas LXRβ-5 had deleted exon 5. LXRβ-6 used an alternative promoter, so N-terminal 79 amino acids were missing. LXRβ-7 had deleted part of exon 10 and LXRβ-8 had deleted exon 7, 8, 9 and part of exon 10. LXRB9 had missing 223 amino acids from N-terminal. The expression of the different variants are indicated in the Figure 3.4. The wild type was detected in all the tissues screened. LXRβ-2 was detected in liver, small intestine, pancreas and brain. LXRβ-3 and LXRβ-9 were detected only in kidney. LXRβ-4 was detected in liver, kidney, heart and brain. LXRβ-5 was detected in kidney, lung, spleen and brain. LXRβ-6 was detected only in liver. LXRβ-7 was detected in liver and pancreas. LXRβ-8 was detected in liver, small intestine and brain. The physiochemical properties of the deduced amino acids of the transcript variants of LXRβ are presented in Table 3.5.

Reduced binding affinity of the novel transcript variants of porcine LXRα and LXRβ towards ligand T0901317 compared to the wild type proteins

In the absence of crystal structures for porcine LXRα and LXRβ, we opted to develop homology models (Figure 3.5 & Figure 3.6). The molecular interactions of LXRα transcript variants with synthetic ligand T0901317 are presented in Figure 3.7

and Figure 3.8. The binding affinity, interacting amino acids in LBD, and hydrogen bond distance of different LXRα transcript variants with T0901317 is presented in Table 3.5. The results showed that the wild type protein LXRα-1 has the highest binding affinity (Glide score of -5.11 Kcal/mol). The other transcript variants had reduced binding affinity for the synthetic ligand. LXRα-8 showed lowest binding affinity (Glide score of -2.14 Kcal/mol). The three dimensional conformations of the novel splice variant proteins have been changed due to splicing. The disturbed 3-D conformation may be the reason behind reduced binding affinity towards its ligand.

Similarly, the docked conformations of LXRβ transcript variants with synthetic ligand is presented in Figure 3.10 and Figure 3.11. The binding affinity, interacting amino acids in LBD, and hydrogen bond distance of different LXRβ transcript variants with T0901317 is presented in Table 3.7. The results showed that the wild type protein LXRβ-1 had highest affinity energy -5.50 kcal/mol towards T0901317. The other splice variants had reduced affinity for the synthetic ligand. The splice variants LXRβ-3, LXRβ-7, LXRβ-8 and LXRβ-9 showed low binding affinity.

T0901317 and GW3965 modulates the expression of LXRs and their downstream target genes in porcine primary hepatocytes

T0901317 [28] and GW3965 [26] are effective, synthetic, non-steroidal agonists of LXRs and are the most commonly used agonists for investigating the physiological role of LXRs. Both the ligands upregulated LXRs transcripts in porcine primary hepatocytes (Figure 3.12).

SREBP1 and FASN are two well documented downstream target gene of LXRs [29]. Upon T0901317 and GW3965 treatment, expressions of LXR target genes SREBP-1 and FASN were up-regulated on a dose dependent manner in primary porcine hepatocytes (Figure 3.13).

Liver X receptor agonists modulate the expression of genes involved in xenobiotic metabolism in porcine primary hepatocytes

To gain understanding how LXRs are involved in the xenobiotic metabolism pathways, we induced LXRs by addition of synthetic ligands and studied the expressions of the most important genes involved in xenobiotic metabolism and its regulation. We treated primary hepatocytes with T0901317 and GW3965 to activate LXRs and studied the expression of phase-I, phase-II drug metabolism genes and phase-III transporters to understand the involvement of LXRs in xenobiotic metabolism pathways. Treatment of both T0901317 and GW3965 caused a significant increase of CYP2B22, CYP2C42, CYP3A and CYP7A1; all the other CYPs remain unchanged (Figure 3.14). T0901317 caused higher fold changes than GW3965. Phase II drug metabolism genes remained unchanged. All the three nuclear receptors studied (ABCB1, ABCC2, ABCG1 and ABCG2) were upregulated (Figure 3.14). From the results of the study, it can be concluded that activated LXRs induce the expression of CYP2B22, CYP2C42, CYP3A and CYP7A1 and the transporters (ABCB1, ABCC2, ABCG1 and ABCG2).

Discussion

Nuclear receptors are master regulators of a wide variety of metabolism including endogenous metabolites and exogenous xenobiotics that integrate the homeostatic control of almost all biological processes [13]. Nuclear receptors regulate transcription through the recruitment of coactivator proteins to the ligand binding domain (LBD) [30]. The liver X receptors, LXR alpha (NR1H3) and LXR beta (NR1H2) are transcription factors belonging to the nuclear receptor superfamily that function as intracellular receptors for cholesterol metabolites, different endogenous metabolites and xenobiotics [7,12,31]. The LXRs form heterodimers with the retinoid X receptor to regulate the important aspects of homeostasis through their target genes [32–34]. In the present study, eight novel splice variants of both LXRα and LXRβ were identified. The splice variants had truncated amino acids in the protein sequences (Table 3.4 and Table 3.5). In human, three novel LXRα isoforms were reported by Chen et al., 2005 [35] and another two novel LXR α isoforms were reported by Endo-Umeda et al., 2012 [36]. LXRα2 lacks the N-terminal 45 amino acids of LXRα1 and LXRα3 lacks 50 amino acids in the ligand binding domain [35]. LXRα3 mRNA is generated by removal of exon 6 through alternative splicing [35]. No information of LXRβ isoforms in human is available.

Synthetic nonsterol LXR agonists have been identified, including T0901317 [26], a lipophilic tertiary sulfonamide that contains an acidic bis-trifluoromethyl carbinal group. Structural and biochemical studies reveal that the coactivator contains a short alpha helical sequence known as NR box that binds the nuclear receptor LBD. The NR box is capped by a charge clamp on the surfaceof the LBD formed by a lysine

on helix 3 and a glutamic acid on the C-terminal AF2 helix [37]. The molecular modeling of porcine LXRα and LXRβ with synthetic ligand T0901317 shows that Trp-443 and Trp-457 play a significant role in ligand binding respectively (Figure 3.10). Crystal structure of human LXRβ also reveals that the residue is Trp-457 and His-435 is important for ligand activation [39]. The X-ray three dimentional structure of the human LXRβ showed that the ligand binding pocket of LXRβ is a large hydrophobic cavity that is surrounded by H3, H5, H6, H7, H11 and H12 [3]. In human homology model of LXRα indicated that Trp-443 plays a role in the activation of the receptor [38]. Agonists bind to LXRα in an orientation that generates a hydrogen bond between the ligand and Trp^{443} [38]. Similar findings are observed in the molecular modeling studies with porcine LXRα and T0901317 (Figure 3.8).

To gain understanding how LXRs are involved in the xenobiotic metabolism pathways, we induced LXRs by addition of synthetic ligands and studied the expressions of the most important genes involved in xenobiotic metabolism and its regulation. Treatment of both T0901317 and GW3965 caused a significant increase of CYP2B22, CYP2C42, CYP3A and CYP7A1 (Figure 3.14). In case of human, regulation of CYP3A , CYP 2B 6 and CYP7A1 by LXR has been reported [40].

Figures and Tables

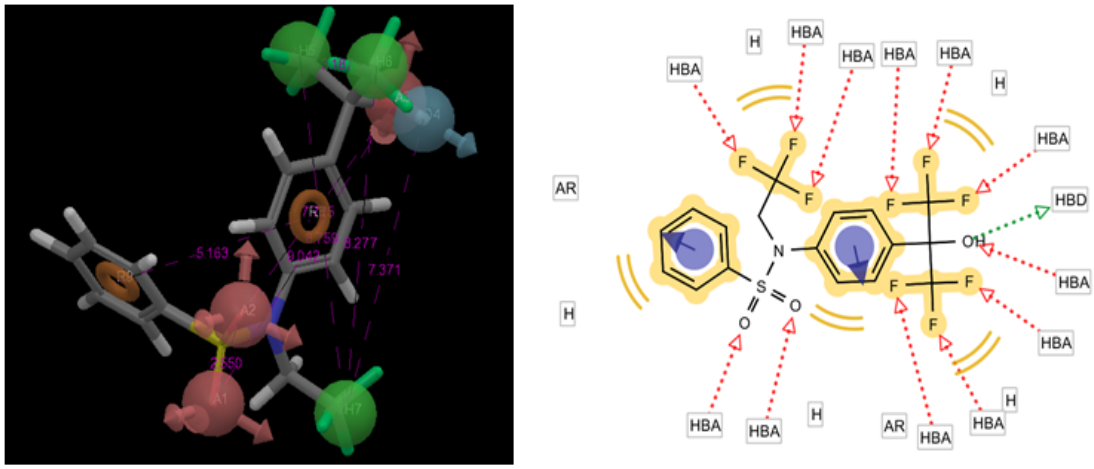

Figure 3.1. Pharmacophore sites of T0901317

HBA denotes hydrogen bond acceptor, HBD denotes hydrogen bond donor, H denotes hydrophobic group and AR denotes aromatic ring.

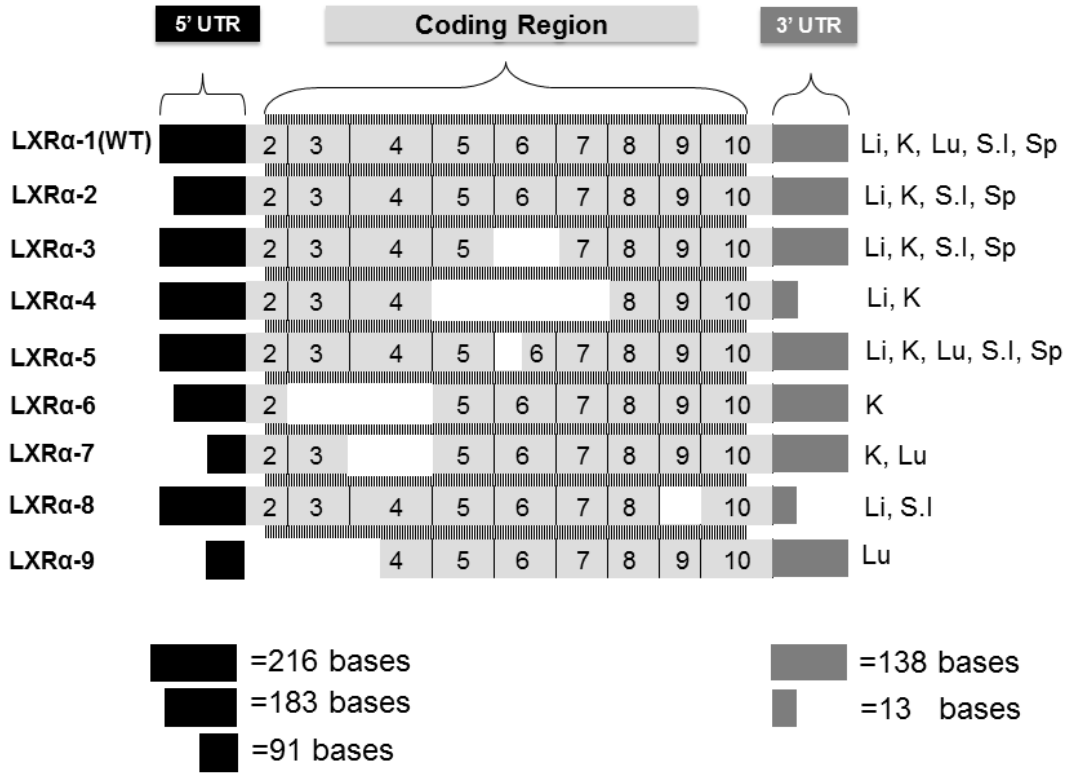

Figure 3.2. Identified transcript variants of LXRα

The tissue distribution of the splice variants are indicated in the right side.

Li, Liver; K, Kidney; Lu, Lung; S.I, Small Intestine, Sp: Spleen

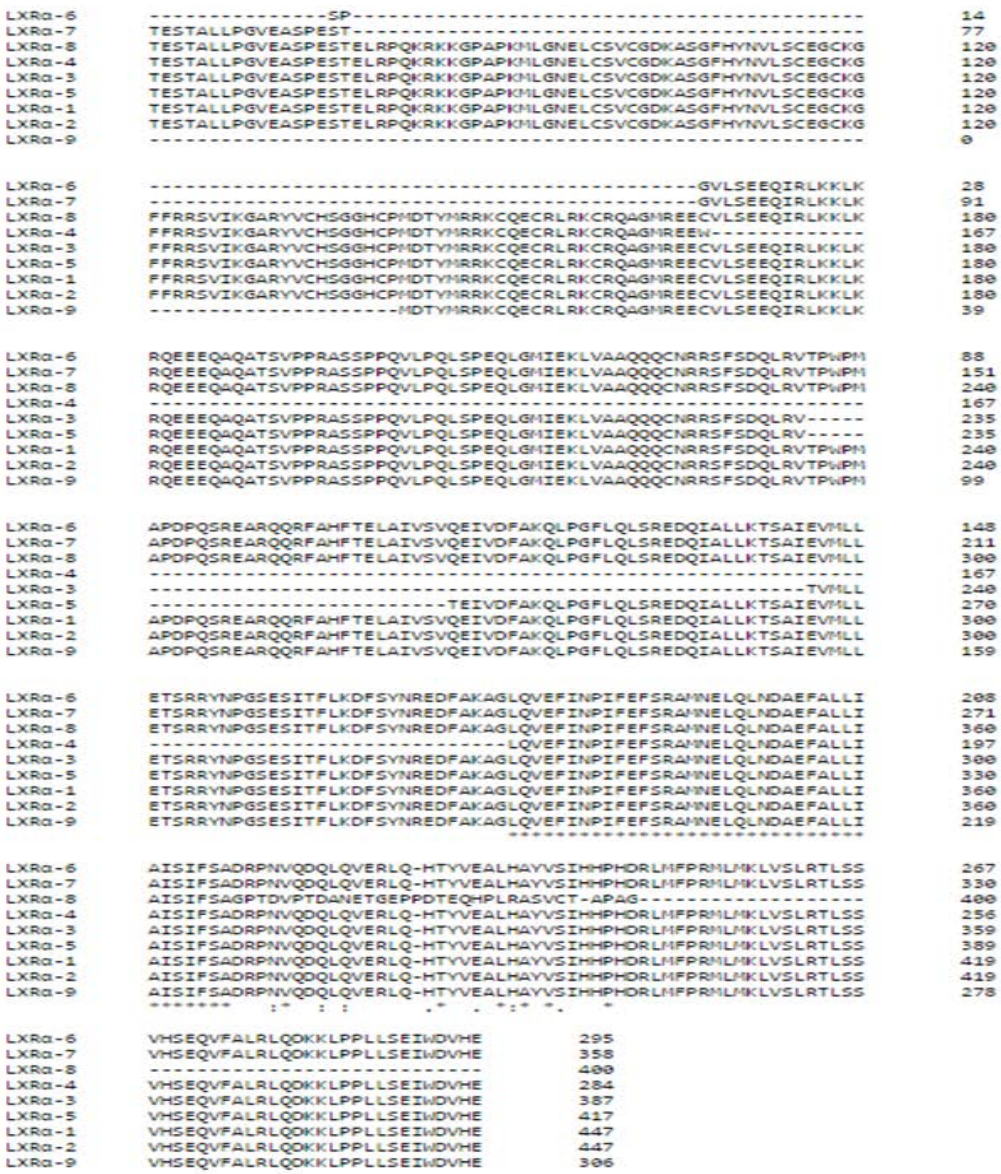

Figure 3.3. Multiple sequence alignment of LXRα transcript variants

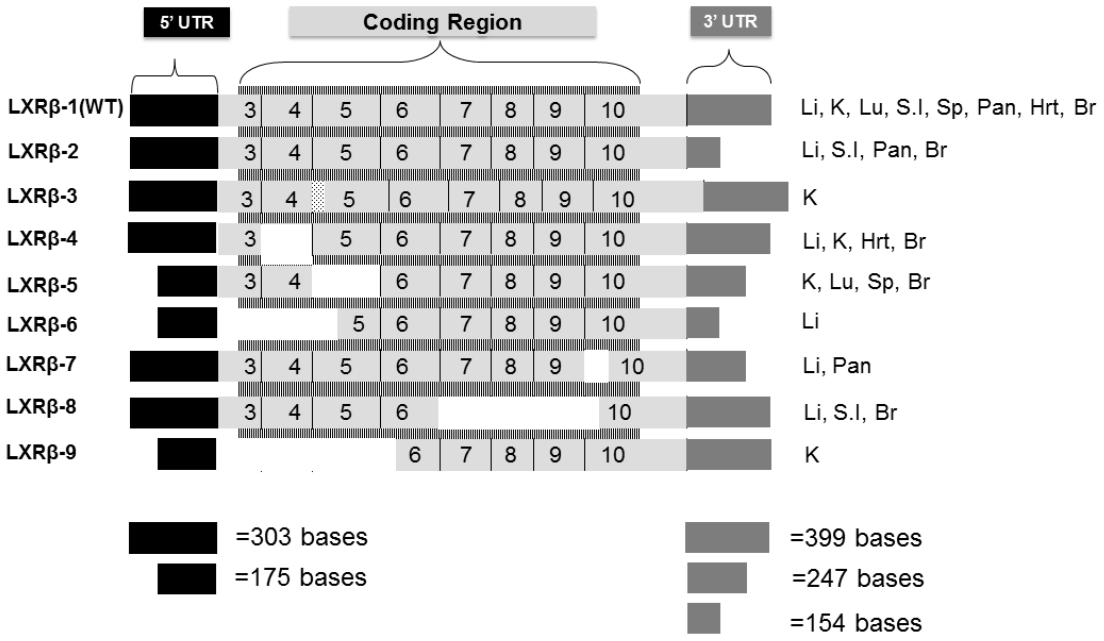

Figure 3.4. Identified transcript variants of LXRβ

The tissue distribution of the splice variants are indicated in the right side.

Li, Liver; K, Kidney; Lu, Lung; SI, Small Intestine; Sp, Spleen; Pan, Pancreas; Hrt, Heart; Br, Brain

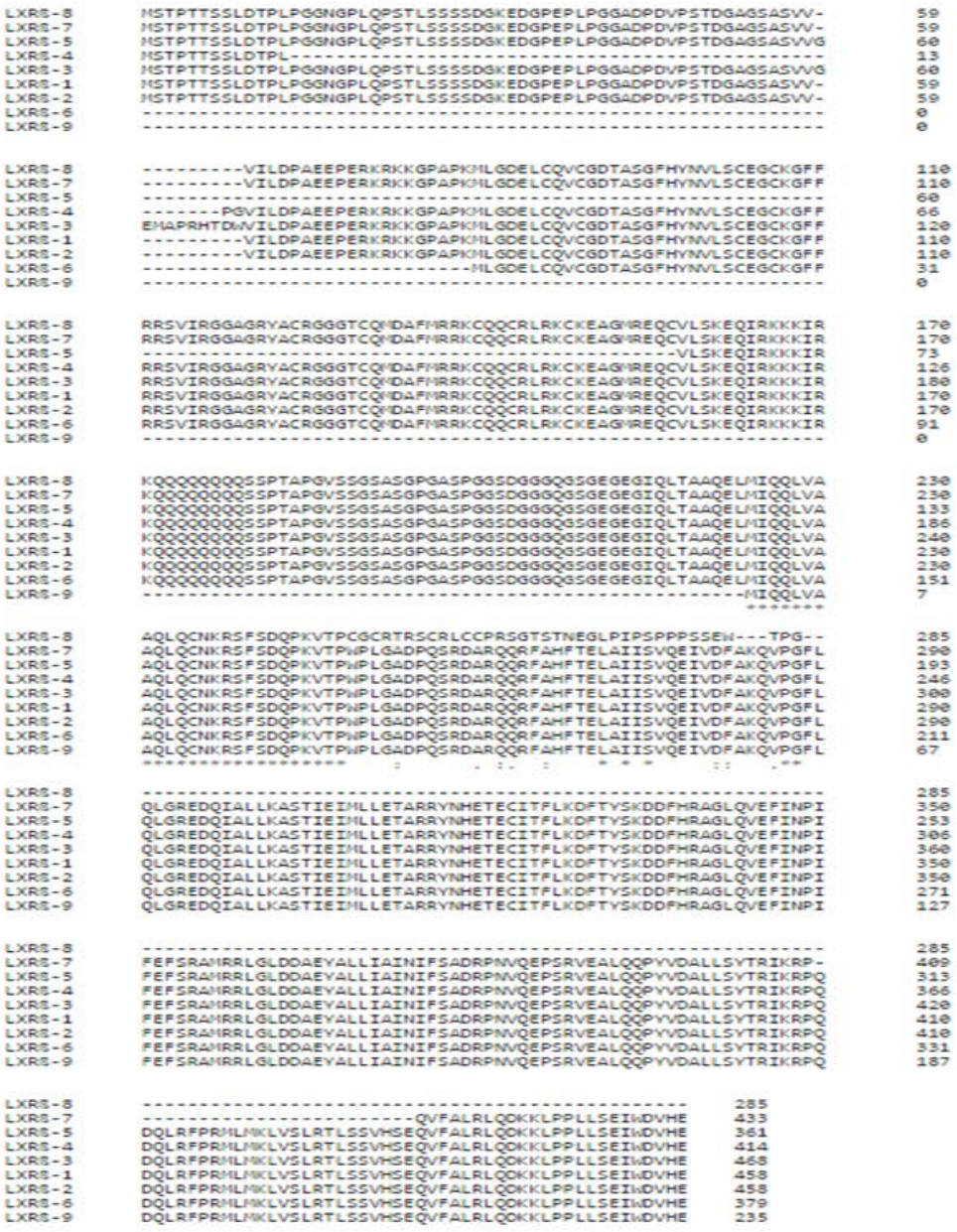

Figure 3.5. Multiple sequence alignment of LXRβ transcript variants

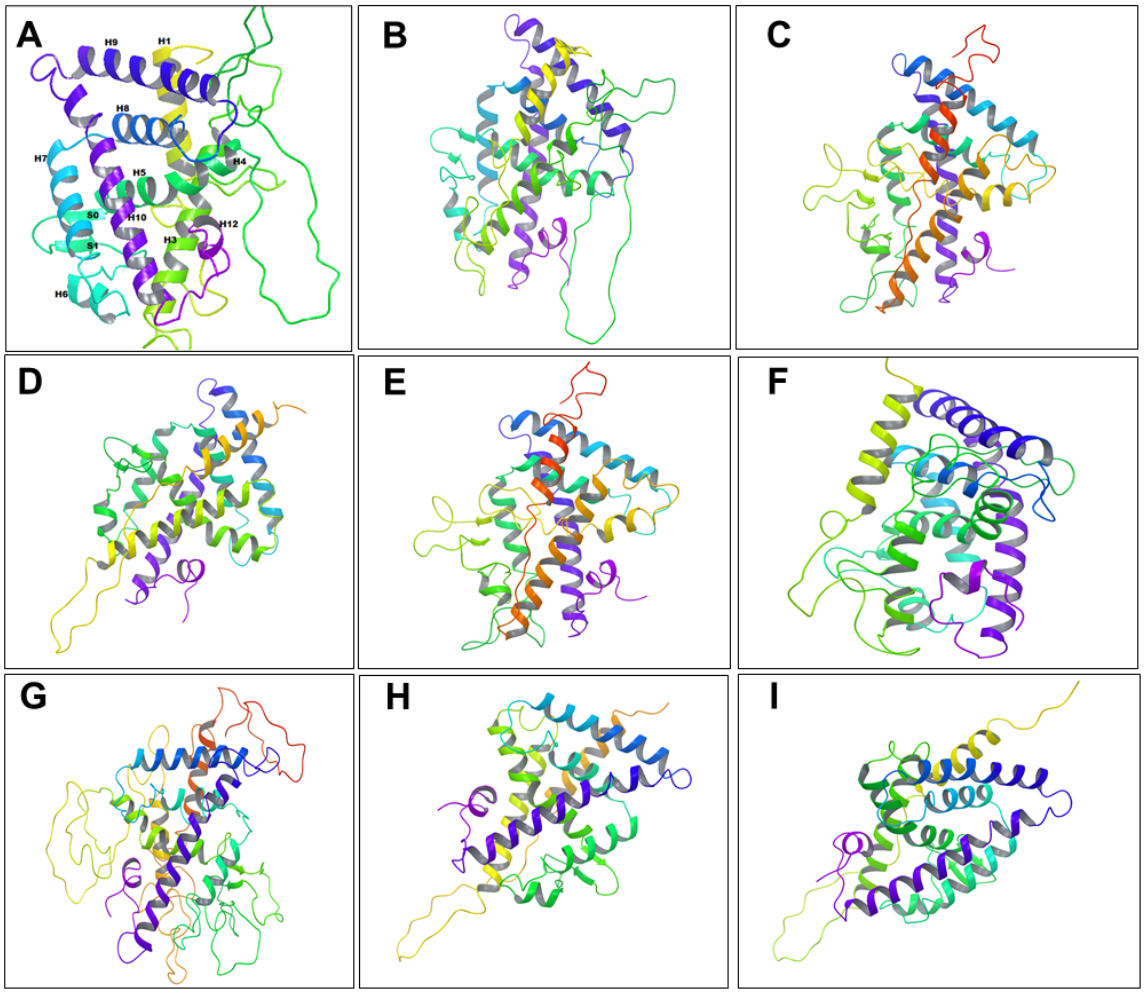

Figure 3.6. Homology modeled LXRα transcript variants

A, LXRα-1; B, LXRα-2; C, LXRα-3; D, LXRα-4; E, LXRα-5; F, LXRα-6; G, LXRα-7; H, LXRα-8; I, LXRα-9

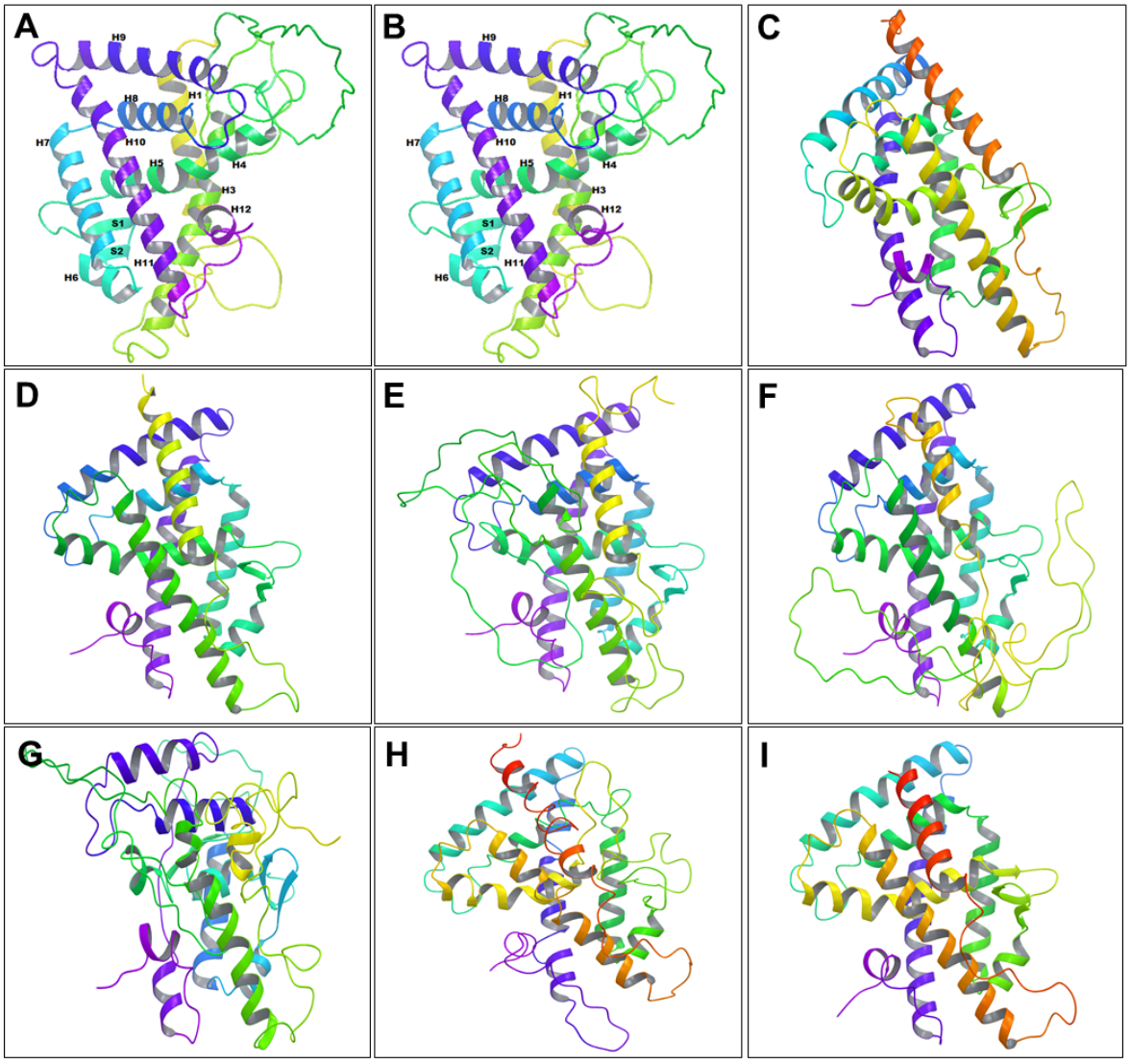

Figure 3.7. Homology modeled LXRβ transcript variants

A, LXRβ-1; B, LXRβ-2; C, LXRβ-3; D, LXRβ-4; E, LXRβ-5; F, LXRβ-6; G, LXRβ-7; H, LXRβ-8; I, LXRβ-9

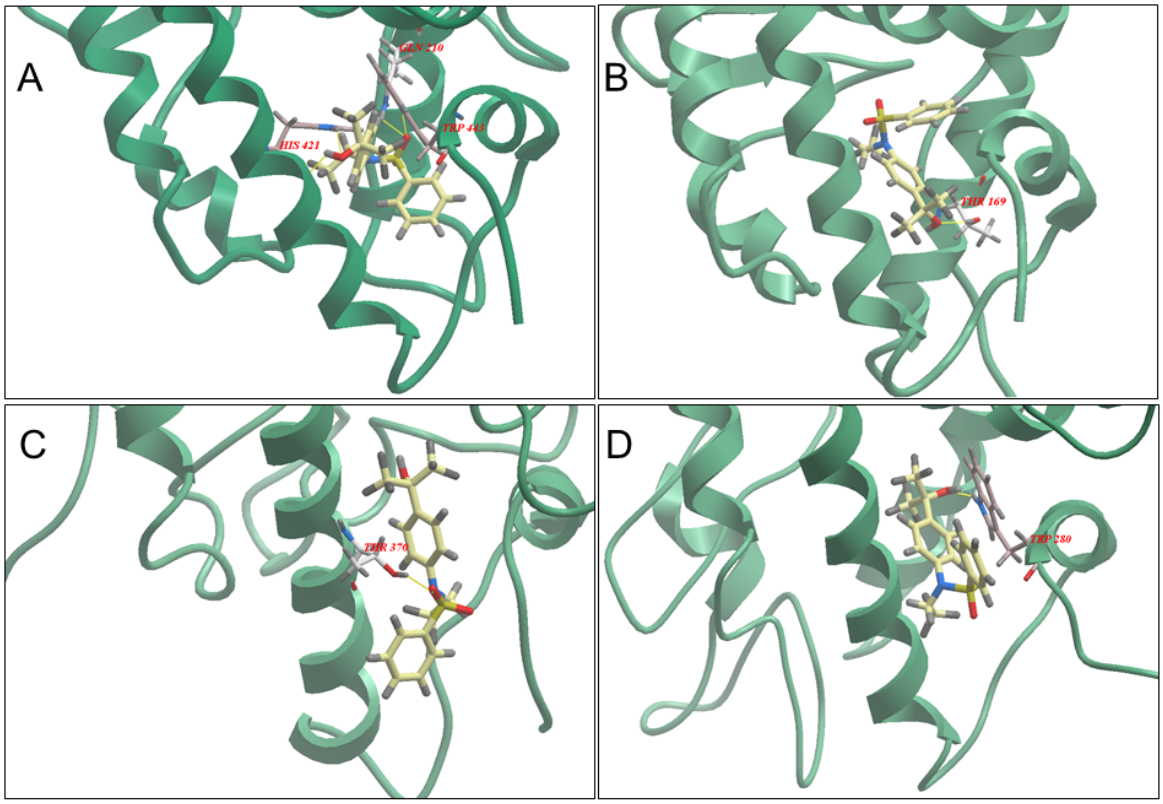

Figure 3.8. Molecular modeling interactions of LXRα transcript variants with its synthetic ligand T0901317

A. Wild type (LXRα-1); B, LXRα-7; C, LXRα-8; D, LXRα-9

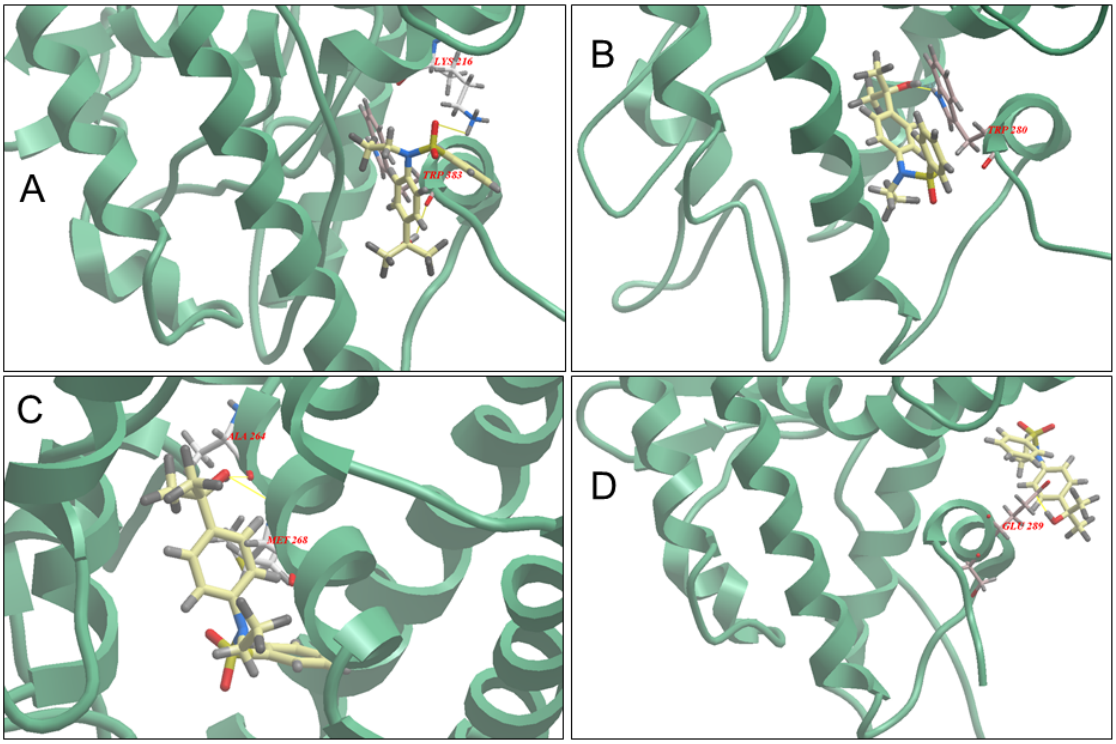

Figure 3.9. Molecular modeling interactions of LXRα transcript variants with its synthetic ligand T0901317

A, LXRα-2B; B, LXRα-3; C, LXRα-5; D, LXRα-6

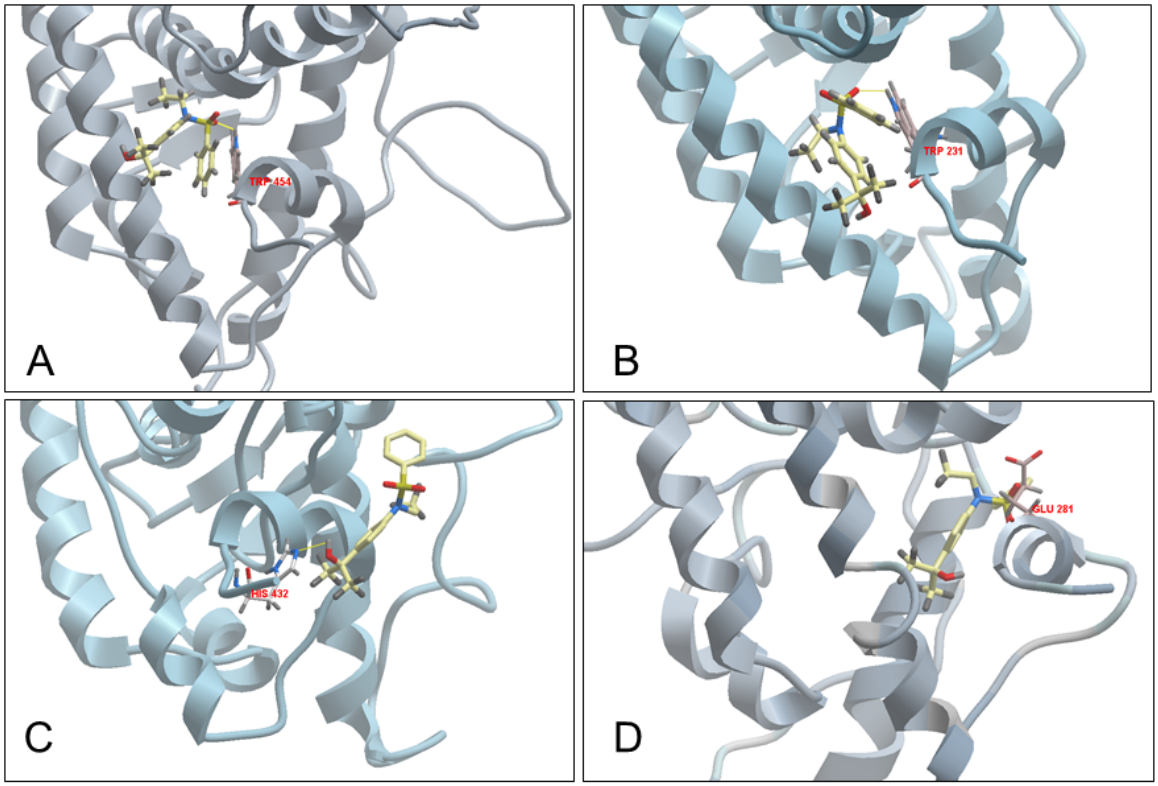

Figure 3.10. Molecular modeling interactions of LXRα transcript variants with its synthetic ligand T0901317

A, Wild type (LXRβ-1); B, LXRβ-9; C, LXRβ-7; D, LXRβ-8

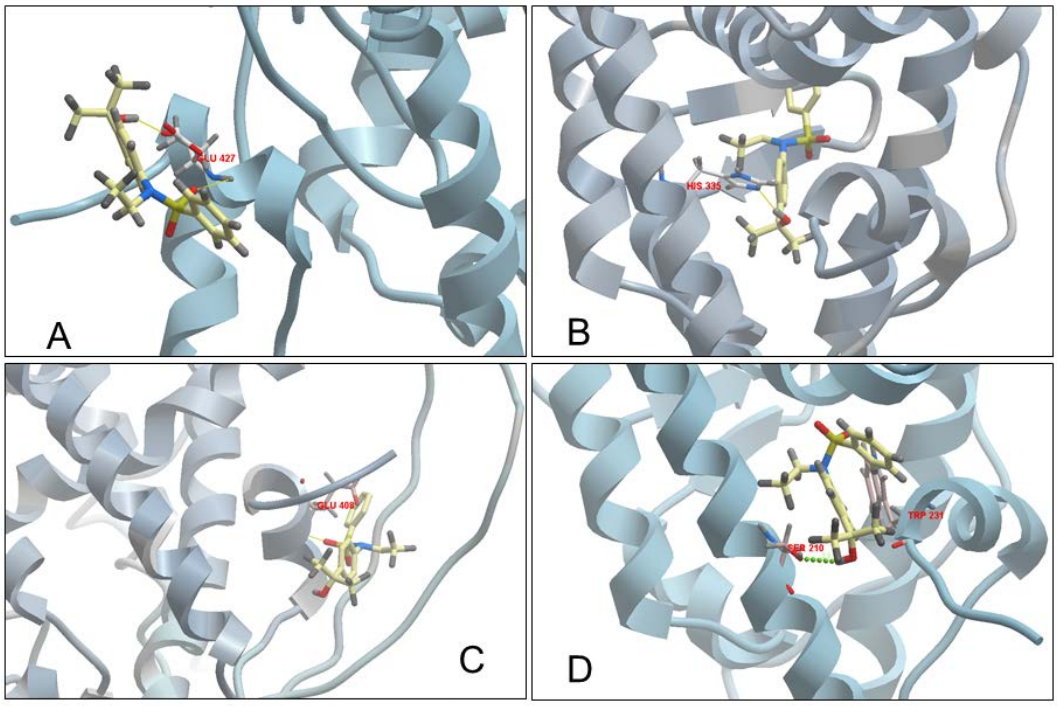

Figure 3.11. Molecular modeling interactions of LXRα transcript variants with its synthetic ligand T0901317

A, LXRβ-2; B, LXRβ-3; C, LXRβ-4; D, LXRβ-5

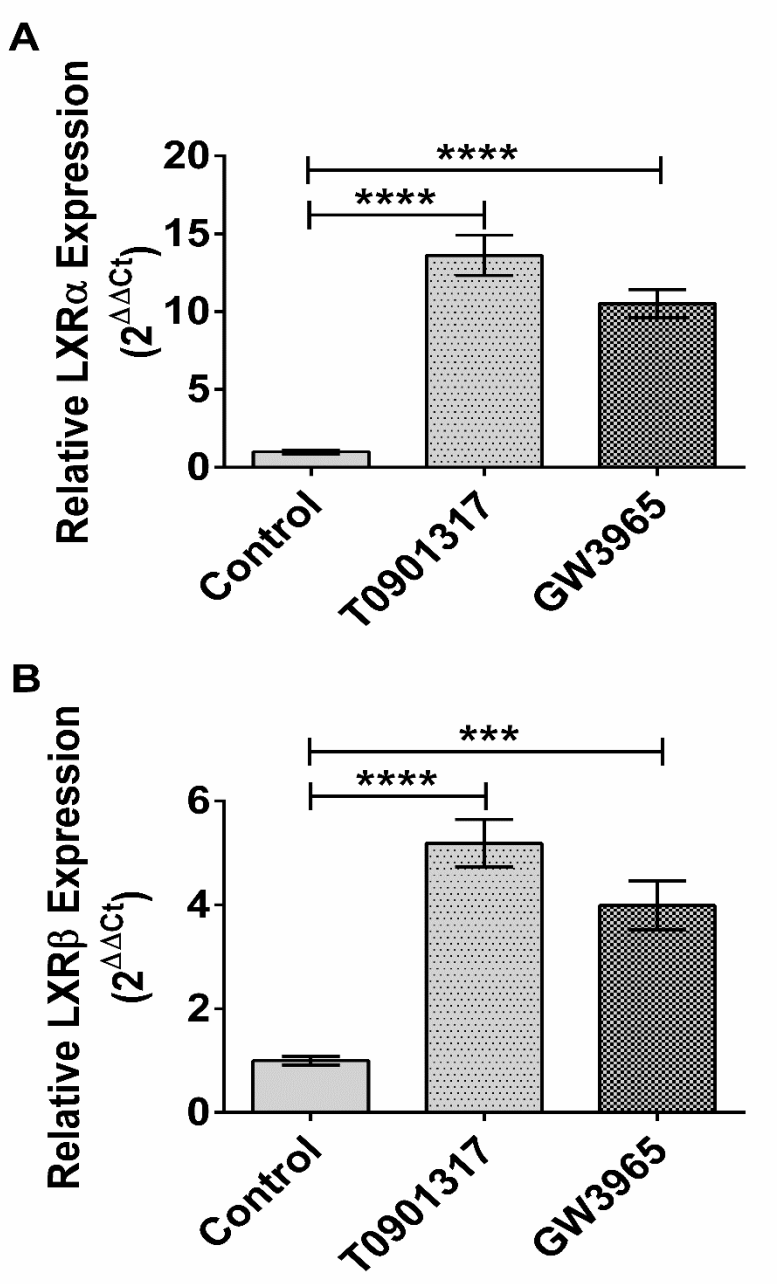

Figure 3.12. Effect of T0901317 and GW3965 on expression of LXRα and LXRβ transcripts in primary porcine hepatocytes

Real time RT-PCR was performed to analyze the effect of LXR ligands T0901317 and GW3965 (10 μM) on expression of LXRα and LXRβ transcripts in primary hepatocytes. The values and error bars represent average and standard deviations of three independent set of experiments. One-way analysis of variance (ANOVA) followed by Dunnett post-test was performed to find out significant difference among control and treatments. *** denotes $p \leq 0.001$; **** denotes $p \leq 0.0001$.

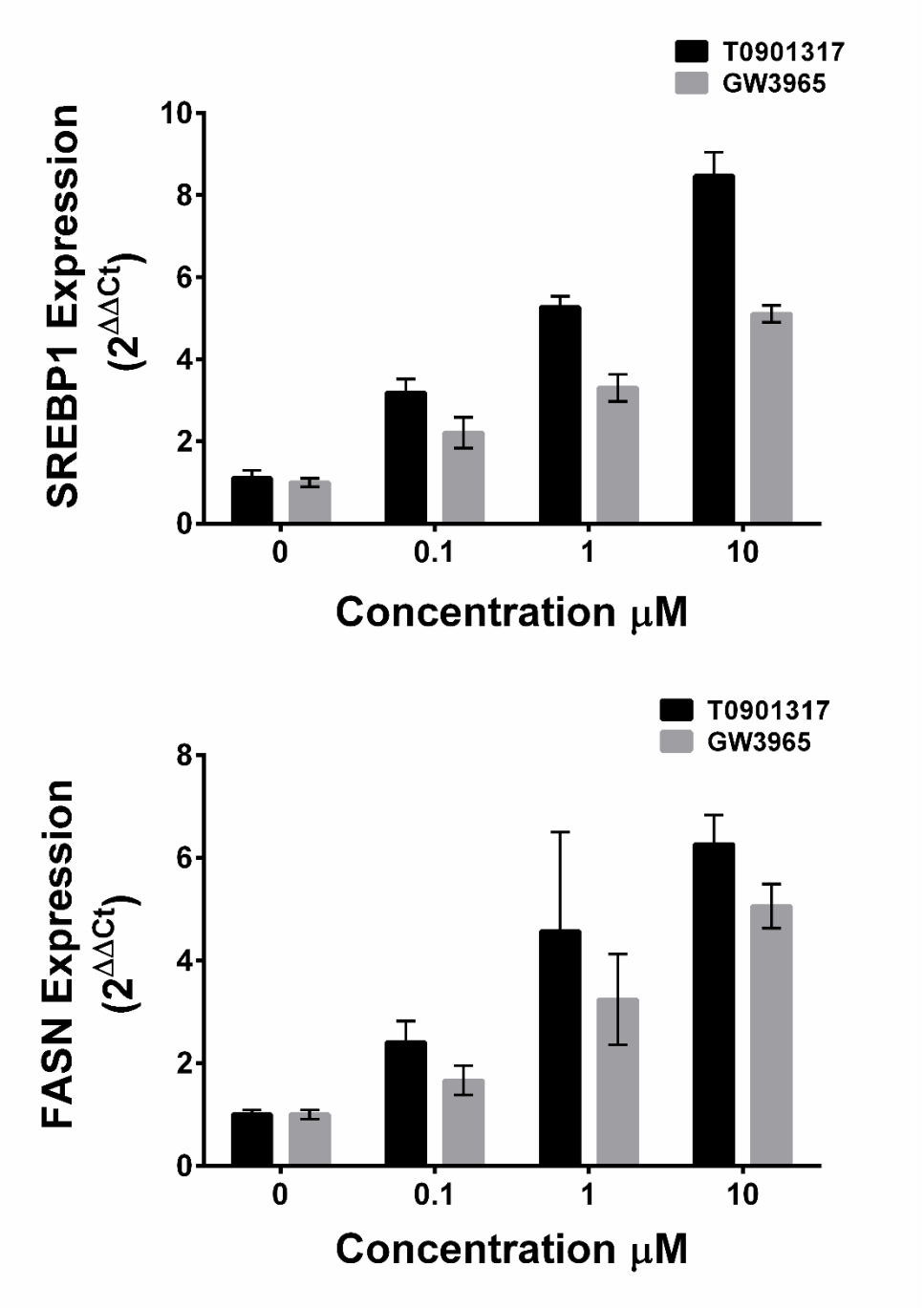

Figure 3.13. Effect of T0901317 and GW3965 on expression of LXR target genes SREBP1 and FASN transcripts

Real time RT-PCR was performed to analyze the effect of LXR ligands T0901317 and GW3965 on expression of two downstream target genes of LXR, SREBP1 and FASN. The values and error bars represent average and standard deviations of three independent set of experiments.

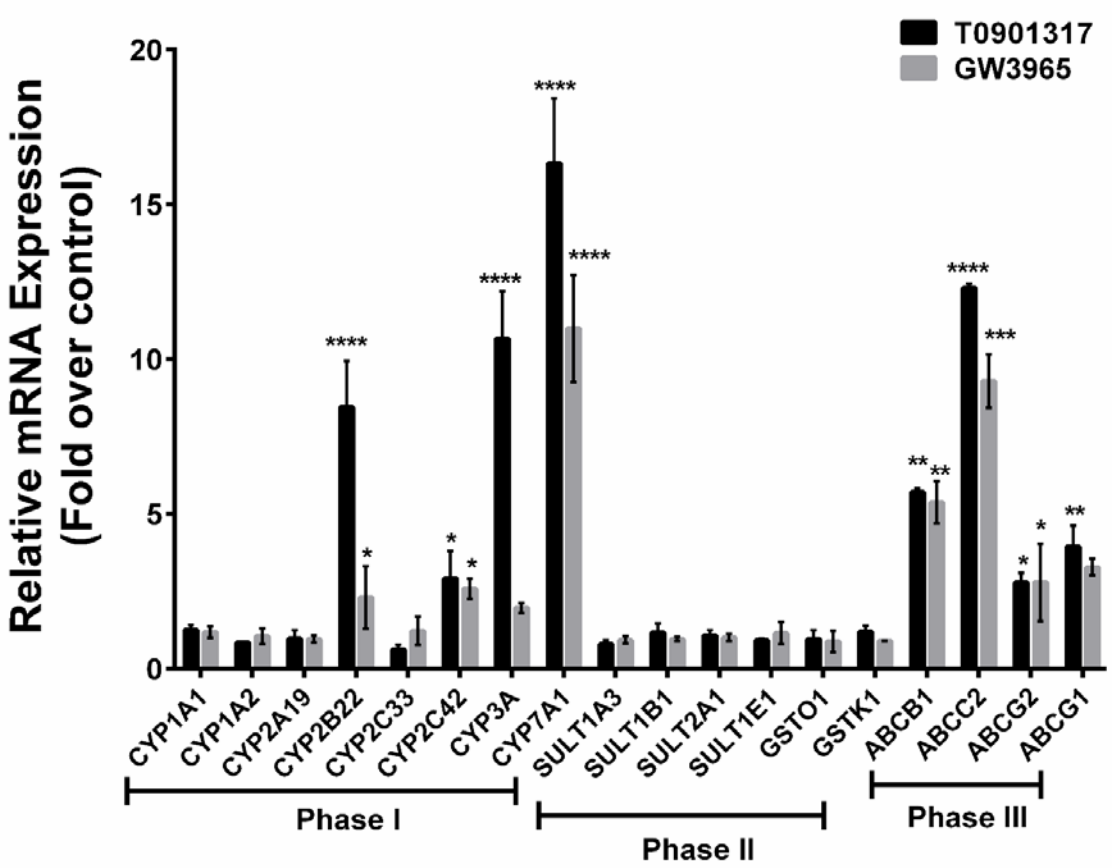

Figure 3.14. Effect of T0901317 and GW3965 on expression of phase-I, phase-II and Phase-II DME transcripts

Real time RT-PCR was performed to analyze the effect of LXR ligands T0901317 and GW3965 (10 µM) on expression of the most important genes involved in regulation of drug metabolism. The values and error bars represent average and standard deviations of three independent set of experiments. One-way analysis of variance (ANOVA) followed by Dunnett post-test was performed to find out significant difference among control and treatments. * denotes p≤0.05; ** denotes p≤0.01; *** denotes p≤0.001; **** denotes p≤0.0001.

Table 3.1

Cloning Primers	
LXRα Forward	GCTCGGACAGTCCCTTGGTA
LXRα Reverse	AGTCACGCCTCAGCCATCTA
LXRβ Forward	CCACTGGTGTTCGGAGAGG
LXRβ Reverse	CCCAGATCTCGGACAGCAAA
CAR Forward	TGAAGGCCACAGAGGTAGAAGTTCCTTG
CAR Reverse	AGCAGCGGCATCATGGTGGACAGTCC
RACE Primers	
3'RACE-outer	Supplied with kit
LXRα- 3'-outer	GAGTTTGCCCTGCTCATTGC
LXRβ- 3'-outer	TGCTTTCCTACACCCGCATC
CAR 3' OUTER	TAAGACACTTCGGCGACTGC
3'RACE-inner	Supplied with kit
LXRα -3'-inner	CTGCATGCCTACGTCTCCA
LXRβ-3'-inner	CACTCCGAGCAGGTCTTCG
CAR 3' INNER	TCTCCGGGACAGGTTTCTCT
5'RACE-outer	Supplied with kit
LXRα -5'-outer	TGCTTGCATCTTGTGCATCTGA
LXRβ -5'-outer	TCCATCGGATGAAGACGACAGA
CAR 5' OUTER	CTTGCAGCCCTCACAAGTCAAG
5'RACE-inner	Supplied with kit
LXRα -5'-inner	TCTCTTCCTGGAGCCCTGGACATT
LXRβ -5'-inner	TTGTGGGGGTCTCCTACTTTTGTTGC
CAR5' INNER	CCGCACACAGCACAGTTCCTTG

Table 3.1. Primer sequences for LXRs cloning and RACE

Table 3.2

Genes	Primers	Sequences (5'-3')
GAPDH	Forward	GGCAAATTCCACGGCACAGTCA
	Reverse	CTGGCTCCTGGAAGATGGTGAT
ACTB	Forward	GCAAATGCTTCTAGGCGGACTGT
	Reverse	CCAAATAAAGCCATGCCAATCTCA
Porcine Albumin	Forward	TGGTGACTTGGCTGACTGCTG
	Reverse	TGTCGGGGTTATCATTTTTGTGTTG
HNF4A	Forward	AGTCCCAGAGTGGTAGTGGAAAG
	Reverse	CAGATGGTGAAGGGTGGCATTG
G6PC	Forward	ATTGAAAGACGATGACTGTGCCAA
	Reverse	CAAAGGAGGAAGGAGTTCTGAGC
CYP1A1	Forward	AAGAGGCAGAGGTGAAGTGGTGAA
	Reverse	GAGAAGAAGGAAGGCAGTGAAGTGATAG
CYP1A2	Forward	ACACCTTCTCCATTGCCTCAGACC
	Reverse	GCACTCAGCCTCCTTGCTCAC
CYP2A19	Forward	CCGAAGAGTCACCAAGGATACCAAG
	Reverse	ACAGAGCCCAGCATAGGGAACA
CYP2B22	Forward	CAGATGAGTAAACAGAGCCCGAGAA
	Reverse	CGAGAGCCAAGGAGACAGCA
CYP2C33	Forward	TGGAAGAAAAATCACAAGAGGAGAAGG
	Reverse	TTGGAAAGAGACGCAGGGATGT
CYP2C42	Forward	TACAGAGACAACAAGCACCACCA
	Reverse	CTGCCAATCACACGGTCAATC
CYP2C49	Forward	CTTGTGGAGGAGTTGAGAAAAACC
	Reverse	TTGTGGAAAATGATGGAGCAGA
CYP2E1	Forward	ACACCCTGCTGATGGAAATGGA
	Reverse	GTGGTCTCTGTCCCCGCAAA
CYP3A	Forward	TACCTGCCCTTTGGGACTGGAC
	Reverse	AGTTCTGCAGGACTCTGACGA
CYP7A1	Forward	TTCTGCTACCGAGTGATGTTTGAGG
	Reverse	AGGTTGTTTAGGATGAGTGCTTTCTGTG
SULT1A3	Forward	GACCACAGCATCTCAGCCTTCAT
	Reverse	CTGCCATCTTCTCAGCATAGTCG
SULT2A1	Forward	AAATGCTGCAAGAGGTGAGGGAGG
	Reverse	ATCCCCCTTGGAGAGAATCAGGCA
SULT1E1	Forward	GAGAAAGGGGATTGCAGGAGACTG
	Reverse	GTAGACCCCTTCATTTGCTGCTCA
GSTO1	Forward	GAGATTCTGTCCTTTCGCCCAGAG
	Reverse	GATGACTTGATGCCGGATTCCCTT
GSTK1	Forward	GGTACACCATCCACCGTTAGTCTC
	Reverse	CACACAAACACCAGCAAAGACACA
ABCB1	Forward	TGGCAGTGGGACAGGTTAGTTC
	Reverse	CACGGTGCTTGAGCTGTCAATC
ABCB6	Forward	TGTTGTCCCAAGGTGGTGTGTATG
	Reverse	GCTGAAATGGATTTCCCTCCAGGT
ABCC2	Forward	GTGGCTGTTGAGCGAATAAATGAATAC
	Reverse	TGCTGGGCCAACCGTCTG

Table 3.2 (cont.)

Gene Name	Primers	Sequences (5'-3')
ABCC3	Forward	TGATGCAGACGCTGATCTTACACC
	Reverse	ACTCACGTTTGACGGAATTGGTGA
ABCG2	Forward	GATCTTTTCGGGGCTGTTCCTCA
	Reverse	TGAGTCCCGGGCAGAAGTTTTGT
PXR	Forward	GACAACAGTGGGAAAGAGAT
	Reverse	CCCTGAAGTAGGAGATGACT
FXR	Forward	CATTCAACCATCACCACGCAGAGA
	Reverse	GCACATCCCAGACTTCACAGAGA
CAR	Forward	GAAAGCAGGGTTACAGTGGGAGTA
	Reverse	CTTCAGGTGTTGGGATGGTGGTC
LXRA	Forward	TCCAGGTAGAGAGGCTGCAACATA
	Reverse	AGTTTCATTAGCATCCGTGGGAAC
LXRB	Forward	GAGTCTTCCTGAGAGGGGCAGATA
	Reverse	CGTGGTAGGCTTGAGGTGTAAGC
PPARA	Forward	AATAACCCGCCTTTCGTCATACAC
	Reverse	GACCTCCGCCTCCTTGTTCT
PPARG	Forward	CCATGCTGTCATGGGTGAAACTCT
	Reverse	GTCAACCATGGTCACCTCTTGTGA
RXRA	Forward	CCTTCTCGCACCGCTCCATA
	Reverse	CGTCAGCACCCTGTCAAAGATG
RXRG	Forward	CTTCCCGTTCCCCAAACGTGAT
	Reverse	CTTCCAGAAAAGATCCCCAGTCCC
SREBP-1	Forward	ATCGACTACATCCGCTTCCTTCAG
	Reverse	TCCTTCAGAGACTTGCTTTTGTGG
FASN	Forward	AGCTACTGGAGGGGCTATTGCAT
	Reverse	CTGCTTACACTCTTCCCAGGACAA

Table 3.2. Primer sequences for real-time PCR

Table 3.3

S.No	Name	Unit
1	Molecular Weight	481.332709 g/mol
2	Molecular Formula	$C_{17}H_{12}F_9NO_3S$
3	XLogP3	4.9
4	Hydrogen Bond Donor Count	1
5	Hydrogen Bond Acceptor Count	13
6	Rotatable Bond Count	5
7	Exact Mass	481.039418 g/mol
8	Monoisotopic Mass	481.039418 g/mol
9	Heavy Atom Count	31
10	Potential Energy OPLS-2005	123.298

Table 3.3: The Chemical properties of T0901317

Table 3.4

LXRα transcript variants	Amino acid length	MW (kDa)	Isoelectric Point	Ramachandran plot (allowed regions %)
LXRα-1	447	50.328	6.73	89%
LXRα-2	447	50.328	6.73	89%
LXRα-3	387	43.497	7.01	87%
LXRα-4	284	31.846	6.66	88%
LXRα-5	417	46.852	6.67	87%
LXRα-6	295	33.847	5.88	87%
LXRα-7	358	40.142	4.74	87%
LXRα-8	400	44.142	5.23	89%
LXRα-9	306	35.545	7.22	87%

Table 3.4. Properties of deduced LXRα transcript variant proteins

Table 3.5

LXRβ transcript variants	AA length	MW (kDa)	Isoelectric Point	Ramachandran plot (allowed regions %)
LXRβ-1	458	50.283	8.00	86
LXRβ-2	458	50.283	8.00	86
LXRβ-3	468	51.464	7.83	87
LXRβ-4	414	46.194	8.78	88
LXRβ-5	361	39.433	5.47	87
LXRβ-6	379	42.467	8.66	89
LXRβ-7	433	47.329	7.58	88
LXRβ-8	285	29.745	8.44	88
LXRβ-9	235	27.242	7.06	87

Table 3.5. Properties of deduced LXRβ transcript variant proteins

Table 3.6

LXRα transcript variants	GScore (Kcal/mol)	Interacting AAs	Interaction Atoms	HB-distance (Å)
LXRα-1	-5.11	TRP433 GLN210 HIS421	(H…N) (H…N) (H…O)	1.94 2.81 2.99
LXRα-2	-5.11	TRP433 GLN210 HIS421	(H…N) (H…N) (H…O)	1.94 2.81 2.99
LXRα-3	-4.01	TRP383 LYS216	(H…O) (N…O)	2.16 2.72
LXRα-4	-4.03	TRP280	(N…O)	2.83
LXRα-5	-3.20	MET268 ALA264	(N…O) (O…H)	2.72 2.86
LXRα-6	-3.50	GLU289	(O…H)	2.32
LXRα-7	-3.20	THR169	(O…H)	2.84
LXRα-8	-2.14	THR370	(O…H)	3.58
LXRα-9	-3.09	HIS280	(N…O)	2.78

Table 3.6. Binding affinity and molecular interactions of LXRα transcript variants with its ligand T0901317

Table 3.7

LXRβ transcript variants	GScore (Kcal/mol)	Interacting AAs	Interaction Atoms	HB-distance (Å)
LXRβ-1	-5.50	TRP454	(N…O)	1.74
LXRβ-2	-5.50	TRP454	(N…O)	1.74
LXRβ-3	-2.31	TRP231	(N…O)	2.22
LXRβ-4	-4.03	GLU427	(N…O)	2.83
LXRβ-5	-3.09	HIS335	(O…H)	1.17
LXRβ-6	-3.14	GLU408	(O…N)	2.61
LXRβ-7	-2.20	HIS432	(O…H)	2.73
LXRβ-8	-2.15	GLU281	(H…O)	1.20
LXRβ-9	-2.05	SER210 TRP231	(O…H) (N…O)	2.03 2.61

Table 3.7. Binding affinity and molecular interactions of LXRβ transcript variants with its ligand T0901317

References

1. Chawla A, Repa JJ, Evans RM, Mangelsdorf DJ. Nuclear receptors and lipid physiology: opening the X-files. Science. 2001;294: 1866–70. doi:10.1126/science.294.5548.1866

2. Francis GA, Fayard E, Picard F, Auwerx J. Nuclear receptors and the control of metabolism. Annu Rev Physiol. 2003;65: 261–311. doi:10.1146/annurev.physiol.65.092101.142528

3. Färnegårdh M, Bonn T, Sun S, Ljunggren J, Ahola H, Wilhelmsson A, et al. The Three-dimensional Structure of the Liver X Receptor β Reveals a Flexible Ligand-binding Pocket That Can Accommodate Fundamentally Different Ligands. J Biol Chem. 2003;278: 38821–38828. doi:10.1074/jbc.M304842200

4. Gabbi C, Warner M, Gustafsson J-A. Minireview: liver X receptor beta: emerging roles in physiology and diseases. Mol Endocrinol. 2009;23: 129–36. doi:10.1210/me.2008-0398

5. Webster N. The hormone-binding domains of the estrogen and glucocorticoid receptors contain an inducible transcription activation function. Cell. Elsevier; 1988;54: 199–207. doi:10.1016/0092-8674(88)90552-1

6. Teboul M, Enmark E, Li Q, Wikström AC, Pelto-Huikko M, Gustafsson JA. OR-1, a member of the nuclear receptor superfamily that interacts with the 9-cis-retinoic acid receptor. Proc Natl Acad Sci U S A. 1995;92: 2096–100. Available: http://www.pubmedcentral.nih.gov/articlerender.fcgi?artid=42430&tool=pmcentrez&rendertype=abstract

7. Janowski BA, Willy PJ, Devi TR, Falck JR, Mangelsdorf DJ. An oxysterol signalling pathway mediated by the nuclear receptor LXR alpha. Nature. 1996;383: 728–31. doi:10.1038/383728a0

8. Alberti S, Steffensen KR, Gustafsson JA. Structural characterisation of the mouse nuclear oxysterol receptor genes LXRalpha and LXRbeta. Gene. 2000;243: 93–103. Available: http://www.ncbi.nlm.nih.gov/pubmed/10675617

9. Fu X, Menke JG, Chen Y, Zhou G, MacNaul KL, Wright SD, et al. 27-hydroxycholesterol is an endogenous ligand for liver X receptor in cholesterol-loaded cells. J Biol Chem. 2001;276: 38378–87. doi:10.1074/jbc.M105805200

10. Zhang Y, Mangelsdorf DJ. LuXuRies of lipid homeostasis: the unity of nuclear hormone receptors, transcription regulation, and cholesterol sensing. Mol Interv. 2002;2: 78–87. doi:10.1124/mi.2.2.78

11. Chuu C-P, Kokontis JM, Hiipakka RA, Liao S. Modulation of liver X receptor signaling as novel therapy for prostate cancer. J Biomed Sci. 2007;14: 543–53. doi:10.1007/s11373-007-9160-8

12. Lehmann JM, Kliewer SA, Moore LB, Smith-Oliver TA, Oliver BB, Su JL, et al. Activation of the nuclear receptor LXR by oxysterols defines a new hormone response pathway. J Biol Chem. 1997;272: 3137–40. Available: http://www.ncbi.nlm.nih.gov/pubmed/9013544

13. Jakobsson T, Treuter E, Gustafsson J-Å, Steffensen KR. Liver X receptor biology and pharmacology: new pathways, challenges and opportunities. Trends Pharmacol Sci. 2012;33: 394–404. doi:10.1016/j.tips.2012.03.013

14. Steffensen KR, Gustafsson J-A. Putative metabolic effects of the liver X receptor (LXR). Diabetes. 2004;53 Suppl 1: S36–42. Available: http://www.ncbi.nlm.nih.gov/pubmed/14749264

15. Brinkman BMN. Splice variants as cancer biomarkers. Clin Biochem. 2004;37: 584–94. doi:10.1016/j.clinbiochem.2004.05.015

16. Robinson-Rechavi M. The nuclear receptor superfamily. J Cell Sci. 2003;116: 585–586. doi:10.1242/jcs.00247

17. Ruau D, Duarte J, Ourjdal T, Perrière G, Laudet V, Robinson-Rechavi M. Update of NUREBASE: nuclear hormone receptor functional genomics. Nucleic Acids Res. 2004;32: D165–7. doi:10.1093/nar/gkh062

18. Schook LB, Collares TV, Darfour-Oduro KA, De AK, Rund LA, Schachtschneider KM, et al. Unraveling the swine genome: implications for human health. Annu Rev Anim Biosci. Annual Reviews; 2015;3: 219–44. doi:10.1146/annurev-animal-022114-110815

19. Forster R, Ancian P, Fredholm M, Simianer H, Whitelaw B. The minipig as a platform for new technologies in toxicology. J Pharmacol Toxicol Methods. 2010;62: 227–235. doi:10.1016/j.vascn.2010.05.007

20. Fiser A, Sali A. Modeller: generation and refinement of homology-based protein structure models. Methods Enzymol. 2003;374: 461–91. doi:10.1016/S0076-6879(03)74020-8

21. Martí-Renom MA, Stuart AC, Fiser A, Sánchez R, Melo F, Sali A. Comparative

protein structure modeling of genes and genomes. Annu Rev Biophys Biomol Struct. 2000;29: 291–325. doi:10.1146/annurev.biophys.29.1.291

22. Laskowski RA, MacArthur MW, Moss DS, Thornton JM. PROCHECK: a program to check the stereochemical quality of protein structures. J Appl Crystallogr. International Union of Crystallography; 1993;26: 283–291. doi:10.1107/S0021889892009944

23. Collins JL, Fivush AM, Watson MA, Galardi CM, Lewis MC, Moore LB, et al. Identification of a nonsteroidal liver X receptor agonist through parallel array synthesis of tertiary amines. J Med Chem. 2002;45: 1963–6. Available: http://www.ncbi.nlm.nih.gov/pubmed/11985463

24. Ferreira M, Cabado AG, Chapela M-J, Fajardo P, Atanassova M, Garrido A, et al. Cytotoxic activity of extracts of marine sponges from NW Spain on a neuroblastoma cell line. Environ Toxicol Pharmacol. 2011;32: 430–7. doi:10.1016/j.etap.2011.08.012

25. Halgren TA, Murphy RB, Friesner RA, Beard HS, Frye LL, Pollard WT, et al. Glide: a new approach for rapid, accurate docking and scoring. 2. Enrichment factors in database screening. J Med Chem. American Chemical Society; 2004;47: 1750–9. doi:10.1021/jm030644s

26. Schultz JR, Tu H, Luk A, Repa JJ, Medina JC, Li L, et al. Role of LXRs in control of lipogenesis. Genes Dev. 2000;14: 2831–8. Available: http://www.pubmedcentral.nih.gov/articlerender.fcgi?artid=317060&tool=pmcentrez&rendertype=abstract

27. Yip DK, Auersperg N. The dye-exclusion test for cell viability: Persistence of differential staining following fixation. In Vitro. 1972;7: 323–329. doi:10.1007/BF02661722

28. Lo Sasso G, Bovenga F, Murzilli S, Salvatore L, Di Tullio G, Martelli N, et al. Liver X receptors inhibit proliferation of human colorectal cancer cells and growth of intestinal tumors in mice. Gastroenterology. 2013;144: 1497–507, 1507.e1–13. doi:10.1053/j.gastro.2013.02.005

29. Yoshikawa T, Shimano H, Amemiya-Kudo M, Yahagi N, Hasty AH, Matsuzaka T, et al. Identification of liver X receptor-retinoid X receptor as an activator of the sterol regulatory element-binding protein 1c gene promoter. Mol Cell Biol. 2001;21: 2991–3000. doi:10.1128/MCB.21.9.2991-3000.2001

30. Xu C, Li CY-T, Kong A-NT. Induction of phase I, II and III drug metabolism/transport by xenobiotics. Arch Pharm Res. 2005;28: 249–68. Available: http://www.ncbi.nlm.nih.gov/pubmed/15832810

31. Peet DJ, Turley SD, Ma W, Janowski BA, Lobaccaro J-MA, Hammer RE, et al. Cholesterol and Bile Acid Metabolism Are Impaired in Mice Lacking the Nuclear Oxysterol Receptor LXRα. Cell. 1998;93: 693–704. doi:10.1016/S0092-8674(00)81432-4

32. Repa JJ, Turley SD, Lobaccaro JA, Medina J, Li L, Lustig K, et al. Regulation of absorption and ABC1-mediated efflux of cholesterol by RXR heterodimers. Science. 2000;289: 1524–9. Available: http://www.ncbi.nlm.nih.gov/pubmed/10968783

33. Schwartz K, Lawn RM, Wade DP. ABC1 gene expression and ApoA-I-mediated

cholesterol efflux are regulated by LXR. Biochem Biophys Res Commun. 2000;274: 794–802. doi:10.1006/bbrc.2000.3243

34. Venkateswaran A, Laffitte BA, Joseph SB, Mak PA, Wilpitz DC, Edwards PA, et al. Control of cellular cholesterol efflux by the nuclear oxysterol receptor LXRalpha. Proc Natl Acad Sci. 2000;97: 12097–12102. doi:10.1073/pnas.200367697

35. Chen M, Beaven S, Tontonoz P. Identification and characterization of two alternatively spliced transcript variants of human liver X receptor alpha. J Lipid Res. 2005;46: 2570–9. doi:10.1194/jlr.M500157-JLR200

36. Endo-Umeda K, Uno S, Fujimori K, Naito Y, Saito K, Yamagishi K, et al. Differential expression and function of alternative splicing variants of human liver X receptor α. Mol Pharmacol. 2012;81: 800–10. doi:10.1124/mol.111.077206

37. Nolte RT, Wisely GB, Westin S, Cobb JE, Lambert MH, Kurokawa R, et al. Ligand binding and co-activator assembly of the peroxisome proliferator-activated receptor-gamma. Nature. 1998;395: 137–43. doi:10.1038/25931

38. Spencer TA, Li D, Russel JS, Collins JL, Bledsoe RK, Consler TG, et al. Pharmacophore analysis of the nuclear oxysterol receptor LXRalpha. J Med Chem. 2001;44: 886–97. Available: http://www.ncbi.nlm.nih.gov/pubmed/11300870

39. Williams S, Bledsoe RK, Collins JL, Boggs S, Lambert MH, Miller AB, et al. X-ray crystal structure of the liver X receptor beta ligand binding domain: regulation by a histidine-tryptophan switch. J Biol Chem. 2003;278: 27138–43. doi:10.1074/jbc.M302260200

40. Duniec-Dmuchowski Z, Ellis E, Strom SC, Kocarek TA. Regulation of CYP3A4 and CYP2B6 expression by liver X receptor agonists. Biochem Pharmacol. 2007;74: 1535–40. doi:10.1016/j.bcp.2007.07.040

Chapter 4: Porcine Constitutive Androstane Receptor (CAR) - Identification of splice variants and its role in regulation of xenobiotic metabolism in an *in vitro* porcine model

Abstract

Constitutive androstane receptor (CAR) is a member of the nuclear hormone receptor superfamily of ligand-activated transcription factors and has been emerged as a key regulator of xenobiotic metabolism. The purpose of the present study was to identify and characterize novel splice variants of porcine CAR. A total of five novel transcript variants of CAR were detected. Molecular modeling studies with a synthetic ligand indicate a reduction of the binding affinity of the splice variants compared to the wild type proteins. Expression profiles of the splice variants in different porcine tissues were also investigated. The role of CAR in xenobiotic metabolism in an *in vitro* porcine model was investigated and it was found that CAR modulates expression of a number of cytochrome P450 enzymes to regulate the metabolism of xenobiotics.

Introduction

Constitutive androstane receptor (CAR, NR1I3) has been emerged as a key regulator of drug and xenobiotic metabolism and disposition [1]. Together with other xenobiotic nuclear receptors, CAR senses xenobiotic ligands and activates phase I and phase II drug metabolizing enzymes and phase III transporters for elimination of the xenobiotics [2,3]. CAR was identified in 1994 as constitutively active nuclear receptor modulating retinoic acid signaling but the ligand and target genes were not known at that time [4,5]. Research in past decade has identified diverse xenobiotics including drugs, pesticides, environmental contaminants, industrial chemicals and many more as ligands of CAR [6]. Now, CAR has been established as a crucial sensor for xenobiotics [7]. CAR also plays important role in regulation of cellular homeostasis and metabolism of several endogenous compounds like steroids, bile acids, vitamin D, thyroid hormone and bilirubin [8]. As a typical nuclear receptor, CAR has N-terminal AF1 dommain, DNA-binding domain and ligand-binding domain (LBD) [1]. CAR forms heterodimer with retinoid X receptor (RXR) and binds to the xenobiotic response element (XRE) of its target gene [9]. Involvement of CAR in controlling of hepatic carbohydrate and lipid metabolism has been reported recently [10–13].

CAR is complexed with heat shock protein 90 and cytoplasmic retention protein in the cytoplasm in unexposed condition [14] and exposure to xenobiotics leads to nuclear translocation and activation of target genes. Phosphorylation and de-phosphorylation play important role in regulating the nuclear translocation of CAR

[15] . The CAR gene is expressed in in tissues with high capacity of xenobiotic metabolism such as liver and intestine [1].

Alternative splicing, has been thought to be one of the major contributors of protein diversity, as it often results in the expression of protein isoforms [16]. It is also a common phenomenon in the nuclear receptor family. In human, alternative splicing has been reported in a number of nuclear receptors like Vitamin D receptor and pregnane X receptor and constitutive androstane receptor [17,18]. The objective of the present study was to identify and characterize transcript variants of porcine CAR and investigate the role of CAR in regulation of xenobiotic metabolism in an in vitro porcine model. In this study we identified 5 novel transcript variants of CAR and investigated the properties of the transcript variants by molecular modeling studies.

Materials and Methods

Reagents

All chemicals were purchased from Sigma-Aldrich (USA) unless stated otherwise. Cell culture plastics were from Midsci, USA.

RNA Isolation and cDNA synthesis

Total RNA was isolated from porcine tissues using RNeasy Mini Kit (Qiagen) as per manufacturer's protocol. RNA pellets were dissolved in nuclease-free water and stored at -80°C until analysis. Quality of the RNA was determined by using Nano Drop spectrophotometer. The concentration of the RNA was determined by Qubit®

RNA HS Assay Kit (Thermo Fisher Scientific, Life Technologies) as per manufacturer's protocol.

Reverse transcription of RNA was performed from 1 µg total RNA in the presence of RNase inhibitor, random hexamer primers (50 ng/µl), deoxynucleotides (dNTPs, 10mM), SuperScript III reverse transcriptase (200 U/µl) and reverse transcriptase buffer in a 20 µl final reaction volume using SuperScript III First-Strand Synthesis System for RT-PCR kit (Invitrogen, Life Technologies, IN, USA).

Cloning and sequencing of CAR gene

Based on the exonic regions of the porcine CAR (NR1I3) gene, cDNAs that together encode the complete ORF of both the genes were amplified using the primer sets (Table 4.1). PCR reactions were performed in a 25 µl reaction volume containing 50 ng cDNA as the template, 0.5 M of each primer, 2X PCR buffer (including 1.5 mM $MgCl_2$), 200 mM dNTPs, and 0.625 units of Taq DNA polymerase. PCR reaction conditions were as follows: denaturation at 95 °C for 5 min, followed by 35 cycles of 95 °C for 30 s, 60°C for for 30 s, and 72 °C for 2 min, with a final extension at 72 °C for 20 min. Then, the 5′ and 3′ untranslated regions of CAR transcript from various tissues were amplified using total RNA and the FirstChoiceTM RNA ligase-mediated (RLM)-RACE kit (Ambion, Austin, TX). This procedure used primers supplied with the kit and the nested gene-specific primers listed in Supplementary Table 4.1. These products were cloned into pCRTOPO2.1 vector and sequenced. The cDNAs and deduced amino acid sequences were analyzed using the Biology Workbench (http://workbench.sdsc.edu/).

Generation of 3-D structure of CAR and its splice variants through homology modeling

In the absence of crystal structures of porcine CAR, we opted to develop homology model. The deduced amino acid sequences of CAR were analyzed by the Geneious R6 software (www.geneious.com). The query sequence was submitted in protein-protein BLAST (Basic Local Alignment Search Tool) program to find out the related protein structure with maximum sequence identity, highest score and least *E*-value to be used as a template (http://www.ncbi.nlm.nih.gov/BLAST). The proteins (PDB ID: 1XNX) and was used as templates for CAR homology modeling. The sequences of the template proteins were retrieved from the protein data bank (www.rcsb.org).

CAR transcript variant sequences were aligned and trimmed by Bioedit v7.2.5 software (http://www.mbio.ncsu.edu/bioedit/bioedit.html). The short sequences as well as ambiguous alignments were removed. Further, the entropy values were predicted. All deduced protein sequences of CAR transcript variants were modeled using MODELLER v9.1 (http://salilab.org/modeller) program [19,20]. The sequence-structure matches were established using a variety of fold assignment methods, including sequence-sequence, profile sequence, and alignments. Each model was evaluated using a multiple scoring algorithm that includes length of modeled sequence, identity of structure-sequence alignment, gap of alignment, compactness of model, and potential Z-scores. Representative models were ranked based on statistical potential value of Discrete Optimizes Potential Energy (DOPE) and the best one was selected.

Evaluation and validation of the3-D structures

The final modeled structures were validated by Procheck [21] (http://services.mbi.ucla.edu/PROCHECK/). Procheck was used to perform full geometric analysis as well as stereochemical quality of protein structures. Ramachandran plot statistics was used to evaluate the stability of the models.

Molecular docking analysis to investigate the interaction of LXRα, LXRβ and their splice variants with a synthetic ligand

CITCO is a well-known synthetic ligand for CAR [22]. To gain an understanding of the molecular interactions during ligand binding, molecular docking analysis of CAR splice variants with a synthetic ligand CITCO was done. The chemical properties of CITCO are presented in Table 4.2.

Protein and Ligand preparation

Each modeled proteins were prepared using protein preparation wizard of Schrodinger LLC., Portland, USA (http://www.schrodinger.com). This adds hydrogen atoms charges, and does energy minimization of the structures using Impact Refinement module using OPLS (2005) force field. The minimization was terminated when the energy converged or Root Mean Square Deviation (RMSD) reached a maximum cutoff of 0.03Å.

The ligand CITCO (Figure 4.1) was obtained from Pubchem database (http://www.pubchem.com). This ligand was built with Chemsketch v12.0 (ACD Labs, USA; http://www.acdlabs.com), and the 3D structure was further energy

minimized by LigPrep program (Schrodinger suite LLC., Portland, USA) using the OPLS 2005 force field at pH 7.0 and keeping rest of the parameter values as default.

The pharmacophore model was developed using PHASE 3D-QSAR software [23] which utilizes conformational sampling and other scoring parameters to identify the common 3D pharmacophore. The pharmacophore model of CITCO is presented in Figure 4.1.

Molecular docking

The molecular docking was carried out using Glide program [24] of the Schrodinger suite. Glide is designed to assist in high-throughput screening of potential ligand based on binding mode and affinity for a given receptor molecule. Glide provides three different level of docking precisions (HTVS, High-Throughput Virtual Screening; SP, Standard Precision; XP, Xtra Precision). The entire Glide program was run using default mode. Minimization cycle for conjugate gradient and steepest descent minimization were used with default value of 0.05 Å for initial step size and 1.0 Å for maximum step size. In the coincide criteria for minimization, both the energy change criteria and gradient criteria were used with default value of 10^{-7} and 0.001 kcal/mol respectively. All conformations were considered for docking and in the docking process the Glide score was used to select the best conformation for the ligand.

Effects of ClTCO on transcript expression CAR and genes involved in phase I, Phase II drug metabolism, phase II transport and nuclear receptors

CAR is a well-documented potent synthetic agonist of CAR [22]. To gain insight into the role of CAR in porcine xenobiotic metabolism, the effect of the synthetic ligand on the expressions of the most important drug metabolism and regulation genes in porcine primary hepatocytes were investigated.

Cell culture and treatments

Primary hepatocytes were isolated by using a simplified manual perfusion method. Immediately after the animal was euthanized, a single liver lobe was resected, washed 2-3 times with ice cold phosphate buffer saline and transported to the laboratory in ice cold Krebs Ringer Solution. Then the liver sample was cannulated with suitable pipette into visible blood vessels on the cut surface and was flushed with 500 ml of buffer A containing 8.3 g/l NaCl, 0.5 g/l KCl, 2.4 g/l HEPES and 0.19 g/l EGTA at pH 7.4 and 37°C. This was followed by perfusion of 500 ml buffer B containing 8.3 g/l NaCl, 0.5 g/l KCl and 2.4 g/l HEPES. Continuous recirculating perfusion was then carried out on the tissue using a pre-warmed digestion buffer (Buffer C) solution containing 3.9 g/l NaCl, 0.5 g/l KCl, 2.4 g/l HEPES, 0.7 g/l $CaCl_2$ X $2H_2O$ and 0.1 % collagenase (type IV). Following sufficient digestion, the liver capsule was removed and dissolved cells were liberated by gentle shaking of the liver specimen in ice cold buffer D containing 9.91 g/l Hanks buffered salt without calcium and magnesium, 2.4 g/l HEPES and 2.0 g/l bovine serum albumin. A scalpel was used to cut through the regions which were not well perfused to release cells contained within. The resulting cell suspension was filtered through

a nylon mesh with 100 µm pore size and centrifuged at 50 g for 3 min at 4°C. After, we employed a cell incubation step for 10 min with DNase1 containing buffer at 4°C during which cell clumps were broken and damaged cells digested. Then the resulting suspension was filtered through 70 µm nylon mesh and cells were harvested by 50 g for 3 min. This was followed by three washing in ice cold buffer D. The resulting cell clumps were finally re-suspended in culture medium (William's E supplemented with 100 mU/ml penicillin, 100 µg/ml streptomycin, 2mM glutamate and 10% Fetal bovine serum). Viability of hepatocytes was determined by trypan blue dye exclusion test [25].

Freshly isolated hepatocytes were cultured in William's E medium supplemented with 100 mU/ml penicillin, 100 µg/ml streptomycin, 2 mM glutamate and 10% fetal bovine serum. Prior to experiments, cells were washed twice with PBS followed by incubation in medium containing CITCO.

Real time PCR

Total RNA isolation and cDNA synthesis have been done as described previously. Relative quantification of the genes involved in phase-I, phase-II drug metabolism, phase III transport and nuclear receptors was performed by using Power SYBR green PCR Master Mix (2X) (Applied Biosystems) in Taqman ABI 7900 Real-Time PCR system (Applied Biosystems). The thermal cycling conditions for real-time PCR were one cycle of 50 °C for 2 min (AmpErase uracil-N-glycosylase activation) and 95°C for 10 min (AmpliTaq Gold activation), followed by 40 cycles of 95°C for 15 sec (denaturation) and 60°C for 1 min (annealing and extension).The housekeeping genes GAPDH and ACTB were used as endogenous control to

normalize for RNA loading or differences in reverse transcription efficiency. The information on the primers is presented in Table 4.2. The relative expression levels were calculated with respect to the normalized expression of the controls by delta delta Ct (ΔΔCt) method.

Results

Identification of novel transcript variants of porcine CAR

Total five novel CAR transcript variants (CAR-2 to Car-6) were detected in different porcine tissues (Figure 4.2). CAR-1 (wild type) transcript consists of eight exons which code for 348 amino acids. CAR-2 had deleted exon 6 during splicing. CAR-3 had a twelve nucleotide insert between exon 5 and exon 6. CAR-4 had a nine nucleotide insert between exon 3 and exon 4 and exon 6 were missing. Exons 3, 4 and 5 were missing in CAR-5, whereas exons 3, 4, 5 and 6 were missing in CAR-6. The physiochemical properties of the deduced amino acids of the CAR transcript variants are presented in Table 4.4.

The expression of the different variants are indicated in the Figure 4.2. The wild type was detected in all the tissues screened. CAR-2 was detected in kidney, small intestine, and spleen. CAR-3 was detected in liver, small intestine and spleen. CAR-4 was detected in only liver. CAR-5 and CAR-6 were detected in only kidney

Reduced binding affinity of the novel transcript variants of porcine CAR towards ligand (CITCO) compared to the wild type protein

In the absence of a crystal structure for porcine CAR, we opted to develop homology model for porcine wild type CAR (Figure 4.4F) and the identified transcript

variants (Figure 4.4A-E). Wild type CAR ligand binding domain contain 11 α-helices and 3 short β-strands and the ligand binding pocket is made up of by helices 2-7 and 10 and three β-sheets which is consistent with human [22,26].The molecular interactions of CAR transcript variants with synthetic ligand CITCO are presented in Figure 4.5 to Figure 4.8. The binding affinity, interacting amino acids in LBD, and hydrogen bond distance of different CAR transcript variants with CITCO is presented in Table 4.5. The results showed that the wild type protein CAR-1 has the highest binding affinity (Glide score of -11.0 Kcal/mol) towards its ligand. The other transcript variants had reduced binding affinity for the synthetic ligand. CAR-4 and CAR-5 did not show any binding affinity towards the ligand. The three dimensional conformations of the novel splice variant proteins have been changed due to splicing. The disturbed 3-D conformation may be the reason behind the reduction in the binding affinity towards the ligand.

CAR agonist modulates the expression of genes involved in xenobiotic metabolism in porcine primary hepatocytes

To gain understanding how CAR is involved in xenobiotic metabolism pathways, we induced CAR by addition of the synthetic ligand CITCO and studied the expression of the key genes involved in xenobiotic metabolism and its regulation. We treated primary hepatocytes with CITCO to activate CAR and studied the expression of phase-I, phase-II drug metabolism genes and phase-III transporters to understand the involvement of CAR in xenobiotic metabolism pathways. Treatment of CITCO upregulated CAR transcript expression in porcine primary hepatocytes (Figure 4.9) indicating that CITCO is a good agonist for porcine CAR.

Treatment of CITCO caused a significant increase of CYP2B22, CYP2C33, CYP2C42 and CYP3A; all the other CYPs remain unchanged (Figure 4.10). Phase II drug metabolism genes SULT1A1 and GSTO1 were upregulated following CITCO treatment. Among nuclear receptors studied, ABCB1 and ABCC2, were upregulated (Figure 4.10). From the results of the study, it can be concluded that activated LXRs induce the expression of CYP2B22, CYP 2C33, CYP2C42, CYP3A and the transporters (ABCB1 and ABCC2).

Discussion

Nuclear receptors are master regulators of a wide variety of metabolism including endogenous metabolites and exogenous xenobiotics that integrate the homeostatic control of almost all biological processes [27]. Nuclear receptors regulate transcription through the recruitment of coactivator proteins to the ligand binding domain (LBD) [28].

Exons 2 and 3 and part of exon 4 encode the DNA binding domain (DBD) and the hinge regions, whereas the ligand binding domain (LBD) is encoded by the rest of exon 4 and exon 5 to exon 9. In the present study, five novel splice variants of CAR were identified. The splice variants had truncated amino acids in the protein sequences (Table 4.4). At least 26 splice variants has been reported in human, most of which codes for a premature stop codon or code for a truncated protein [29,30]. Due to changes in the LBD structures, differences in ligand binding affinity has been reported between human wild-type CAR and isoforms [31,32]. In the present study also, a reduction in the binding affinity was found in splice variants (CAR-2, CAR-3 and CAR-4) towards a synthetic ligand (Table 4.5). Two identified splice variants

(CAR-5 and CAR-6) did not bind at all to the synthetic ligand CITCO. In CAR-5, exons 4, 5 and 6 was deleted and in CAR-6, exons 4, 5, 6 and 7 was deleted. As exons exons 4, 5 and 6 form the ligand binding domain for the wild type CAR, deletion of these impairs the binding of the ligand.

To gain understanding on how LXRs are involved in the xenobiotic metabolism pathways, we induced LXRs by addition of synthetic ligands and studied the expressions of the most important genes involved in xenobiotic metabolism and its regulation. Treatment of CITCO caused a significant increase of CYP2B22, CYP 2C33, CYP2C42, and CYP3A among phase I drug metabolism enzymes, SULT1A1 and GSTO1 among phase II enzymes and ABCB1 and ABCC2 among transporters (Figure 4.10). In human, the hepatic induction of phase I (e.g. CYP2B6, CYP2C9, CYP3A4) and phase II (e.g. UGT1A1, GSTA1) drug metabolizing enzymes and of transporters (e.g. MRP2, SLC21A6) by CAR in response to structurally diverse chemicals has been reported [33,34].

Figures and Tables

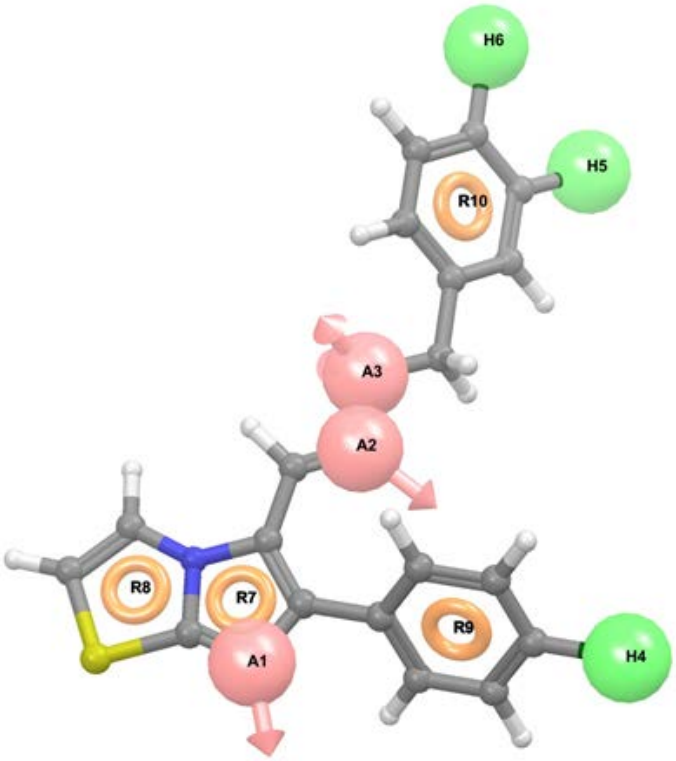

Figure 4.1. Chemical structure of CITCO

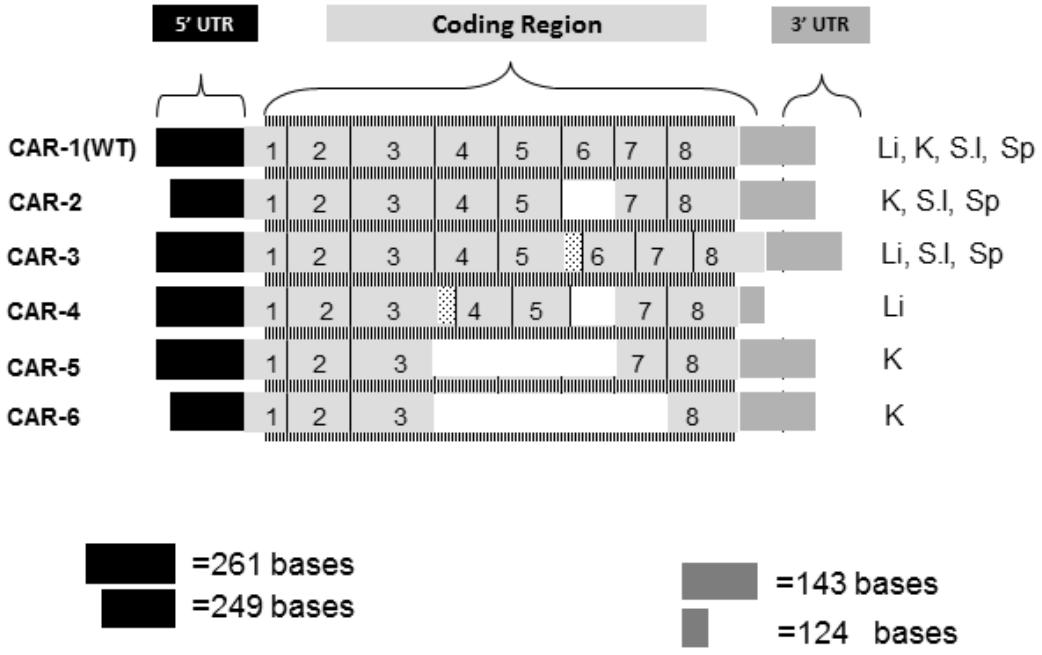

Figure 4.2. Identified transcript variants of CAR

The tissue distribution of the splice variants are indicated in the right side.

Li, Liver; K, Kidney; S.I, Small Intestine; Sp, Spleen

```
CAR_1      MASGEDEPRNCAVCGDRATGYHFHALTCEGCKGFFRRTVNKSTSLICPFAGSCKVNKAQR 60
CAR_2      MASGEDEPRNCAVCGDRATGYHFHALTCEGCKGFFRRTVNKSTSLICPFAGSCKVNKAQR 60
CAR_4      MASGEDEPRNCAVCGDRATGYHFHALTCEGCKGFFRRTVNKSTSLICPFAGSCKVNKAQR 60
CAR_3      MASGEDEPRNCAVCGDRATGYHFHALTCEGCKGFFRRTVNKSTSLICPFAGSCKVNKAQR 60
CAR_5      MASGEDEPRNCAVCGDRATGYHFHALTCEGCKGFFRRTVNKSTSLICPFAGSCKVNKAQR 60
CAR_6      MASGEDEPRNCAVCGDRATGYHFHALTCEGCKGFFRRTVNKSTSLICPFAGSCKVNKAQR 60
           ************************************************************

CAR_1      RHCPACRLQKCLDAGMKKDMILSAEVLALRRARQVQRRAQQASLQLSKEQKALVQILLGA 120
CAR_2      RHCPACRLQKCLDAGMKKDMILSAEVLALRRARQVQRRAQQASLQLSKEQKALVQILLGA 120
CAR_4      RHCPACRLQKCLDAGMKKDMILSAEVLALRRARQVQRRAQQASLQLSKEQKALVQILLGA 120
CAR_3      RHCPACRLQKCLDAGMKKDMVLSAEVLALRRARQVQRRAQQASLQLSKEQKALVQILLGA 120
CAR_5      RHCPACRLQKCLDAGMKKDM---------------------------------------- 80
CAR_6      RHCPACRLQKCLDAGMKKD----------------------------------------- 79
           ******************

CAR_1      HTRHMGTMFDQFVQFR---PPAHLFIHHQHLPPLVPELSLLMHFADINTFMIQQIIKFTK 177
CAR_2      HTRHMGTMFDQFVQFR---PPAHLFIHHQHLPPLVPELSLLMHFADINTFMIQQIIKFTK 177
CAR_4      HTRHMGTMFDQFVQFRQKKPPAHLFIHHQHLPPLVPELSLLMHFADINTFMIQQIIKFTK 180
CAR_3      YTRHMGTMFDQFVQFR---PPAHLFIHHQHLPPLVPELSLLMHFVDINTFMIQQIIKFTK 177
CAR_5      ------------------------------------------------------------ 80
CAR_6      ------------------------------------------------------------ 79


CAR_1      DLPLFRSLPMEDQISLLKGAAVEICQIVLNTTFCLQTQKFLCGPLRYTIEDGAH----VG 233
CAR_2      DLPLFRSLPMEDQISLLKGAAVEICQIVLNTTFCLQTQKFLCGPLRYAIEDGAH------ 231
CAR_4      DLPLFRSLPMEDQISLLKGAAVEICQIVLNTTFCLQTQKFLCGPLRYAIEDGAH------ 234
CAR_3      DLPLFRSLPMEDQISLLKGAAVEICQIVLNTTFCLQTQKFLCGPLRYTIEDGAHVSPTVG 237
CAR_5      ------------------------------------------------------------G 81
CAR_6      ------------------------------------------------------------ 79


CAR_1      FQEEFLELLFGFHKTLRRLQLQEPEYVLMVAVALFSPDRPGVTQRKEIDQLQEEMALTLQ 293
CAR_2      -----------------------------------DRPGVTQRKEIDQLQEEMALTLQ 254
CAR_4      -----------------------------------DRPGVTQRKEIDQLQEEMALTLQ 257
CAR_3      FQEEFLELLFGFHKTLRRLQLQEPEYVLMVAVALFSPDRPGVTQRKEIDQLQEEMALTLQ 297
CAR_5      FQEEFLELLFGFHKTLRRLQLQEPEYVLMVAVALFSPDRPGVTQRKEIDQLQEEMALTLQ 141
CAR_6      -----------------------------------NRPGVTQRKEIDQLQEEMALTLQ 102
                                             :**********************


CAR_1      SYIKGQQPSLRDRFLYAKLLGLLAELRSINKEYWYQIQNIQGLSTMMPLLQEICS      348
CAR_2      SYIKGQQPSLRDRFLYAKLLGLLAELRSINKEYWYQIQNIQGLSTMMPLLQEICS      309
CAR_4      SYIKGQQPSLRDRFLYAKLLGLLAELRSINKEYWYQIQNIQGLSTMMPLLQEICS      312
CAR_3      SYIKGQQPSLRDRFLYAKLLGLLAELRSINKEYWYQIQNIQGLSTMMPLLQEICS      352
CAR_5      SYIKGQQPSLRDRFLYAKLLGLLAELRSINKEYWYQIQNIQGLSTMMPLLQEICS      196
CAR_6      SYIKGQQPSLRDRFLYAKLLGLLAELRSINKEYWYQIQNIQGLSTMMPLLQEICS      157
           ******************************************************
```

Figure 4.3. Multiple sequence alignment of CAR transcript variants

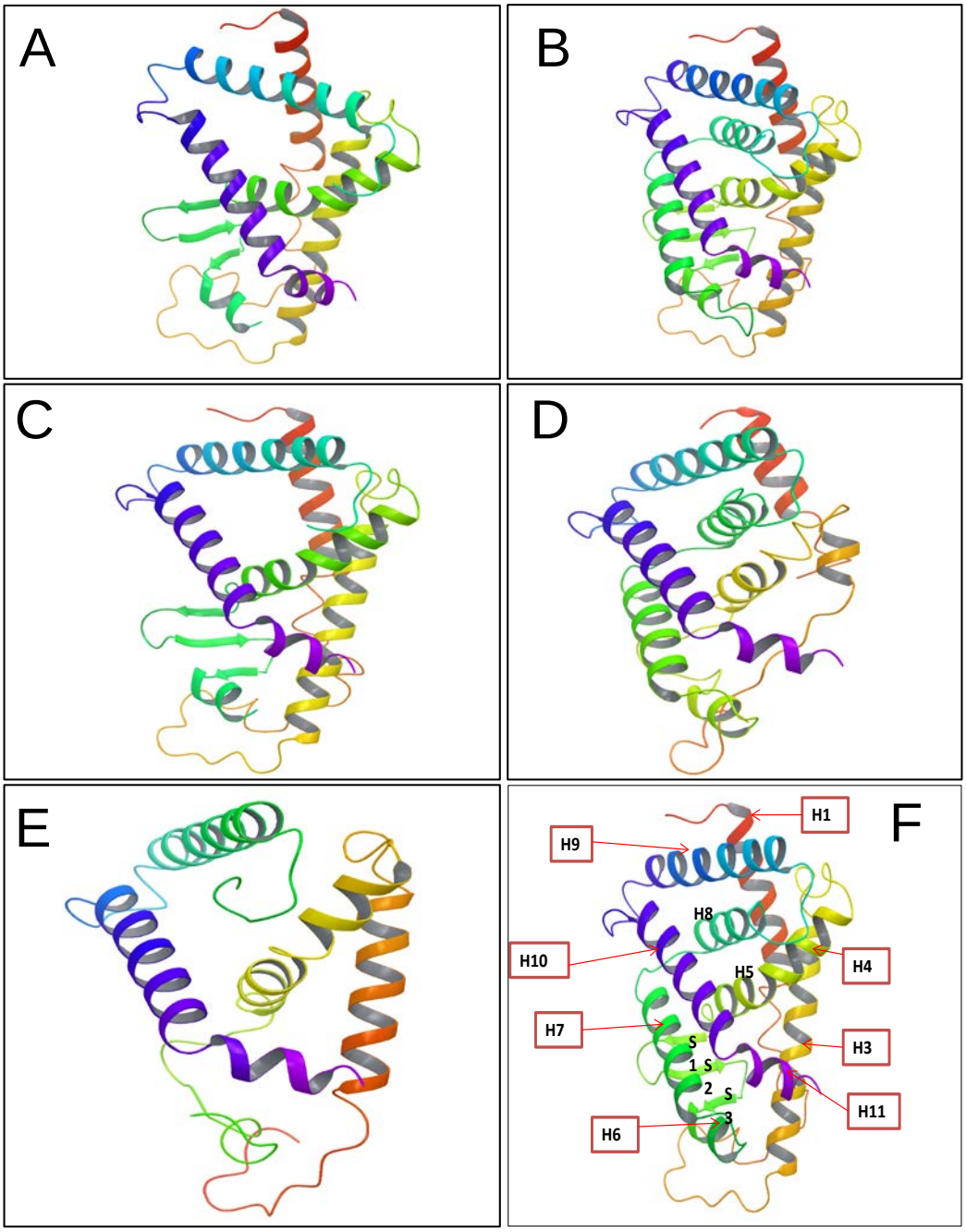

Figure 4.4. 3D structure of porcine CAR splice variants by homology modeling

A, CAR-2; B, CAR-3; C, CAR-4; D, CAR-5; E: CAR-6; F, CAR-1

H denotes helix and S denotes β-sheet

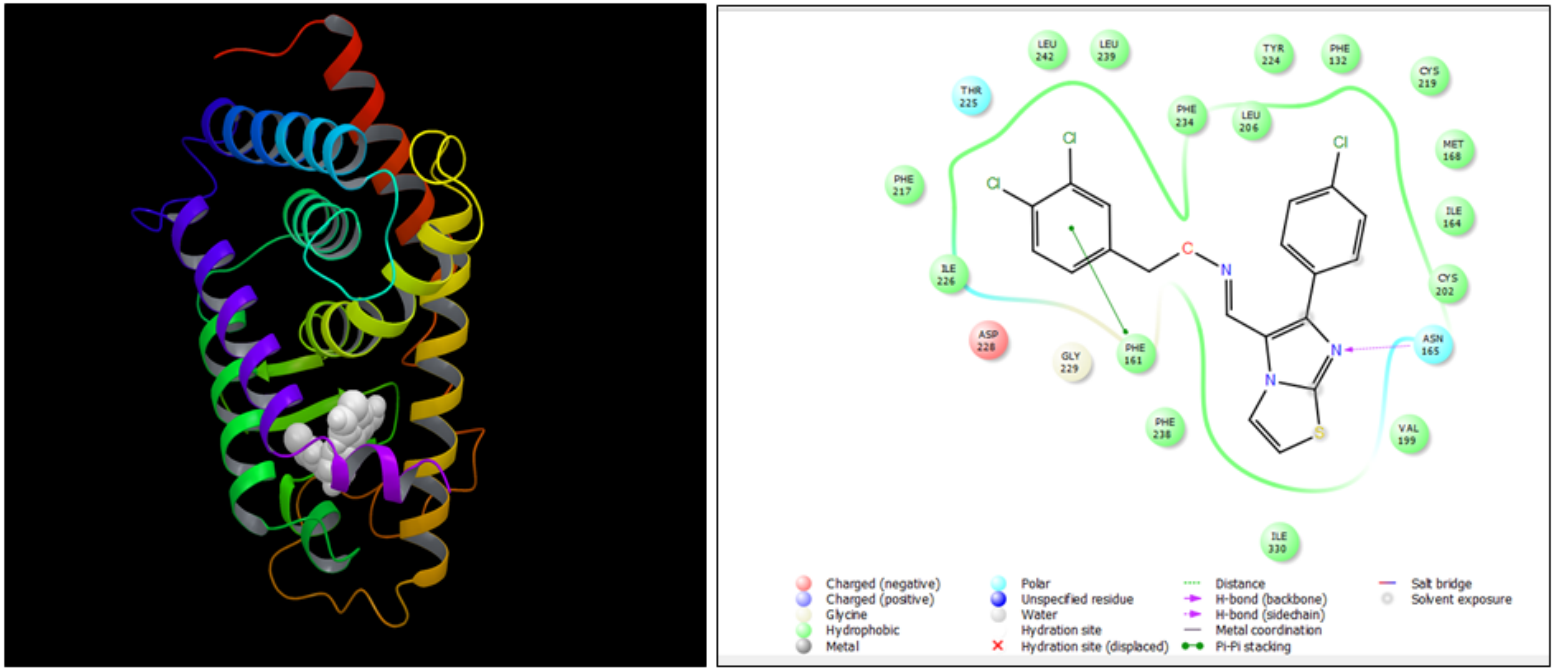

Figure 4.5. Molecular modeling interactions of CAR-1 with CITCO

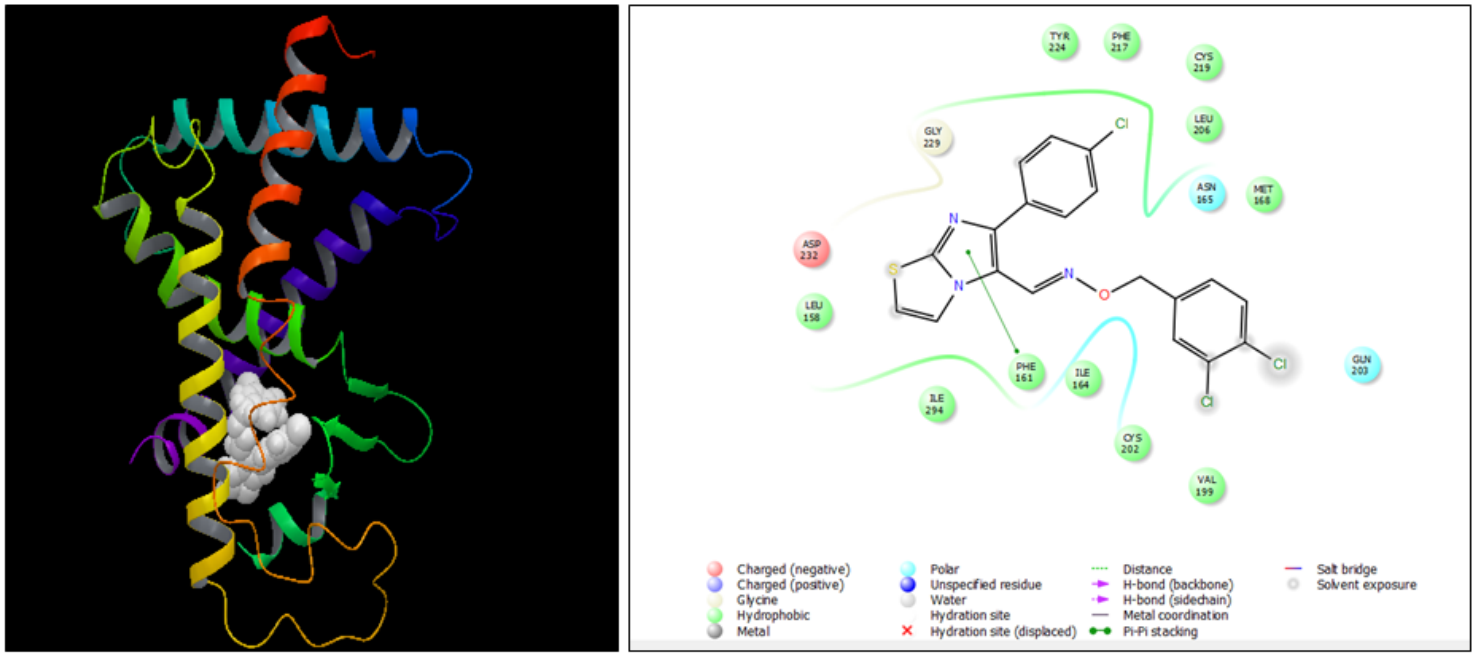

Figure 4.6. Molecular modeling interactions of CAR-2 with CITCO

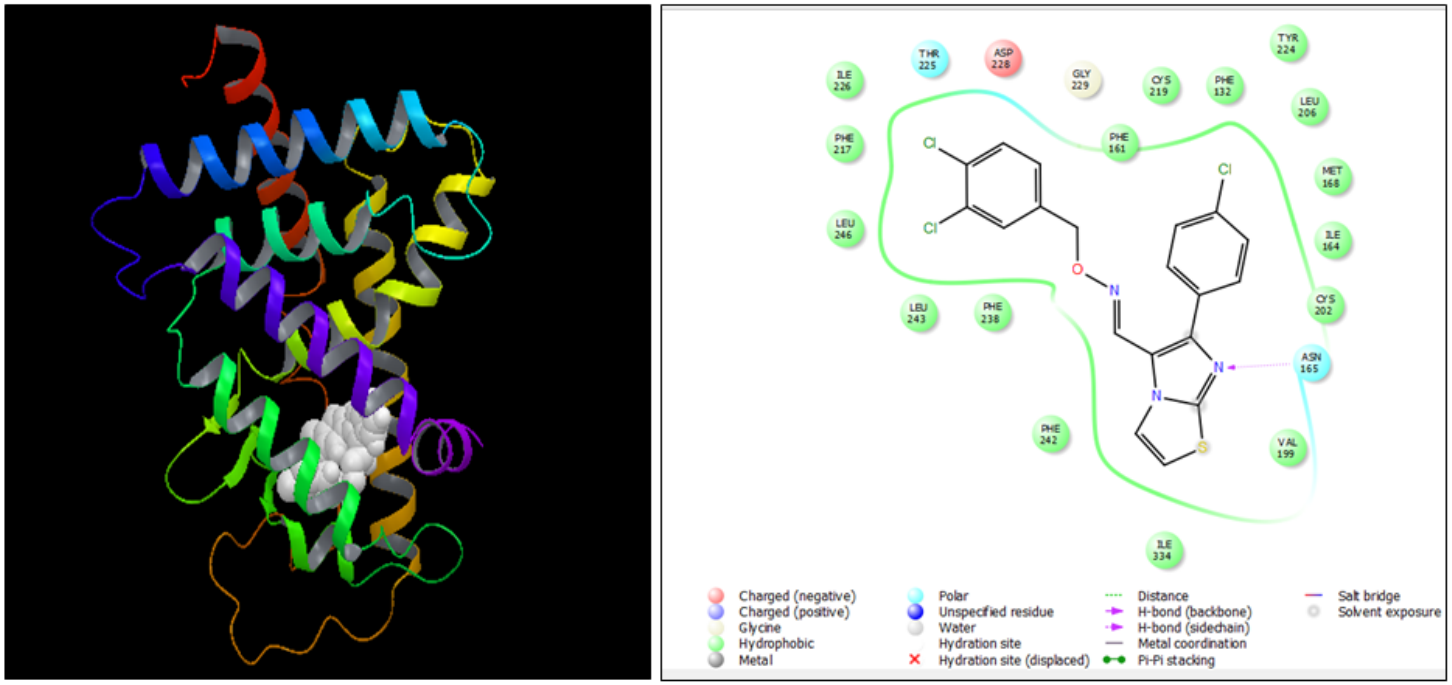

Figure 4.7. Molecular modeling interactions of CAR-3 with CITCO

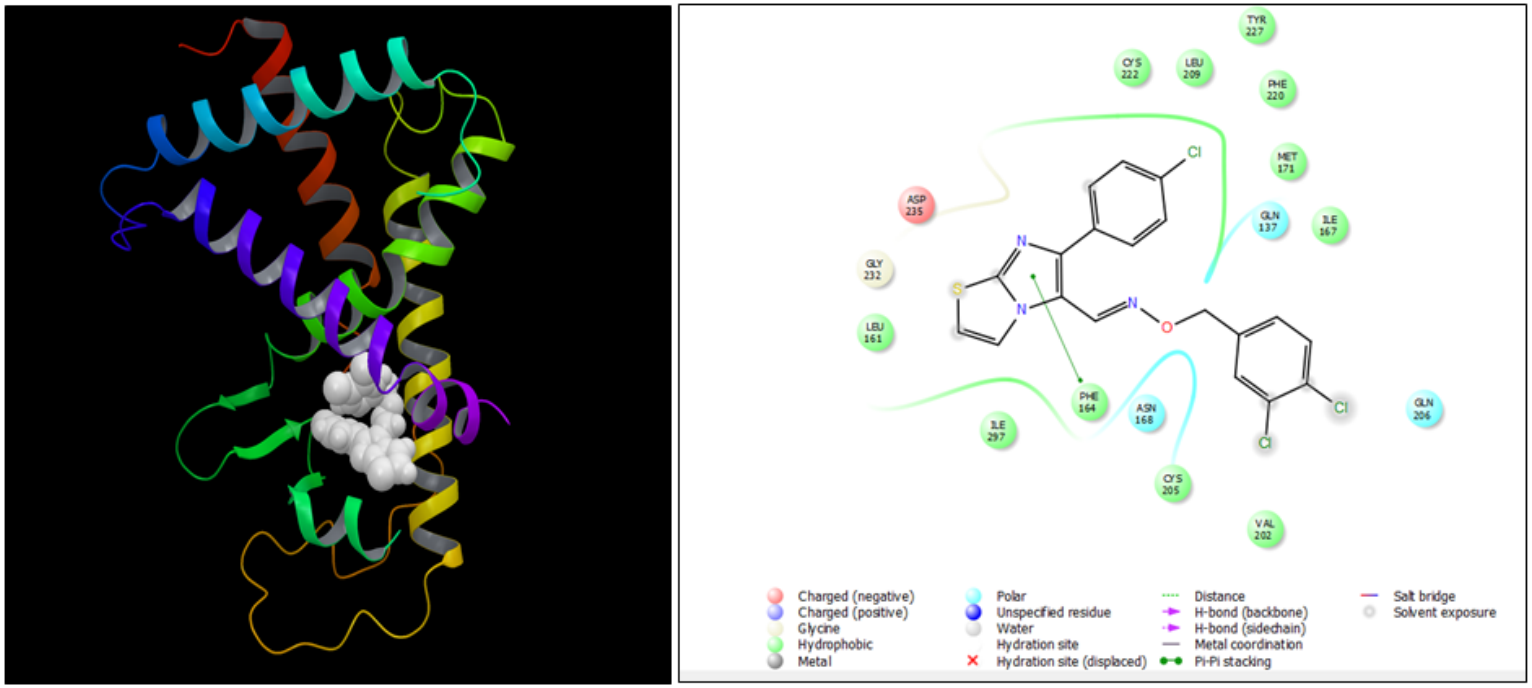

Figure 4.8. Molecular modeling interactions of CAR-4 with CITCO

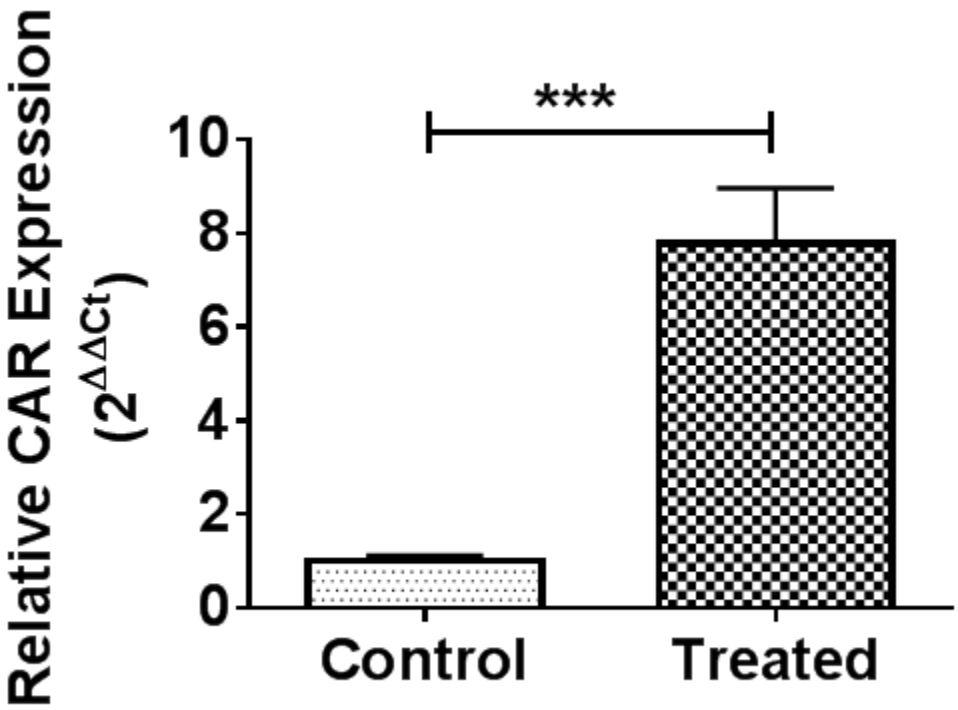

Figure 4.9. Effect of CITCO on expression of CAR transcript in primary porcine hepatocytes

Real time RT-PCR was performed to analyze the effect of CAR ligand CITCO (10 µM) on expression of CAR transcript in primary hepatocytes. The values and error bars represent average and standard deviations of three independent set of experiments. One-way analysis of variance (ANOVA) followed by Dunnett post-test was performed to find out significant difference among control and treatments. *** denotes p≤0.001

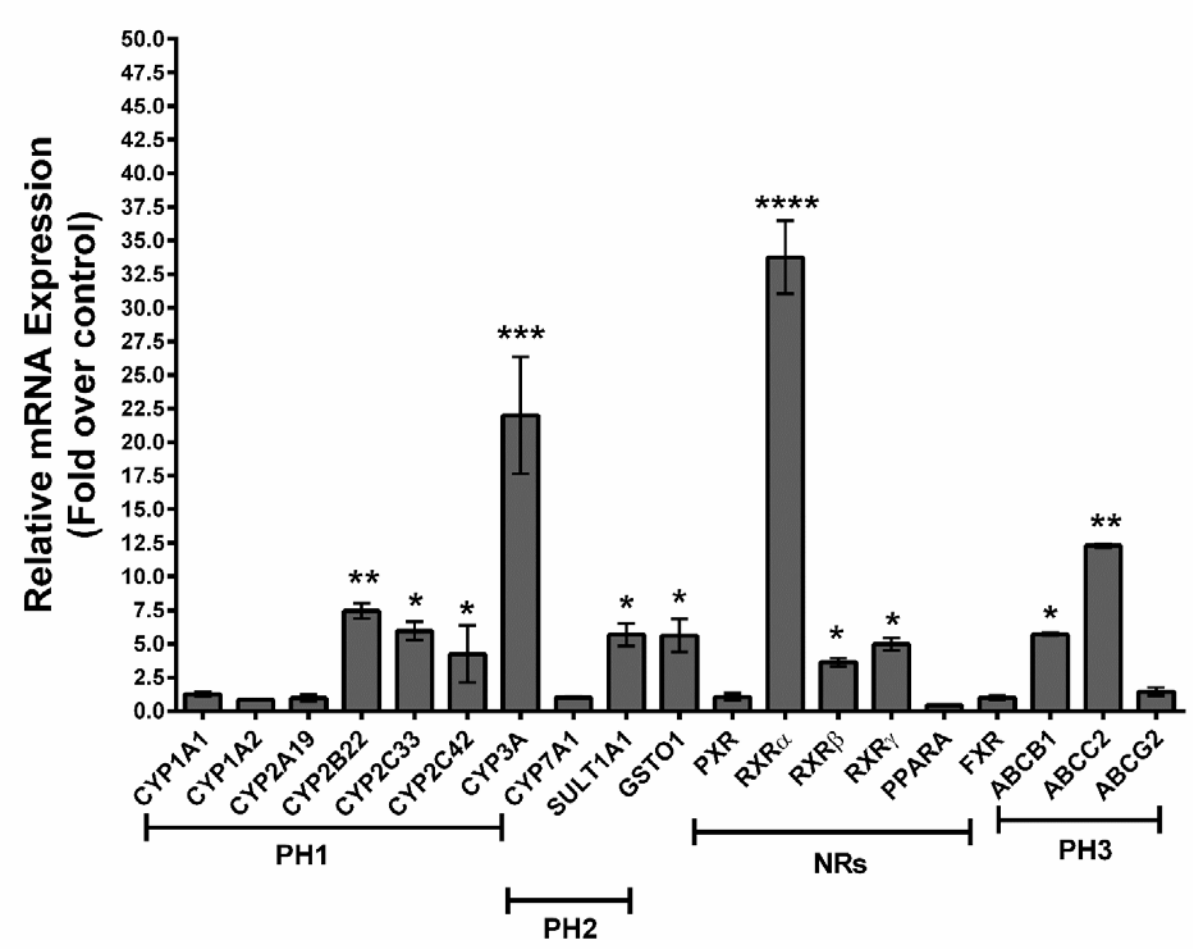

Figure 4.10. Effect of CITCO on expression of phase-I, phase-II and Phase-II DME transcripts

Real time RT-PCR was performed to analyze the effect of CAR ligand CITCO (10 μM) on expression of the most important genes involved in regulation of drug metabolism. The values and error bars represent average and standard deviations of three independent set of experiments. One-way analysis of variance (ANOVA) followed by Dunnett post-test was performed to find out significant difference among control and treatments. * denotes p≤0.05; ** denotes p≤0.01; *** denotes p≤0.001; **** denotes p≤0.0001.

Table 4.1

Cloning Primers	
CAR Forward	TGAAGGCCACAGAGGTAGAAGTTCCTTG
CAR Reverse	AGCAGCGGCATCATGGTGGACAGTCC
RACE Primers	
3’RACE-outer	Supplied with kit
CAR 3' OUTER	TAAGACACTTCGGCGACTGC
3’RACE-inner	Supplied with kit
CAR 3' INNER	TCTCCGGGACAGGTTTCTCT
5’RACE-outer	Supplied with kit
CAR 5' OUTER	CTTGCAGCCCTCACAAGTCAAG
5’RACE-inner	Supplied with kit
CAR5' INNER	CCGCACACAGCACAGTTCCTTG

Table 4.1. Cloning and RACE primers for CAR

Table 4.2

Molecular Weight	436.74208 g/mol
XLogP3	7.3
Hydrogen Bond Donor Count	0
Hydrogen Bond Acceptor Count	4
Rotatable Bond Count	5
Exact Mass	434.976666 g/mol
Monoisotopic Mass	434.976666 g/mol
Topological Polar Surface Area	67.1 A^2
Heavy Atom Count	27
Formal Charge	0
Complexity	520
Isotope Atom Count	0
Defined Atom Stereocenter Count	0
Undefined Atom Stereocenter Count	0
Defined Bond Stereocenter Count	1
Undefined Bond Stereocenter Count	0
Covalently-Bonded Unit Count	1

Table 4.2. Chemical properties of CITCO

Table 4.3

Gene Name	Primers	Sequences (5'-3')
GAPDH	Forward	GGCAAATTCCACGGCACAGTCA
	Reverse	CTGGCTCCTGGAAGATGGTGAT
ACTB	Forward	GCAAATGCTTCTAGGCGGACTGT
	Reverse	CCAAATAAAGCCATGCCAATCTCA
Porcine Albumin	Forward	TGGTGACTTGGCTGACTGCTG
	Reverse	TGTCGGGGTTATCATTTTTGTGTTG
HNF4A	Forward	AGTCCCAGAGTGGTAGTGGAAAG
	Reverse	CAGATGGTGAAGGGTGGCATTG
G6PC	Forward	ATTGAAAGACGATGACTGTGCCAA
	Reverse	CAAAGGAGGAAGGAGTTCTGAGC
CYP1A1	Forward	AAGAGGCAGAGGTGAAGTGGTGAA
	Reverse	GAGAAGAAGGAAGGCAGTGAAGTGATAG
CYP1A2	Forward	ACACCTTCTCCATTGCCTCAGACC
	Reverse	GCACTCAGCCTCCTTGCTCAC
CYP2A19	Forward	CCGAAGAGTCACCAAGGATACCAAG
	Reverse	ACAGAGCCCAGCATAGGGAACA
CYP2B22	Forward	CAGATGAGTAAACAGAGCCCGAGAA
	Reverse	CGAGAGCCAAGGAGACAGCA
CYP2C33	Forward	TGGAAGAAAAATCACAAGAGGAGAAGG
	Reverse	TTGGAAAGAGACGCAGGGATGT
CYP2C42	Forward	TACAGAGACAACAAGCACCACCA
	Reverse	CTGCCAATCACACGGTCAATC
CYP2C49	Forward	CTTGTGGAGGAGTTGAGAAAAACC
	Reverse	TTGTGGAAAATGATGGAGCAGA
CYP2E1	Forward	ACACCCTGCTGATGGAAATGGA
	Reverse	GTGGTCTCTGTCCCCGCAAA
CYP3A	Forward	TACCTGCCCTTTGGGACTGGAC
	Reverse	AGTTCTGCAGGACTCTGACGA
CYP7A1	Forward	TTCTGCTACCGAGTGATGTTTGAGG
	Reverse	AGGTTGTTTAGGATGAGTGCTTTCTGTG
SULT1A3	Forward	GACCACAGCATCTCAGCCTTCAT
	Reverse	CTGCCATCTTCTCAGCATAGTCG
SULT2A1	Forward	AAATGCTGCAAGAGGTGAGGGAGG
	Reverse	ATCCCCCTTGGAGAGAATCAGGCA
SULT1E1	Forward	GAGAAAGGGGATTGCAGGAGACTG
	Reverse	GTAGACCCCTTCATTTGCTGCTCA
GSTO1	Forward	GAGATTCTGTCCTTTCGCCCAGAG
	Reverse	GATGACTTGATGCCGGATTCCCTT
GSTK1	Forward	GGTACACCATCCACCGTTAGTCTC
	Reverse	CACACAAACACCAGCAAAGACACA
ABCB1	Forward	TGGCAGTGGGACAGGTTAGTTC
	Reverse	CACGGTGCTTGAGCTGTCAATC
ABCB6	Forward	TGTTGTCCCAAGGTGGTGTGTATG
	Reverse	GCTGAAATGGATTTCCCTCCAGGT
ABCC2	Forward	GTGGCTGTTGAGCGAATAAATGAATAC
	Reverse	TGCTGGGCCAACCGTCTG

Table 4.3 (cont.)

Gene Name	Primers	Sequences (5'-3')
ABCC3	Forward	TGATGCAGACGCTGATCTTACACC
	Reverse	ACTCACGTTTGACGGAATTGGTGA
ABCG2	Forward	GATCTTTTCGGGGCTGTTCCTCA
	Reverse	TGAGTCCCGGGCAGAAGTTTTGT
PXR	Forward	GACAACAGTGGGAAAGAGAT
	Reverse	CCCTGAAGTAGGAGATGACT
FXR	Forward	CATTCAACCATCACCACGCAGAGA
	Reverse	GCACATCCCAGACTTCACAGAGA
CAR	Forward	GAAAGCAGGGTTACAGTGGGAGTA
	Reverse	CTTCAGGTGTTGGGATGGTGGTC
LXRA	Forward	TCCAGGTAGAGAGGCTGCAACATA
	Reverse	AGTTTCATTAGCATCCGTGGGAAC
LXRB	Forward	GAGTCTTCCTGAGAGGGGCAGATA
	Reverse	CGTGGTAGGCTTGAGGTGTAAGC
PPARA	Forward	AATAACCCGCCTTTCGTCATACAC
	Reverse	GACCTCCGCCTCCTTGTTCT
PPARG	Forward	CCATGCTGTCATGGGTGAAACTCT
	Reverse	GTCAACCATGGTCACCTCTTGTGA
RXRA	Forward	CCTTCTCGCACCGCTCCATA
	Reverse	CGTCAGCACCCTGTCAAAGATG
RXRG	Forward	CTTCCCGTTCCCCAAACGTGAT
	Reverse	CTTCCAGAAAAGATCCCCAGTCCC

Table 4.3. Primer sequences for real-time PCR

Table 4.4

Name	Protein length	Molecular Weight (kDa)	Isoelectric Point
CAR-1	348	39.809	8.72
CAR-2	309	35.200	8.96
CAR-3	352	40.233	8.71
CAR-4	312	35.585	9.23
CAR-5	196	22.421	8.41
CAR-6	157	17.810	8.86

Table 4.4: Physiochemical properties of transcript variants of CAR

Table 4.5

Ligand Name	G_Score (Kcal/mol)	AA-Name	Interaction Atom	HB-distance (Å)
CAR1(WT)	-11.0	ASN165 PHE161	N-H pi-pi	3.2
CAR2	-6.2	PHE161	pi-pi	3.4
CAR3	-9.2	ASN165	N-H	3.6
CAR4	-6.6	PHE164	pi-pi	3.5
CAR5	-	-	-	-
CAR6	-	-	-	-

Table 4.5: Molecular Docking interactions of CAR transcript variants with its ligand CITCO GScore indicates Glide Score; AA indicates amino acid name; HB indicates hydrogen bond.

References

1. Molnár F, Küblbeck J, Jyrkkärinne J, Prantner V, Honkakoski P. An update on the constitutive androstane receptor (CAR). Drug Metabol Drug Interact. 2013;28: 79–93. doi:10.1515/dmdi-2013-0009

2. Maglich JM, Sluder A, Guan X, Shi Y, McKee DD, Carrick K, et al. Comparison of complete nuclear receptor sets from the human, Caenorhabditis elegans and Drosophila genomes. Genome Biol. 2001;2: RESEARCH0029. Available: http://www.pubmedcentral.nih.gov/articlerender.fcgi?artid=55326&tool=pmcentrez&rendertype=abstract

3. Xie W, Barwick JL, Simon CM, Pierce AM, Safe S, Blumberg B, et al. Reciprocal activation of xenobiotic response genes by nuclear receptors SXR/PXR and CAR. Genes Dev. 2000;14: 3014–23. Available: http://www.pubmedcentral.nih.gov/articlerender.fcgi?artid=317112&tool=pmcentrez&rendertype=abstract

4. Baes M, Gulick T, Choi HS, Martinoli MG, Simha D, Moore DD. A new orphan member of the nuclear hormone receptor superfamily that interacts with a subset of retinoic acid response elements. Mol Cell Biol. 1994;14: 1544–52.

5. Choi HS, Chung M, Tzameli I, Simha D, Lee YK, Seol W, et al. Differential transactivation by two isoforms of the orphan nuclear hormone receptor CAR. J Biol Chem. 1997;272: 23565–71. Available: http://www.ncbi.nlm.nih.gov/pubmed/9295294

6. di Masi A, De Marinis E, Ascenzi P, Marino M. Nuclear receptors CAR and PXR:

Molecular, functional, and biomedical aspects. Mol Aspects Med. 2009;30: 297–343. doi:10.1016/j.mam.2009.04.002

7. Poso A, Honkakoski P. Ligand recognition by drug-activated nuclear receptors PXR and CAR: structural, site-directed mutagenesis and molecular modeling studies. Mini Rev Med Chem. 2006;6: 937–47. Available: http://www.ncbi.nlm.nih.gov/pubmed/16918499

8. Wagner M, Zollner G, Trauner M. Nuclear receptor regulation of the adaptive response of bile acid transporters in cholestasis. Semin Liver Dis. 2010;30: 160–77. doi:10.1055/s-0030-1253225

9. Honkakoski P. Characterization of a Phenobarbital-responsive Enhancer Module in Mouse P450 Cyp2b10 Gene. J Biol Chem. 1997;272: 14943–14949. doi:10.1074/jbc.272.23.14943

10. Gao J, Xie W. Targeting xenobiotic receptors PXR and CAR for metabolic diseases. Trends Pharmacol Sci. 2012;33: 552–8. doi:10.1016/j.tips.2012.07.003

11. Ueda A, Hamadeh HK, Webb HK, Yamamoto Y, Sueyoshi T, Afshari CA, et al. Diverse roles of the nuclear orphan receptor CAR in regulating hepatic genes in response to phenobarbital. Mol Pharmacol. 2002;61: 1–6. Available: http://www.ncbi.nlm.nih.gov/pubmed/11752199

12. Locker J, Tian J, Carver R, Concas D, Cossu C, Ledda-Columbano GM, et al. A common set of immediate-early response genes in liver regeneration and hyperplasia. Hepatology. 2003;38: 314–25. doi:10.1053/jhep.2003.50299

13. Columbano A, Ledda-Columbano GM, Pibiri M, Cossu C, Menegazzi M, Moore DD, et al. Gadd45beta is induced through a CAR-dependent, TNF-independent pathway in murine liver hyperplasia. Hepatology. 2005;42: 1118–26. doi:10.1002/hep.20883

14. Kobayashi K, Sueyoshi T, Inoue K, Moore R, Negishi M. Cytoplasmic accumulation of the nuclear receptor CAR by a tetratricopeptide repeat protein in HepG2 cells. Mol Pharmacol. 2003;64: 1069–75. doi:10.1124/mol.64.5.1069

15. Yan J, Chen B, Lu J, Xie W. Deciphering the roles of the constitutive androstane receptor in energy metabolism. Acta Pharmacol Sin. 2015;36: 62–70. doi:10.1038/aps.2014.102

16. Kawamoto T, Kakizaki S, Yoshinari K, Negishi M. Estrogen activation of the nuclear orphan receptor CAR (constitutive active receptor) in induction of the mouse Cyp2b10 gene. Mol Endocrinol. 2000;14: 1897–905. doi:10.1210/mend.14.11.0547

17. Crofts LA, Hancock MS, Morrison NA, Eisman JA. Multiple promoters direct the tissue-specific expression of novel N-terminal variant human vitamin D receptor gene transcripts. Proc Natl Acad Sci U S A. 1998;95: 10529–34. Available: http://www.pubmedcentral.nih.gov/articlerender.fcgi?artid=27928&tool=pmcentrez&rendertype=abstract

18. Fukuen S, Fukuda T, Matsuda H, Sumida A, Yamamoto I, Inaba T, et al. Identification of the novel splicing variants for the hPXR in human livers. Biochem Biophys Res Commun. 2002;298: 433–8. Available: http://www.ncbi.nlm.nih.gov/pubmed/12413960

19. Fiser A, Sali A. Modeller: generation and refinement of homology-based protein structure models. Methods Enzymol. 2003;374: 461–91. doi:10.1016/S0076-6879(03)74020-8

20. Martí-Renom MA, Stuart AC, Fiser A, Sánchez R, Melo F, Sali A. Comparative protein structure modeling of genes and genomes. Annu Rev Biophys Biomol Struct. 2000;29: 291–325. doi:10.1146/annurev.biophys.29.1.291

21. Laskowski RA, MacArthur MW, Moss DS, Thornton JM. PROCHECK: a program to check the stereochemical quality of protein structures. J Appl Crystallogr. International Union of Crystallography; 1993;26: 283–291. doi:10.1107/S0021889892009944

22. Suino K, Peng L, Reynolds R, Li Y, Cha J-Y, Repa JJ, et al. The nuclear xenobiotic receptor CAR: structural determinants of constitutive activation and heterodimerization. Mol Cell. 2004;16: 893–905. doi:10.1016/j.molcel.2004.11.036

23. Ferreira M, Cabado AG, Chapela M-J, Fajardo P, Atanassova M, Garrido A, et al. Cytotoxic activity of extracts of marine sponges from NW Spain on a neuroblastoma cell line. Environ Toxicol Pharmacol. 2011;32: 430–7. doi:10.1016/j.etap.2011.08.012

24. Halgren TA, Murphy RB, Friesner RA, Beard HS, Frye LL, Pollard WT, et al. Glide: a new approach for rapid, accurate docking and scoring. 2. Enrichment factors in database screening. J Med Chem. American Chemical Society; 2004;47: 1750–9. doi:10.1021/jm030644s

25. Yip DK, Auersperg N. The dye-exclusion test for cell viability: Persistence of

differential staining following fixation. In Vitro. 1972;7: 323–329. doi:10.1007/BF02661722

26. Xu RX, Lambert MH, Wisely BB, Warren EN, Weinert EE, Waitt GM, et al. A structural basis for constitutive activity in the human CAR/RXRalpha heterodimer. Mol Cell. 2004;16: 919–28. doi:10.1016/j.molcel.2004.11.042

27. Jakobsson T, Treuter E, Gustafsson J-Å, Steffensen KR. Liver X receptor biology and pharmacology: new pathways, challenges and opportunities. Trends Pharmacol Sci. 2012;33: 394–404. doi:10.1016/j.tips.2012.03.013

28. Xu C, Li CY-T, Kong A-NT. Induction of phase I, II and III drug metabolism/transport by xenobiotics. Arch Pharm Res. 2005;28: 249–68. Available: http://www.ncbi.nlm.nih.gov/pubmed/15832810

29. Arnold KA, Eichelbaum M, Burk O. Alternative splicing affects the function and tissue-specific expression of the human constitutive androstane receptor. Nucl Recept. 2004;2: 1. doi:10.1186/1478-1336-2-1

30. Lamba JK, Lamba V, Yasuda K, Lin YS, Assem M, Thompson E, et al. Expression of constitutive androstane receptor splice variants in human tissues and their functional consequences. J Pharmacol Exp Ther. 2004;311: 811–21. doi:10.1124/jpet.104.069310

31. Faucette SR, Zhang T-C, Moore R, Sueyoshi T, Omiecinski CJ, LeCluyse EL, et al. Relative activation of human pregnane X receptor versus constitutive androstane receptor defines distinct classes of CYP2B6 and CYP3A4 inducers. J Pharmacol Exp Ther. 2007;320: 72–80. doi:10.1124/jpet.106.112136

32. Dring AM, Anderson LE, Qamar S, Stoner MA. Rational quantitative structure-activity relationship (RQSAR) screen for PXR and CAR isoform-specific nuclear receptor ligands. Chem Biol Interact. 2010;188: 512–25. doi:10.1016/j.cbi.2010.09.018

33. Honkakoski P, Sueyoshi T, Negishi M. Drug-activated nuclear receptors CAR and PXR. Ann Med. Taylor & Francis; 2009;35: 172–182. doi:10.1080/07853890310008224

34. Huang W, Zhang J, Chua SS, Qatanani M, Han Y, Granata R, et al. Induction of bilirubin clearance by the constitutive androstane receptor (CAR). Proc Natl Acad Sci U S A. 2003;100: 4156–61. doi:10.1073/pnas.0630614100

35. Reschly EJ, Krasowski MD. Evolution and function of the NR1I nuclear hormone receptor subfamily (VDR, PXR, and CAR) with respect to metabolism of xenobiotics and endogenous compounds. Curr Drug Metab. 2006;7: 349–65.

36. Krasowski MD, Yasuda K, Hagey LR, Schuetz EG. Evolutionary selection across the nuclear hormone receptor superfamily with a focus on the NR1I subfamily (vitamin D, pregnane X, and constitutive androstane receptors). Nucl Recept. 2005;3: 2. doi:10.1186/1478-1336-3-2

37. Maglich JM, Parks DJ, Moore LB, Collins JL, Goodwin B, Billin AN, et al. Identification of a novel human constitutive androstane receptor (CAR) agonist and its use in the identification of CAR target genes. J Biol Chem. 2003;278: 17277–83. doi:10.1074/jbc.M300138200

Chapter 5: Development of an *in vitro* porcine model for drug metabolism and toxicity assessment

Abstract

To date, *in vitro* cytotoxicity assays are not highly predictive of *in vivo* toxicity. There is a critical need for more predictive and reliable *in vitro* testing methods. Due to its physiological similarities with humans, pigs have emerged as a suitable and reliable animal model for pharmacological and toxicological studies. To further the pigs' suitability, we have developed and characterized a transformed porcine hepatocyte cell line (pHCC) to support drug toxicity and metabolism assessments. Porcine primary hepatocytes had similar morphology to human and expression values of the most important drug metabolism genes involved in phase I and II drug metabolism, phase-III transport were comparable to human primary hepatocytes. However, primary hepatocytes have a limited life span in culture and usually within 8 days post culture more than 50% of cells undergo apoptosis. Moreover, normal gene expression declines from day 5 in culture. To overcome these limitations, we have generated and characterized transformed hepatocyte cell lines (pHCC) derived from the transgenic Oncopig. Three independent hepatocyte cell lines were developed from three different Oncopigs and all of them expressed hepatocyte specific and most important drug metabolism and regulation genes comparable to those porcine primary hepatocytes. We evaluated the effect of selective CYP modulators on three pHCC and pPH cell lines. All the three independent pHCC cell lines behaved the same way and the gene regulation pattern in pHCC was similar to that of primary hepatocytes and human models. Exposure of pHCC cells to hepatotoxic drugs

caused a concentration-dependent decrease in cell viability comparable to those of human models. These findings indicate that this porcine hepatocyte cell line represents a useful and predictive model for high throughput screening of new drugs as well as studies on metabolism and hepatotoxicity of chemicals.

Introduction

Major reasons that contribute to the failure of a drug in preclinical and clinical studies are toxicity and efficacy. The adverse effects of new drugs are often not discovered until preclinical animal safety studies or even clinical trials; 40% of drugs fail in preclinical animal studies and 89% of those that reach clinical trials fail [1]. There is a critical need for more predictive and reliable *in vitro* testing methods. A good *in vitro* model can identify issues related to toxicity early in the discovery process thereby saving millions of dollars.

Metabolism of a drug or xenobiotics is critical for its pharmacokinetic properties, and the liver is the main organ of drug or xenobiotics biotransformation (Lübberstedt et al., 2011; Tuschl et al., 2009). The cytochrome P450 (CYP) isozymes expressed in the hepatic tissue constitute the major enzyme family capable of catalyzing the oxidative biotransformation of most drugs and lipophilic xenobiotics [4]. Primary human hepatocytes are considered the standard model for drug metabolism and toxicity studies as they provide a complete picture of the metabolic fate of xenobiotics *in vitro* (Lübberstedt et al., 2011; Brandon et al., 2003). However, primary human hepatocytes have limited availability and undergo early and variable phenotypic alterations in culture [5]. Most of the human liver cell lines have poor or fractional CYP expression [4,6,7]. To date, the lack of a reliable animal model for assessment

of drug toxicity and metabolism is a major limitation in early high throughput screening of xenobiotics. Immunological and physiological differences between rodents and humans represent major constraints for the use of rodent-based models in drug screening. Therefore, a large animal model surrogate for human hepatocytes is a very important improvement over the current methods for early screening of novel drugs and xenobiotics.

Over the years, the pig has gained increasing importance as a biomedical model due to similarities in size, anatomy and physiology with humans [8–10]. CYP enzymes have been extensively studied in pigs and enzymes equivalent to human P450 (eg. CYP1A, 2A6, 2E1, 3A4) have been identified in pig liver [11–13]. The sequence identity between human and porcine P450 enzymes is striking, ranging from 72 to 95 % [13]. Biotransformation data indicate that the CYP1A, 2A and 3A enzyme systems seem to be functionally very similar between pigs and humans [14,15]. In addition, the characterization of the porcine pregnane X receptor [16] and farnesoid X receptor [17] has been reported. In the present study, we developed and characterized a porcine hepatocyte cell line (pHCC) to be utilized for screening drug toxicity and metabolism assessment.

Materials and Methods

Reagents

All chemicals were purchased from Sigma-Aldrich (USA) unless stated otherwise. Cell culture plastics were from Midsci, USA.

Animals

All animal studies and procedures were approved by The University of Illinois Institutional Animal Care and Use Committee (IACUC; Protocol number 11221). Transgenic Oncopigs carrying Cre recombinase inducible transgenes encoding $KRAS^{G12D}$ and $TP53^{R167H}$, which represent a commonly mutated oncogene and tumor suppressor in human cancers [18], were utilized for experiments described here.

Porcine hepatocyte isolation and culture

Porcine primary hepatocytes (pPH) were isolated from three Oncopigs (Pig no 316, 326 and 327) and were denoted as pPH1, pPH2 and pPH3. The modified procedure of Meng's method [19] utilizing manual perfusion along with enzymatic digestion was used to isolate functionally viable hepatocytes from a single lobe of Oncopig liver. Immediately after the animal was euthanized, a portion of the liver lobe was resected, washed 2-3 times with ice cold PBS and transported to the laboratory in ice cold Krebs Ringer Solution. Then the liver sample was cannulated with a suitable pipette into visible blood vessels on the cut surface and flushed with 500 mL of buffer A containing 8.3 g/L NaCl, 0.5 g/L KCl, 2.4 g/L HEPES and 0.19 g/L EGTA at pH 7.4 and 37°C. This was followed by perfusion of 500 mL buffer B containing 8.3 g/L NaCl, 0.5 g/L KCl and 2.4 g/L HEPES. Perfusion was then carried out on the tissue using a pre-warmed (37 °C) digestion buffer (Buffer C) containing 3.9 g/L NaCl, 0.5 g/L KCl, 2.4 g/L HEPES, 0.7 g/L $CaCl_2$ X $2H_2O$ and 0.1 % collagenase (type IV). Following digestion, the liver capsule was removed and dissolved cells were liberated by gentle shaking of the liver specimen in ice cold buffer D containing 9.91 g/L HBSS (without calcium and magnesium), 2.4 g/L HEPES and 2.0 g/L BSA. A scalpel was

used to cut through the regions which were not well perfused to release cells contained within. The resulting cell suspension was filtered through a nylon mesh with 100 µm pore size and centrifuged at 50 X g for 3 min at 4°C. After, cells were incubated in DNase1 containing buffer at 4°C for 10 min to digest cell clumps. Then the resulting suspension was filtered through 70µm nylon mesh and cells were harvested by centrifugation at 50 X g for 3 min. This was followed by three washing in ice cold buffer D. The resulting cell clumps were finally re-suspended in culture medium (William's E supplemented with 100 mU/mL penicillin, 100 µg/mL streptomycin, 2 mM glutamate and 10% FBS). Viability of hepatocytes was determined by trypan blue dye exclusion test [20].

Freshly isolated hepatocytes were cultured in William's E medium supplemented with 100 mU/mL penicillin, 100 µg/mL streptomycin, 2 mM glutamate and 10% FBS in either collagen coated or uncoated flask.

Collagen coating

A final concentration of 1.5 mg/mL rat tail collagen I in DMEM was used for the coating of flasks. The pH of the collagen was adjusted to 7.4 using DMEM. A volume of 1 mL was used for a 25 cm^2 (T25) flask and dried overnight in a tissue culture hood. Approximately, 2 X 10^6 cells were seeded with 5 mL of culture medium into a T25 culture flask. Five hours following seeding, culture medium along with unattached cells were removed and replaced with fresh medium. Medium were replaced with fresh medium every 24 h.

Cell viability and cell proliferation of hepatocytes

The MTT assay was used to assess hepatocyte growth in culture. The reduction of tetrazolium salts is now widely accepted as a reliable way to examine cell proliferation. The yellow tetrazolium MTT (3-(4, 5-dimethylthiazolyl-2)-2, 5-diphenyltetrazolium bromide) is reduced by metabolically active cells, in part by the action of dehydrogenase enzymes, to generate reducing equivalents such as NADH and NADPH. The resulting intracellular purple formazan can be solubilized and quantified by spectrophotometric means. For the MTT assay, hepatocytes were seeded in a 96 well plate at a density of 10^4 cells/100 µL/well. The MTT assay was done by incubating 100 µl MTT reagent (1 mg/mL) per well for 4 h at 37° C. After 4 h, the formazan crystals were dissolved by adding 100 µL of DMSO. Then the optical density was measured at 570 nm in a microplate reader (SpectraMax Plus, Molecular Devices, USA).

Apoptosis assay

The FITC Annexin V/Dead Cell Apoptosis Kit (Invitrogen, Life Technologies, USA) was used for the measurement of apoptosis. In normal live cells, phosphatidylserine (PS) is located on the cytoplasmic surface of the cell membrane. However, in apoptotic cells, PS is translocated from the inner to the outer leaflet of the plasma membrane, thus exposing PS to the external cellular environment [21]. The human anticoagulant, annexin V, is a 35–36 kDa Ca^{2+}-dependent phospholipid-binding protein that has a high affinity for PS [22]. Annexin V labeled with a

fluorophore can identify apoptotic cells by binding to PS exposed on the outer leaflet [23]. Flow cytometric quantification of hepatocyte apoptosis was performed on day 1, 3, 5, 8 and 15 of culture. In brief, the cells were harvested, washed in PBS and stained with Annexin V-FITC and propidium iodide. The cells were incubated at room temperature for 15 min and fluorescence measured by flow cytometry (BD LSR II Flow Cytometer, BD Biosciences, USA). The data was analyzed using FCS Express 4 software.

Ad-Cre activation of the Oncopig primary Hepatocytes

Oncopig [18] hepatocytes were isolated and cultured as described above. On day 2 of culture, the medium was changed to low serum (5% FBS) and Ad5CMVCre-eGFP recombinase (AdCre; University of Iowa Vector Core) was added at multiplicity of infection (MOI) of 200 to 500 as previously described [18]. Cells were incubated for 5 h at 37° C, after which AdCre medium was removed and replaced with fresh medium (10% FBS). Three hepatocyte cell lines (pHCC1, pHCC2 and pHCC3) were developed. The hepatocyte cell lines (pHCCs) were passed after reaching 80% confluence. The expression of transgenes ($KRAS^{G12D}$ and $TP53^{R167H}$) was determined by RT-PCR as described by [18].

Doxorubicin sensitivity assay

Doxorubicin sensitivity of the pPH and pHCC cell lines was determined by MTT assay. Cells were seeded in 96-well plates (1×10^4 cells/well) in William's E medium with 10% FBS. 24 h after plating, the cells were treated with doxorubicin (0-4 µg/mL)

and incubated for 72 h at 37° C in an atmosphere of 5% CO_2. Untreated pHCC cells were used as control. The MTT assay protocol was followed as described above.

DMSO treatment of the pHCC cells

pHCC cells were seeded at low density (2 X 10^4 cells/cm^2) in supplemented William's E (10% FBS, 100 mU/mL penicillin, 100 µg/mL streptomycin, 2 mM glutamate). At confluence, the medium was supplemented with 2% DMSO. The medium was changed every 2-3 days. The cells were cultured in presence of DMSO for 15 days before using for further experiments.

RNA Isolation

Total RNA was isolated from pPH and pHCC cell lines (cultured in presence or absence of DMSO) using RNeasy Mini Kit (Qiagen) as per the manufacturer's protocol. RNA pellets were dissolved in nuclease-free water and stored at -80°C until analysis. Quality of the RNA was determined using NanoDrop spectrophotometer and analyzed by an Agilent 2100 Bioanalyzer to determine RNA integrity as well as the presence/absence of gDNA by the Carver High-Throughput DNA Sequencing and Genotyping Unit (HTS lab, University of Illinois, Urbana, IL, USA). The concentration of the RNA was determined by Qubit® RNA HS Assay Kit (Thermo Fisher Scientific, Life Technologies) as per manufacturer's protocol.

RT-PCR

Reverse transcription of RNA was performed from 1 µg total RNA in the presence of RNase inhibitor, random hexamer primers (50 ng/µL), deoxynucleotides (dNTPs, 10 mM), SuperScript III reverse transcriptase (200 U/µL) and reverse transcriptase buffer in a 20 µL final reaction volume using SuperScript III First-Strand Synthesis System for RT-PCR kit (Invitrogen,Life Technologies, IN, USA). PCR reactions were performed in a 25 µl reaction volume containing 50 ng cDNA as the template, 0.5 M of each primer, 2X PCR buffer (including 1.5 mM $MgCl_2$), 200 mM dNTPs, and 0.625 units of Taq DNA polymerase. The PCR primer sequences and PCR conditions are given in table 5.1.

Quantitative RT-PCR

Reverse transcription of RNA was performed as stated above. Relative quantification of the genes was performed by using Power SYBR green PCR Master Mix (2X) (Applied Biosystems) in a Taqman ABI 7900 Real-Time PCR system (Applied Biosystems). Information on primer used are listed in Table 5.2. The thermal cycling conditions for real-time PCR were one cycle of 50 °C for 2 min (AmpErase uracil-N-glycosylase activation) and 95°C for 10 min (AmpliTaq Gold activation), followed by 40 cycles of 95°C for 15 sec (denaturation) and 60°C for 1 min (annealing and extension).The housekeeping genes GAPDH and ACTB were used as endogenous controls to normalize for RNA loading or differences in reverse transcription efficiency. Gene expression levels were calculated using the $2^{-\Delta\Delta Ct}$ method relative to the internal control.

Evaluation of the effect of selective CYP modulators

The effects of selective CYP modulators on the expression of a number of drug metabolism enzymes (DMEs) in pPH and pHCC cells (+DMSO) were evaluated. The compounds were well-documented selective modulators of CYPA1/2 (3-methylcholanthrene), CYP3A (Rifampicin) and CYP2A6, CYP2B6, CYP3A (Phenobarbital) [24]. Porcine primary hepatocytes (day 1 of culture) and pHCC cells (pass 8) were exposed to 2 µM 3-methylcholanthrene or 1 mM phenobarbital or 50 µM rifampicin in separate experiments. The culture medium was removed and replaced with serum free medium containing test compound and incubated for 24 h. The mRNA levels corresponding to major drug metabolizing porcine P450 enzymes were measured by quantitative RT-PCR.

Evaluation of drug cytotoxicity

The effects of four reference hepatotoxic drugs, namely Aflatoxin B1 (AFB_1), amiodarone, chlorpromazine and acetaminophen were evaluated on porcine primary hepatocytes (day 1 of culture) and pHCC cell lines cultured in presence of DMSO at two different passages (8^{th} and 15^{th}) at 72 h after exposure. Incubations were performed with medium free from DMSO and FBS. At the end of the incubation time, the MTT assay was performed as described above.

Statistical analysis

Data are expressed as mean ± SD. Statistical significance was evaluated by using one-way analysis of variance (ANOVA) followed by Dunnett post-test or by

using a paired student's t test (two-tailed). Differences were considered significant when $p \leq 0.05$. All data was analyzed by Graphpad-prism 6.

Results

Porcine hepatocytes display similar morphology to human hepatocytes, are epithelial in origin, and express hepatocyte specific functional genes

To determine whether porcine hepatocytes have similar morphology to humans, the morphology of freshly isolated and cultured Oncopig hepatocytes were observed. The freshly isolated viable hepatocytes were bright, translucent and spherical in shape. After 24 h of culture, the hepatocytes had attached, aggregated into clusters and established cell-cell interactions. The arrangement showed typical liver morphological appurtenance with polygonal cells, containing granular cytoplasm and two or more nuclei (Figure 5.1A). The morphology of the cultured hepatocytes was similar to that of human [25]. Immunohistochemistry showed that the cells were positive for cytokeratin (Figure 5.1B) and negative for vimentin (Figure 5.1C) which indicates that they are epithelial in origin. Further characterization showed that each of the three primary hepatocyte cell lines examined expressed the hepatocyte specific genes albumin (ALB), glucose-6-phosphatase (G6PC) and hepatocyte nuclear factor 4 alpha (HNF4A) (Figure 5.3).

Relative abundance of drug metabolizing enzyme genes in porcine primary hepatocytes is consistent with human primary hepatocytes

Relative abundance of the most important drug metabolism enzyme genes in the porcine primary hepatocytes (Day 1 of culture) isolated from three different pigs was

investigated by quantitative PCR. Expression value of the genes was calculated based on the assumption that average expression level of two housekeeping genes GAPDH and ACTB is 1. The results are presented in table 5.3. The expression values of the DME genes were similar in all the three porcine primary hepatocytes and comparable to those of human primary hepatocytes reported by Guo et al., 2011 [7]. Among the phase I DMEs, CYP2C49, CYP2C33, CYP3A and CYP1A2 transcripts were highly abundant. GSTO1 was the most abundant phase II drug metabolism enzyme transcript. Among the transporters, the expression value of ABCC2 transcript was highest. Overall, the relative abundance and expression level of the porcine drug metabolism genes in porcine hepatocytes are comparable to that of human primary hepatocytes.

Primary porcine hepatocytes have limited life span in culture

To determine life span and growth kinetics of primary hepatocytes in culture, a MTT assay was performed on hepatocytes from three different Oncopigs mentioned previously. The growth and viability of the hepatocytes was assessed on days 1, 3, 5, 8, and 15 of culture. Primary hepatocyte from all three above mentioned animals continued to divide up to 5 days after isolation, after which growth receded in both collagen coated and uncoated culture conditions (Figure 5.2A).

We also examined the effect of culture length on hepatocyte apoptosis. The number of apoptotic cells increased with time in culture (Figure 5.2 B-F). Primary hepatocytes on culture day 1 consisted of 6.45 % apoptotic cells, increasing to 18.45, 22.60 and 44.23 % at culture day 5, 8, and 15, respectively (Figure 5.2G). Based on the MTT assay and apoptosis analysis, it is clear that primary hepatocytes have a

limited life span in culture, with more than 50% of cells undergoing apoptosis by day 15 of culture. Human primary hepatocytes also have a limited survival time in culture; survives 2-3 weeks when maintained in standard culture conditions[2,5].

Reduced expression of hepatocyte specific and DME transcripts in primary hepatocytes over time in culture

To study whether primary hepatocytes maintain hepatocyte specific functions in culture, we studied the expression of ALB, G6PC and sixteen other genes involved in drug metabolism and regulation in the three primary hepatocytes (pPH1, pPH2, pPH3) at different days of culture (Table 5.4 and Figure 5.4). In each of the three lines, most of the genes were downregulated from culture day 5, with 3-13 fold reductions in expression observed on culture day 15 (Table 5.4). Overall, transcript levels of CYPs, phase II DMEs, and transporters were not maintained in culture. Similar findings were reported in human primary hepatocytes [26].

Hepatocyte cell lines (pHCC) are highly proliferative and have unlimited life span in culture

To overcome the limitations of primary hepatocytes, we activated the Oncopig primary hepatocytes by Ad-Cre. The three Oncopig primary hepatocyte cell lines were transformed into pHCC lines through exposure to AdCre. Hepatocyte specific functional gene expression was observed in the pHCC cell lines following activation, in addition to oncogenic $KRAS^{G12D}$ and $pTP53^{R167H}$ expression (Figure 5.3). The cells were elongated, and were characterized by a clear cytoplasm and active cell divisions

(Figure 5.1D). The pHCC cells have been maintained in culture for 63 passages and have a recovery rate of more than 90% in cryopreservation.

To further validate that the pHCC cells are transformed and have unlimited life span, we studied the sensitivity of the pHCC cells to doxorubicin *in vitro*, observing a higher sensitivity of the pHCC cells to doxorubicin than the primary hepatocytes (Figure 5.5). Doxorubicin treatment reduced the number of viable pHCC cells to less than 50% at concentrations from 0.5 µg/mL whereas 4 µg/mL doxorubicin was required for the same effect in the primary hepatocytes.

pHCC cells expressed most important drug metabolism and regulator genes at levels significantly lower than primary hepatocytes

We studied the expression of hepatocyte specific functional genes and most important genes involved in drug metabolism, transport and regulation in all the three pHCC cell lines in two passes (pass 8 and pass 15) by qPCR. All the three pHCC cell lines expressed all the major drug metabolism and regulation genes tested (Figure 5.6). However, a significant downregulation of most of the CYP genes was observed in all the three pHCC cells compared to primary hepatocytes, in addition to reduction in the expression of ALB and G6PC (Figure 5.7). Most of the CYPs involved in phase I drug metabolism were downregulated in the range of 4 to 25 fold. The genes involved in phase II drug metabolism showed varying differences in expression (Figure 5.8); SULT1B1, SULT2A1 and GSTO1 were unchanged whereas SULT1A3 was upregulated. Transporter ABCB1, ABCB6 and ABCC3 were upregulated. All the nuclear receptors involved in the regulation of drug metabolism except NR1H4 were downregulated from 2 to 10 fold (Figure 5.9). In brief, although pHCC cells express

the major drug metabolism and regulator genes tested, a marked decline in CYPs and nuclear receptors compared to those of primary hepatocytes was observed (Figure 5.10).

pHCC cells cultured in presence of DMSO express drug metabolism and regulation genes comparable to primary hepatocytes

Many researchers reported that treatment of DMSO improved the expression of CYPs in hepatocyte cell lines [7,26]. To improve the expression level of the drug metabolism and regulator genes, pHCC cells were cultured in the presence of DMSO in culture medium for 15 days. When cultured in William's E medium in presence of 2% DMSO, the all three pHCC cells showed hepatocyte like morphology, granular in shape (Figure 5.1E-F) and expressed hepatocyte specific functional genes like ALB, G6PC and HNF4A (Figure 5.3).

Expressions of the hepatocyte specific functional genes and the most important genes involved in drug metabolism and regulation in all three pHCC cells (+DMSO) of two different passages (Pass 8 and Pass 15) were compared to day 1 cultured Oncopig hepatocytes (Figure 5.7-5.10). The expression of the drug metabolism and regulation genes in all the three independent pHCC cell lines were similar (Figure 5.10). We studied expression of the ten most important CYPs (CYP1A1, CYP1A2, CYP2A19, CYP2B22, CYP2C33, CYP2C42, CYP2C49, CYP2E1, CYP3A and CYP7A1) and all of them except CYP1A1 and CYP7A1 had expressions comparable to those of primary hepatocytes (Figure 5.7). CYP1A1 had reduced expression in both passes and CYP7A1 had reduced expression in passage 8 of pHCC (+DMSO) cells than primary hepatocytes. We studied four genes involved in phase-II drug

metabolism (SULT1A3, SULT1B1, SULT2A1 and GSTO1) and four transporters (ABCB1, ABCC2, ABCB6 and ABCC3). No significant difference in SULT1B1, SULT2A1 and GSTO1 expression between pHCC (+DMSO) and primary hepatocytes was observed whereas an upregulation of SULT1A3 was found in pHCC (+DMSO) (Figure 5.8). The transporter ABCB1 was upregulated in pHCC (+DMSO) compared to cultured primary hepatocytes (Figure 5.8). The relative expressions of seven main nuclear receptors involved in regulation of drug metabolism (NR1I3, NR1I2, NR1H4, RXRA, RXRB, PPARA and PPARG) were compared between pHCC (+DMSO) and primary cultured hepatocytes (Figure 5.9). The expressions of all the nuclear receptors were not significantly different. Overall, when pHCC cells were cultured in presence of 2% DMSO for 15 days, the expression levels of the hepatocyte specific genes and most of the genes involved in drug metabolism and regulation were comparable to primary hepatocytes.

Gene regulation by selective CYP modulators in pHCC cells cultured in presence of DMSO follows a similar pattern as in primary hepatocytes and human models

To validate the effectiveness of the pHCC cells as a model of drug metabolism, the effect of three selective CYP modulators on all three pHCC cells cultured in the presence of DMSO were evaluated and compared to primary hepatocytes and human models. The compounds were known inducers of CYPA1/2 (3-methylcholanthrene), CYP3A (Rifampicin) and CYP2A6, CYP2B6, CYP3A (Phenobarbital) [24]. Treatment of 3-methylcholanthrene caused a significant upregulation of CYPA1 and CYPA2 in both primary hepatocytes and all three pHCC

cell lines (Figure 5.11), while the expressions of other CYPs remained unchanged. Upregulation of CYP2A19, CYP2B22 and CYP3A occurred following exposure to rifampicin. Phenobarbital exposure caused upregulation of several CYPs including CYP2A19 which is equivalent to human CYP2A6 [13], CYP2B22 and CYP3A (Figure 5.11). Interestingly, the results obtained in this study are consistent with those available from human hepatocytes [27] and from human clinical studies [28] supporting the idea that this *in vitro* model is reliable for evaluating the potential of new drugs as P450 modulators.

pHCC cells (+DMSO) recapitulate toxicity responses of primary hepatocytes and human models

To validate the suitability of the pHCC cells as a drug toxicity model, the cytotoxicity of four hepatotoxic compounds was evaluated on three pHCC cells (cultured in presence of DMSO) and compared to primary hepatocytes. Toxicity of four reference hepatotoxic compounds, namely Aflatoxin B1 (AFB_1), amiodarone, chlorpromazine and acetaminophen, was estimated on primary hepatocytes and pHCC cell lines at two different passages (pass 8 and pass 15) using standard MTT assay (Figure 5.12). No significant difference between pHCC cell lines and primary hepatocytes were observed. All four chemicals were toxic for the cell lines and as expected, AFB1 was the most toxic one. At 72 hr, no viable cells were observed with AFB1 concentrations greater than 10 µM. For the other three drugs, cell viability also decreased in a concentration-dependent manner. At 72 hr, the IC_{50}s for amiodarone, chlorpromazine and acetaminophen were around 15 µM, 20 µM and 5 mM

respectively. The IC_{50} values of the compounds on pHCC ((+DMSO) cells were comparable to human hepatocytes and other in *vitro* human models [26].

Discussion

A key challenge in drug candidate screening and development of new chemical entities (NCE) or new biological entities (NBE) as therapeutic agents is accurate determination of their toxicity and metabolism assessment [29,30]. Human primary hepatocytes are generally used for xenobiotic metabolism and toxicity assessment, however they have a lot of limitations [26,31]. Human primary hepatocytes have scarce and unpredictable availability, limited growth activity and undergo early phenotypic alterations [7]. Moreover, the expression levels of all P450s are not similarly maintained over time in culture. Several approaches have been reported to improve the preservation of liver specific functions in primary hepatocyte cultures, including the use of sandwich configuration by an additional layer of extracellular matrix [32]. However, marked phenotypic changes have been observed resulting in reduced expression of several CYPs [26]. An attractive alternative source of hepatocytes would be immortalized cells, which could make the unlimited supply of cells exhibiting the characteristics of differentiated hepatocytes feasible [33]. Most of the human hepatocyte cell lines, whether of tumoral origin or obtained by oncogenic transformation, lack a variable and substantial set of liver specific functions and consequently are unsuitable for mimicking *in vivo* normal parenchyma cells [5]. For example, the HepG2 cell line retains various hepatic functions but contain little CYP activity [25,34]. Immunological and physiological differences between rodents and humans represent major constraints for the use of rodent based models in drug

screening. Moreover, it is well known that induction responses in rats differ from those of humans due to sequence differences in the ligand domain of the nuclear receptor genes and CYP response element [35]. Therefore a large animal *in vitro* model will be highly beneficial for initial screening of novel drugs. In the present study we have developed a porcine hepatocyte cell line (pHCC) which overcomes the limitations of the primary hepatocytes and available human cell lines. pHCC cells have unlimited life span in culture, have a recovery rate of more than 90% in cryopreservation and when cultured in presence of a DMSO, mimic primary hepatocytes in terms of expression of major drug metabolism and regulation enzymes supporting the idea that this *in vitro* model can be a better model for high throughput screening of new drugs as well as studies on metabolism and hepatotoxicity of chemicals.

Cytochrome P450 enzymes responsible for drug metabolism have been extensively studied in pig and enzymes equivalent to human P450s have been identified in pig liver [12]. Porcine and human enzymes from the same P450 subfamily seem to have the highest sequence homology and the same substrate specificity [13,36]. Genetically, pigs bear key sequence homology to humans in xenobiotic receptors, which are divergent in mice that are responsible for modulating the metabolism of drugs [8]. In the present study, we have developed pHCC cell lines originating from transgenic Oncopigs. pHCC cells, when cultured in media containing 2% DMSO, showed hepatocyte like morphology including granular shape and the expression of the hepatocyte specific genes ALB, G6PC, and HNF4A (Figure 5.3).

Porcine hepatocyte cell lines cultured in the presence of DMSO expresses genes involved in phase I and phase II drug metabolism, phase III transporters comparable

to those of day 1 culture of primary hepatocytes (Figure 5.7-5.10). They can be used as a surrogate to hepatocytes to study drug metabolism and toxicity. Ten P450s responsible for the metabolism of 90% of drugs were analyzed. When comparisons were made with primary hepatocytes, the expression level of all the studied P450s except CYP1A1 and CYP7A1 in pHCC (+DMSO) was comparable to primary hepatocytes. In the human HEPG2 cell line, no transcripts were detected for CYPs 2B6, 2C9, 2E1 and 3A4 [5]. Recently, HepaRG cells derived from a human liver hepatocellular carcinoma in presence of DMSO have been shown to express liver function genes and major CYPs at levels markedly lower (5-50 fold) than primary hepatocytes [26,37]. In contrast, porcine pHCC cells have the potential to express most of the CYPs at level comparable to primary hepatocytes. Expression of Glutathione-S-Transferase O1 in the pHCC cell lines was comparable to cultured hepatocytes, while SULT1A1 were upregulated. Nuclear receptors NR1I2, NR1H4, RXR, NR1I3 and PPARA play the most important roles in regulating most of the drug metabolizing enzymes and transporters [38] and have been considered the key xenobiotic sensors for years. These receptors, which are most highly expressed in the liver, were also expressed in the porcine hepatocyte cell lines in presence of DMSO at level comparable to primary hepatocytes (Figure 5.8).

We studied the effect of three selective CYP modulators on hepatocyte cell lines and primary hepatocytes. 3-methylcholanthrene is a selective inducer of CYP1A1/2 [24]. In contrast, phenobarbital and rifampicin increases several enzymes [24,39]. In the present study, 3-methylcholanthrene treatment induced significant increases in the expression of CYP1A2 and CYP1A1 and phenobarbital and rifampicin

significantly increased the expression of several CYPs in both primary hepatocytes and pHCC (+DMSO) cell lines (Figure 5.11). The results obtained in this study are consistent with those of human primary hepatocytes and from clinical studies [27,28,40] which support the idea that this *in vitro* model is reliable for evaluating the potential of new drug entities.

In agreement with the active expression of phase-I and phase-II xenobiotic-metabolizing enzymes, the suitability of the hepatocyte cell lines cells for determination of chemical metabolism profiles was supported by the cytotoxicity effects of several hepatotoxicants (Figure 5.12). Toxicity of AFB1 and acetaminophen is dependent on electrophilic metabolites by P450 dependent reactions [41]. AFB1 and acetaminophen showed marked toxicity on pHCC cells, indicating that they express the different enzymes involved in the biotransformation at suitable levels.

In conclusion, we have developed a hepatocyte cell lines derived from the transgenic Oncopig. Our results demonstrate that, in conditions in which cells attain a differentiated hepatocyte-like morphology, drug metabolism enzymes remain at levels comparable to those measured in primary hepatocytes. hepatocyte cell lines represent a porcine hepatocyte cell line, capable of expressing both phase-I and phase-II drug metabolism enzymes as well as membrane transporters normally found in liver. They represent a prominent alternative to primary hepatocytes. They overcome the limitations of primary hepatocytes and available human cell lines, can be easily cryopreserved and functional activity remain stable over several passages. They have the ability to carry out normal biotransformation reactions by metabolic CYP enzymes, which are required for toxicity of some chemicals, making the cell line

a potentially useful model for toxicological testing. In conclusions, hepatocyte cell lines represent a useful and predictive model for high throughput screening of new drugs as well as studies on metabolism and hepatotoxicity of chemicals.

Figures and Tables

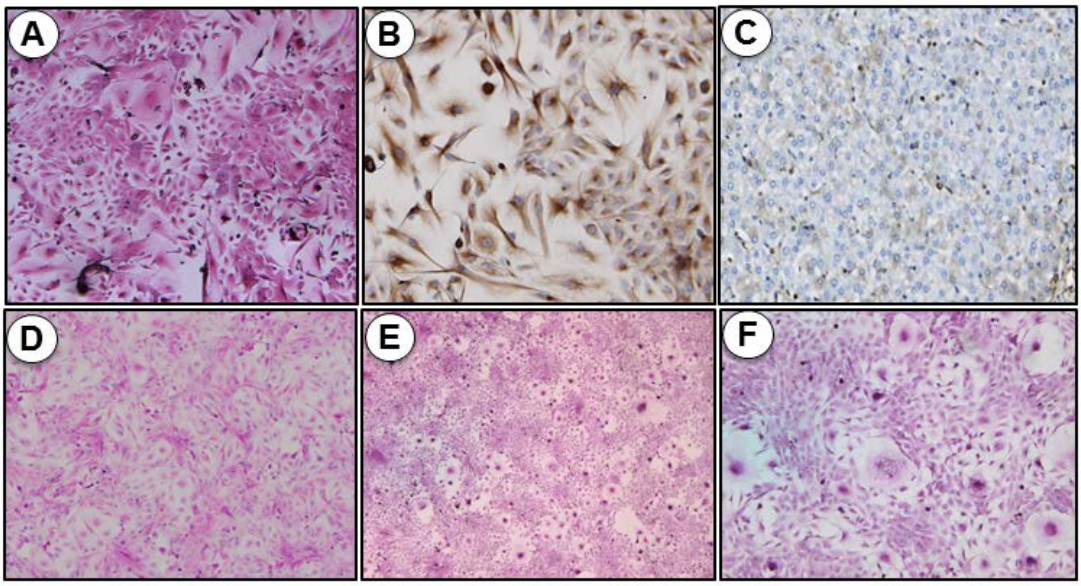

Figure 5.1. Morphology of porcine primary hepatocytes (pHC) and Hepatocyte Cell Lines (pHCC)

All the three porcine primary hepatocytes (pPH) showed similar morphology; pPH1 is presented in the figure. Same is true for hepatocyte cell lines (pHCC)

(A) H&E stained porcine primary hepatocytes; the cells are polygonal in shape with granular cytoplasm. (B) Expression of cytokeratin in primary hepatocytes. (C) Vimentin staining of the primary hepatocytes; primary hepatocytes were negative for vimentin. (D) H&E stained pHCC cells cultured in absence of DMSO (20X). The cells are elongated, characterized by a clear cytoplasm and actively dividing cells. (E) H&E stained pHCC cells cultured in presence of 2% DMSO (10X) (F) H&E stained pHCC cells cultured in presence of 2% DMSO (40X). The cells are granular in shape and show hepatocyte like morphology.

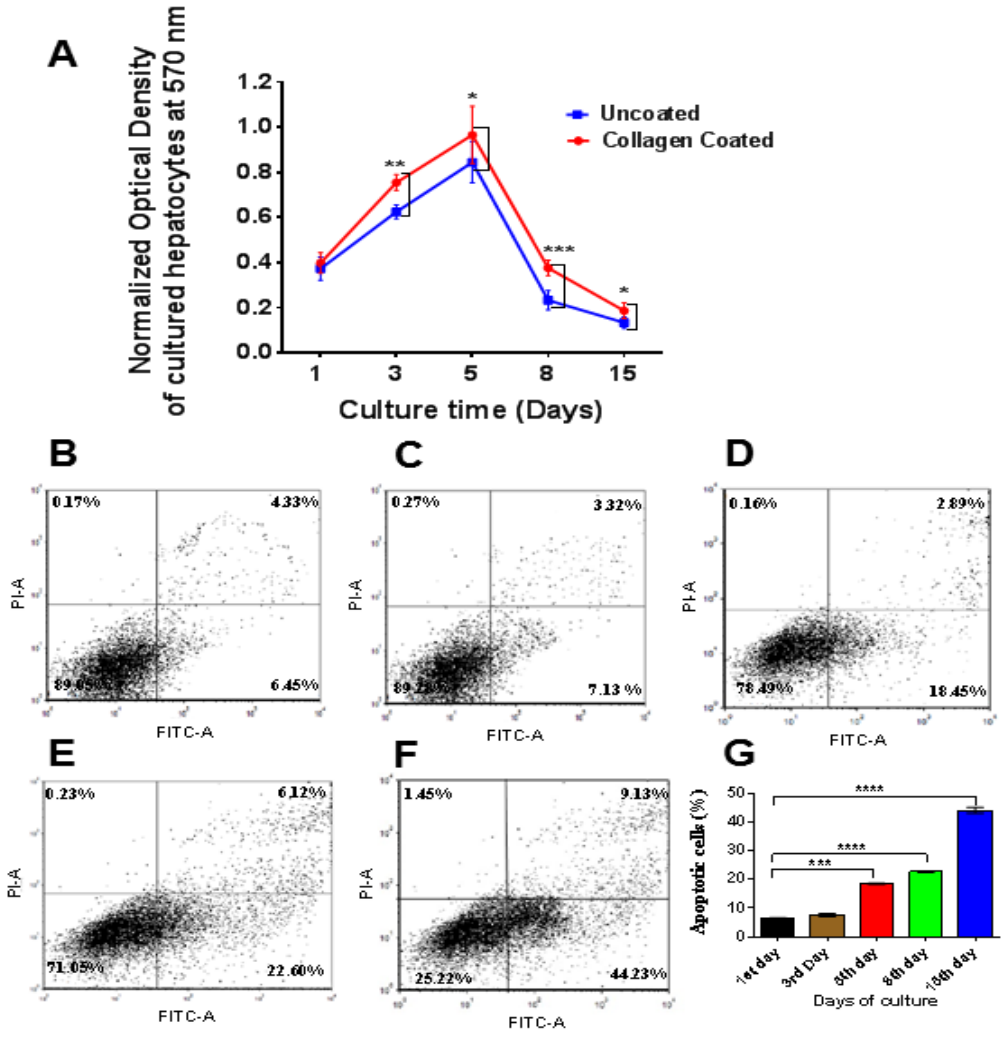

Figure 5.2. Porcine primary hepatocytes have limited life-span in culture

(A) Hepatocyte growth at different days of culture. A MTT assay was done to determine the proliferation of primary hepatocytes in culture. A cell proliferation curve was prepared by plotting the optical density of the hepatocytes against respective days of culture. The values and error bar represent average and standard deviations of three independent set of experiments. Student T test was performed to find out significant differences between two culture conditions. Apoptosis analysis of primary hepatocytes after (B) 1, (C) 3, (D) 5, (E) 8, and (F) 15 days in culture. Apoptotic cells were stained by Annexin-V and detected by flow cytometry. The apoptotic cell death was quantified as Annexin V+ (both PI-negative and AnnexinV-positive) cells. The percentage of apoptotic cells increased over time and after 15 days in culture more than 50% of primary hepatocytes was either apoptotic or dead. (G) The histogram shows the mean number of apoptotic hepatocytes (mean ± SD) from three experiments. One-way analysis of variance (ANOVA) followed by Dunnett post-test was performed to determine significant difference among treatments. * denotes p≤0.05; ** denotes p≤0.01; *** denotes p≤0.001; **** denotes p≤0.0001

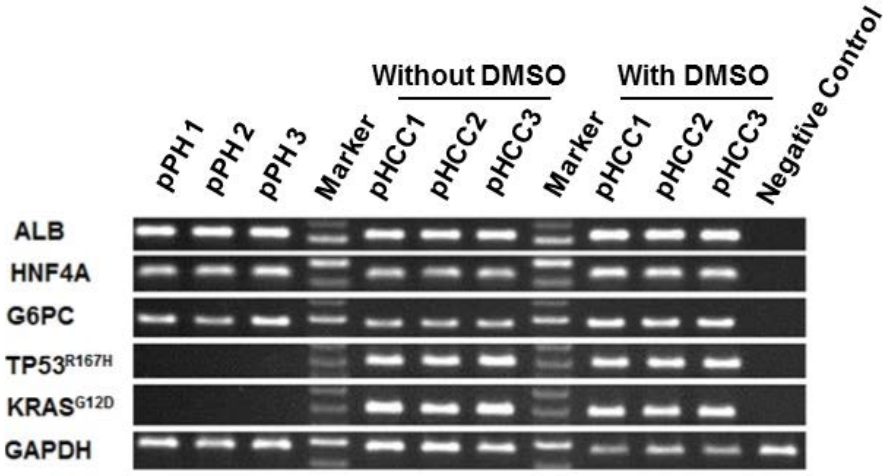

Figure 5.3. Primary hepatocytes and pHCC cells express hepatocyte specific genes

Agarose Gel electrophoresis of RT-PCR products of hepatocyte-specific marker genes; porcine albumin (ALB); HNF4 alpha (HNF4A) and Glucose-6-phosphatase (G6PC). pHCC cells expressed the transgenes ($KRAS^{G12D}$ and $TP53^{R167H}$) while primary hepatocytes did not. Oncopig fibroblasts were used as a negative control. pPH denotes porcine primary hepatocytes and pHCC denotes porcine hepatocyte cell line

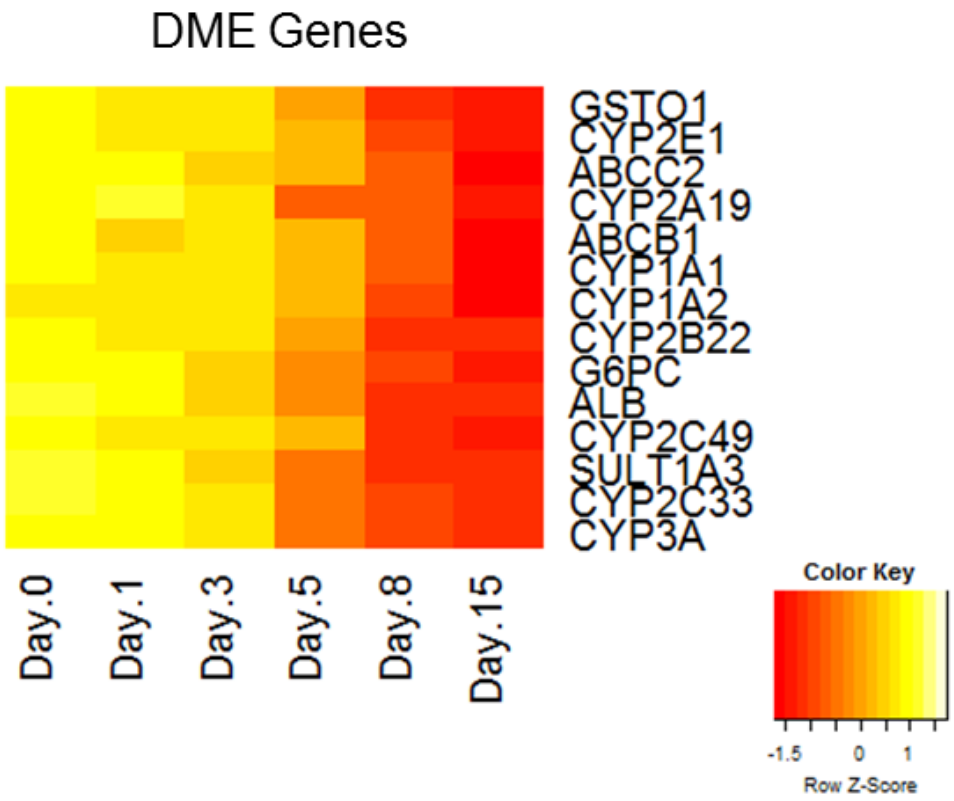

Figure 5.4. Expression profiles of drug metabolism genes in different days of culture of primary porcine hepatocytes. Heatmap of the normalized expression level of genes commonly involved in drug metabolism. Expression is represented as z-scores.

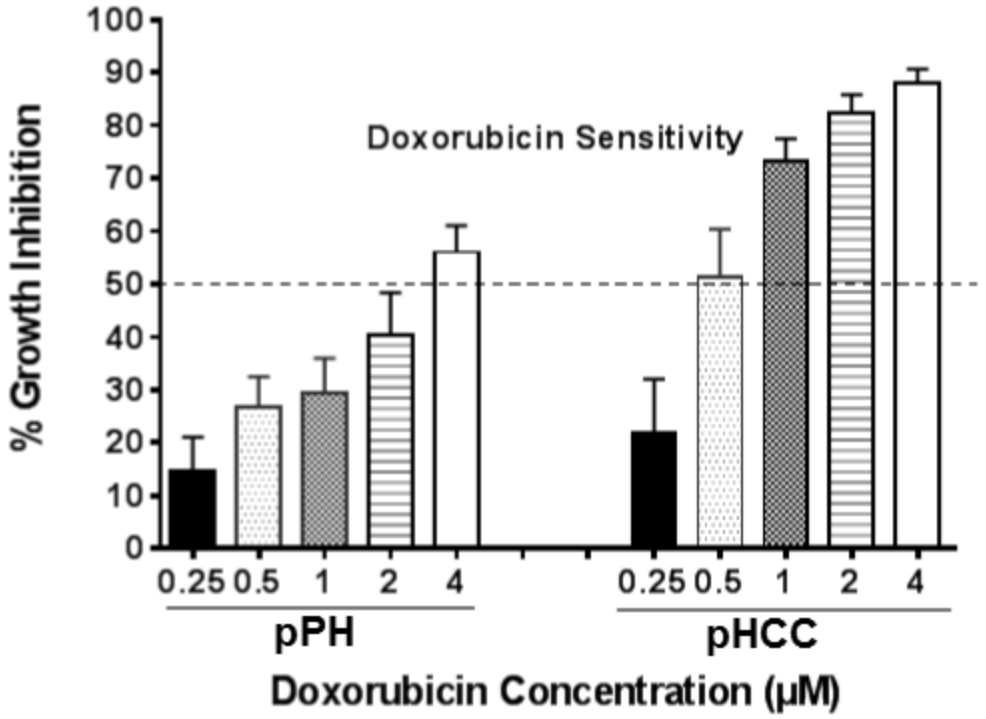

Figure 5.5. pHCC cells are more sensitive to doxorubicin

All the three pHCC cell lines showed more sensitivity towards doxorubicin; the figure represents average values. Doxorubicin sensitivity assay shows pHCC cells are more sensitive to doxorubicin toxicity than primary hepatocytes. Doxorubicin treatment reduced the number of viable pHCC cells to less than 50% at concentrations from 0.5 µg/ml. 4 µg/ml doxorubicin was required for the same effect in the primary hepatocytes. pPH denotes porcine primary hepatocytes and pHCC denotes porcine hepatocyte cell line

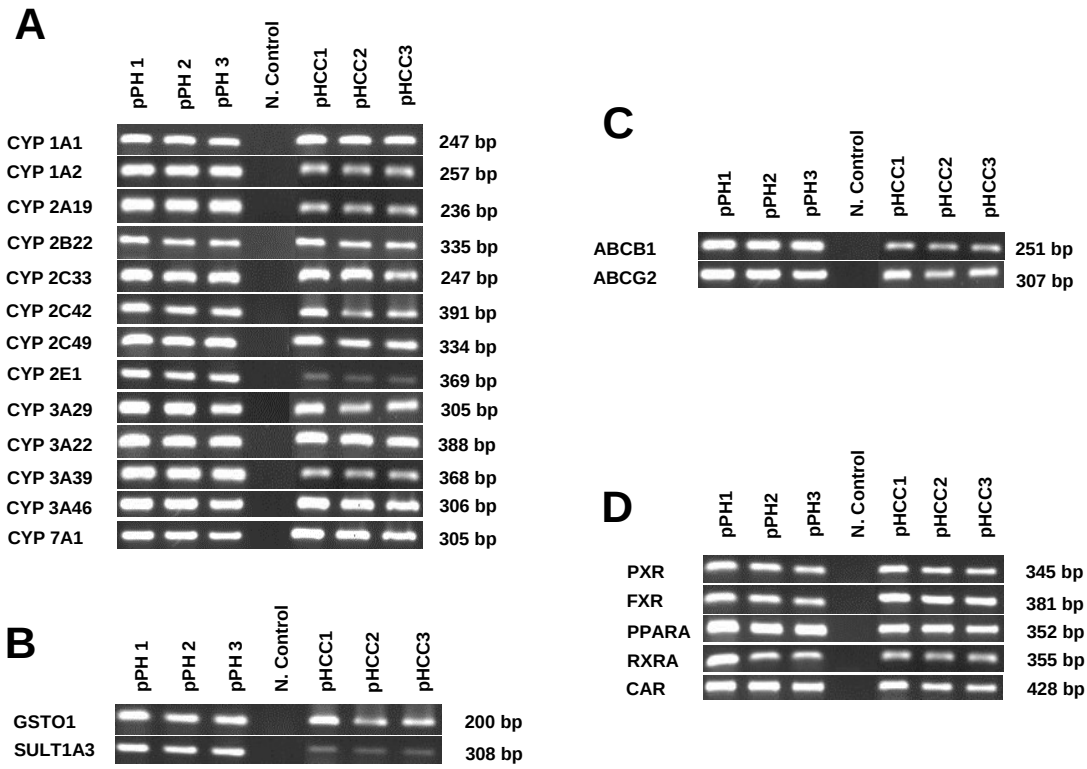

Figure 5.6. Porcine primary hepatocytes (pPH) and hepatocyte cell lines (pHCC) express drug metabolism and regulation genes. Reverse transcriptase (RT) PCR was done to detect the expression of the genes. N. control denotes negative control.

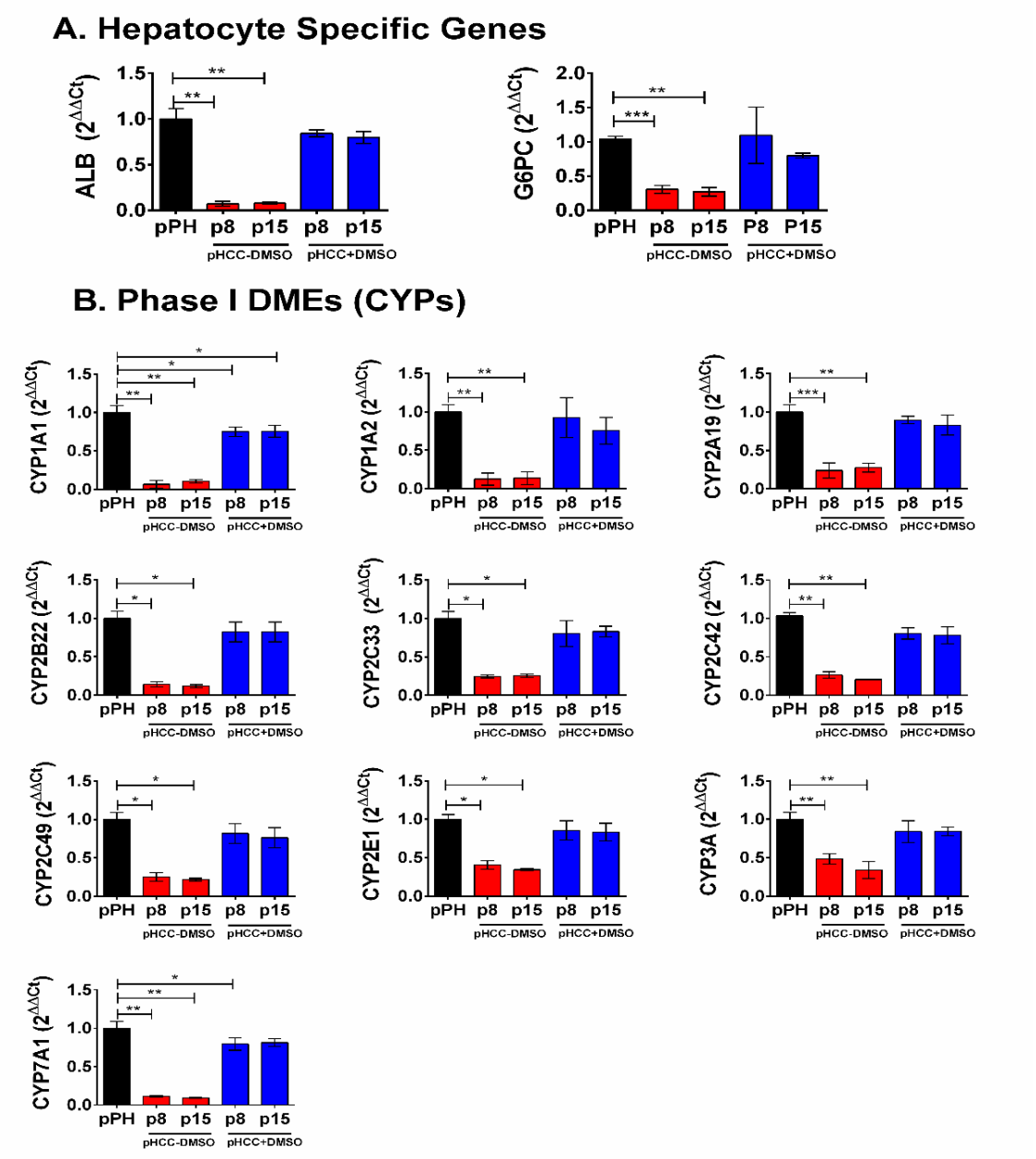

Figure 5.7. Differential expression profiles of hepatocyte specific and phase I DME (CYP) transcripts in primary hepatocytes and pHCC cell lines.

All the three cell lines (pHCC) showed similar expression patterns and the figure represents average values. Real time RT-PCR was performed to analyze the expression of the two hepatocyte specific genes (A) and ten phase I DME genes (B). The values and error bars represent average and standard deviations of three independent set of experiments. One-way analysis of variance (ANOVA) followed by Dunnett post-test was performed to find out significant difference among control and treatments. * denotes p≤0.05; ** denotes p≤0.01; *** denotes p≤0.001; **** denotes p≤0.0001. pPH denotes porcine primary hepatocytes and pHCC denotes porcine hepatocyte cell line.

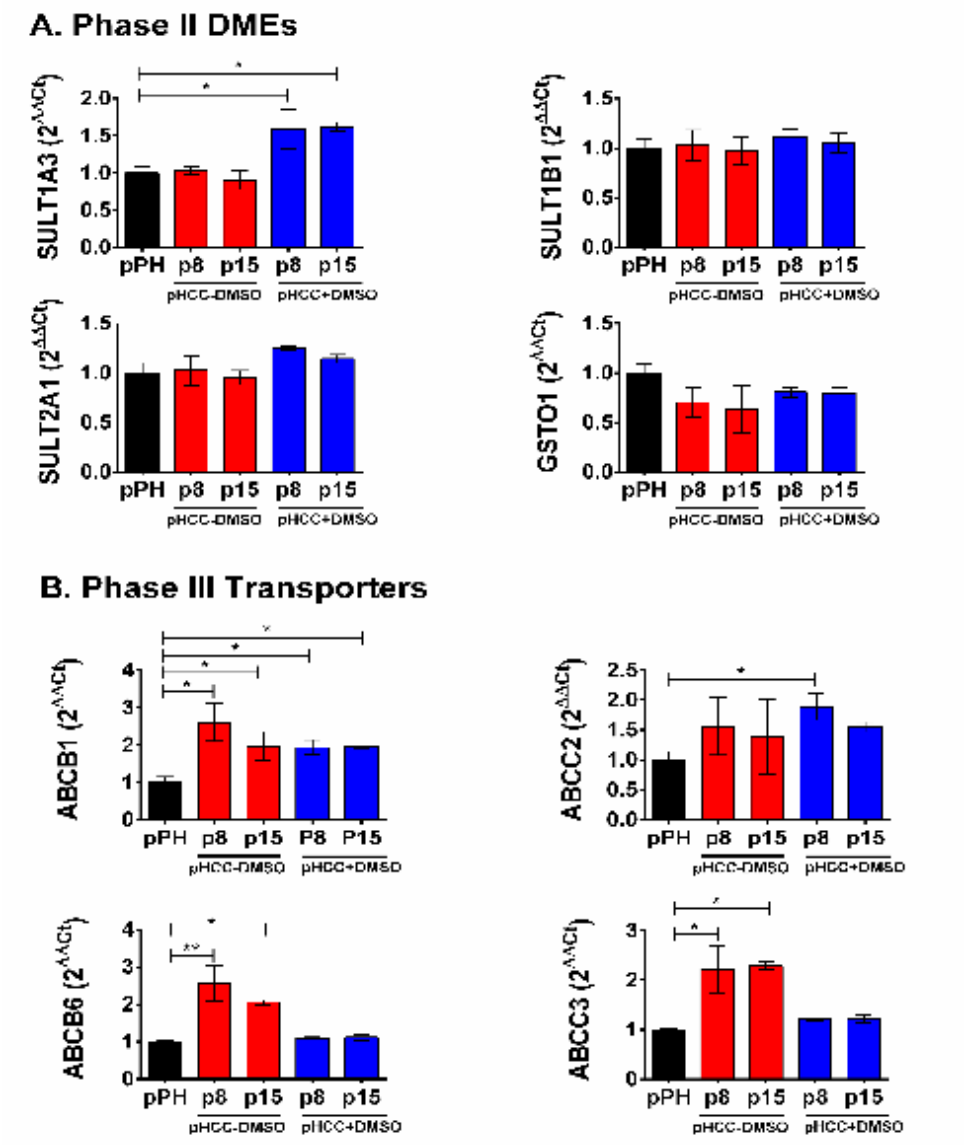

Figure 5.8. Differential expression profiles of phase II and phase III transcripts in primary hepatocytes and pHCC cell lines.

All the three cell lines (pHCC) showed similar expression patterns and the figure represents average values. Real time RT-PCR was performed to analyze the expression of the four phase II DME genes (A) and four phase III transporters (B). The values and error bars represent average and standard deviations of three independent set of experiments. One-way analysis of variance (ANOVA) followed by Dunnett post-test was performed to find out significant difference among control and treatments. * denotes p≤0.05; ** denotes p≤0.01; *** denotes p≤0.001; **** denotes p≤0.0001. pPH denotes porcine primary hepatocytes and pHCC denotes porcine hepatocyte cell line.

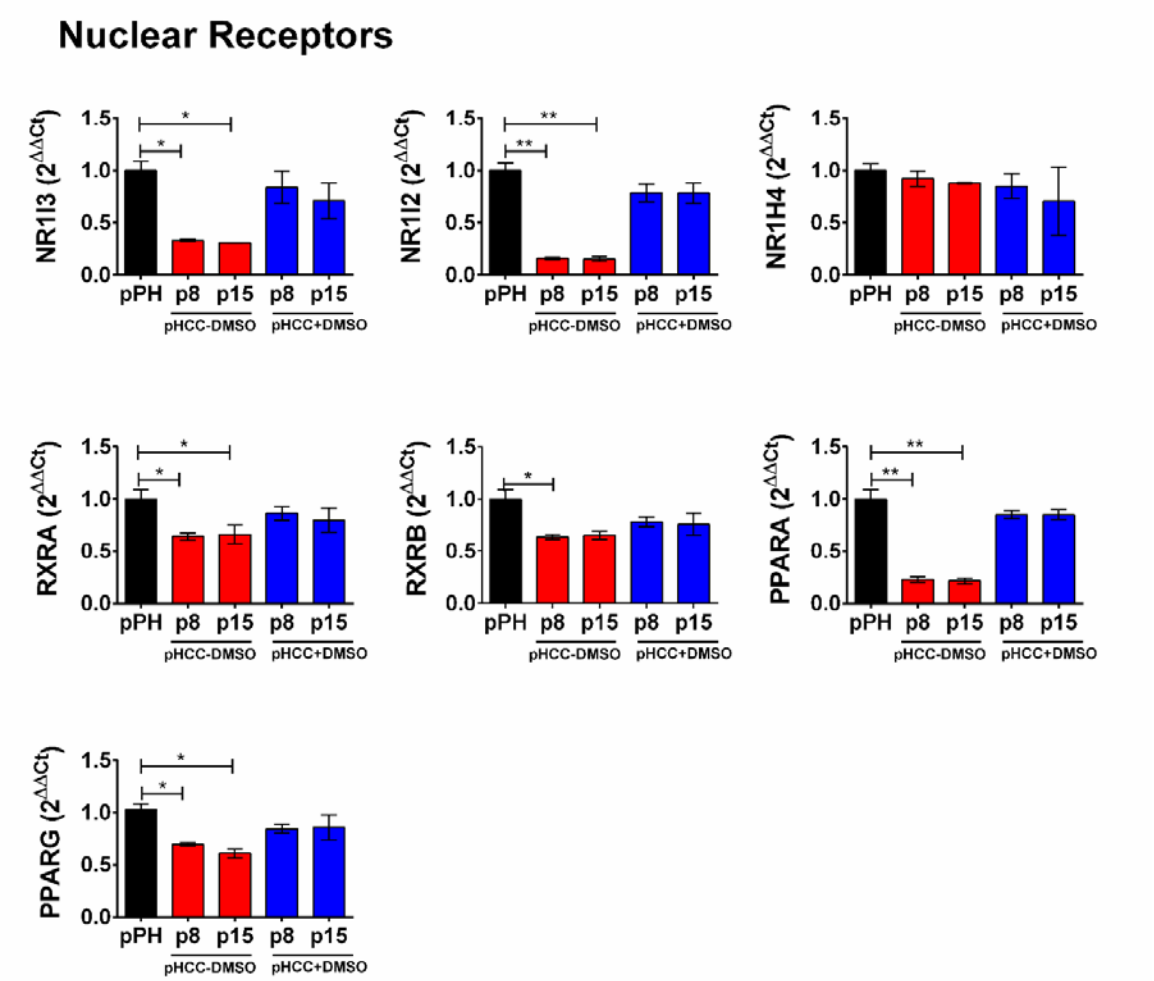

Figure 5.9. Differential expression profiles of nuclear receptor transcripts in primary hepatocytes and pHCC cell lines.

All the three cell lines (pHCC) showed similar expression patterns and the figure represents average values. Real time RT-PCR was performed to analyze the expression of the seven nuclear receptors involved in regulation of drug metabolism. The values and error bars represent average and standard deviations of three independent set of experiments. One-way analysis of variance (ANOVA) followed by Dunnett post-test was performed to find out significant difference among control and treatments. * denotes p≤0.05; ** denotes p≤0.01; *** denotes p≤0.001; **** denotes p≤0.0001. pPH denotes porcine primary hepatocytes and pHCC denotes porcine hepatocyte cell line.

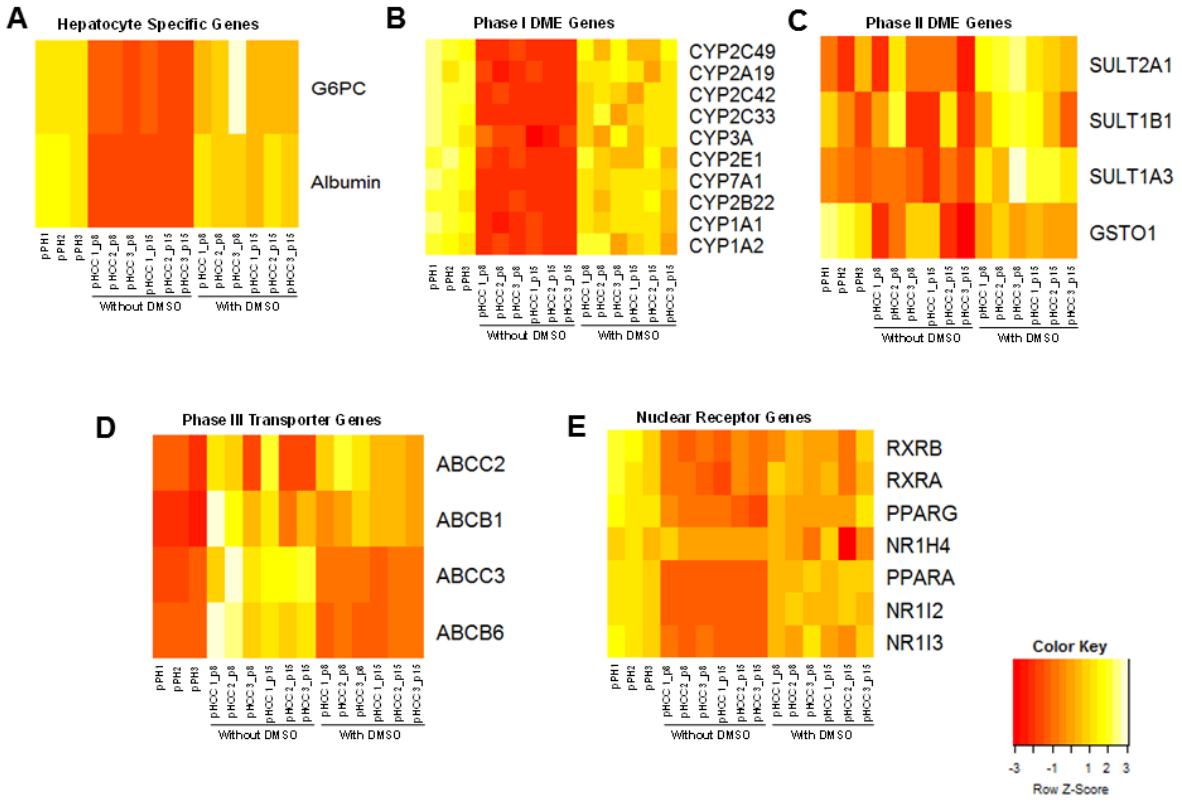

Figure 5.10. Expression profiles of drug metabolism and transport genes in pPH and pHCC cell lines. Heatmap of the normalized expression level of genes commonly involved in drug metabolism and regulation, grouped by their functional categories. Expression is represented as z-scores.

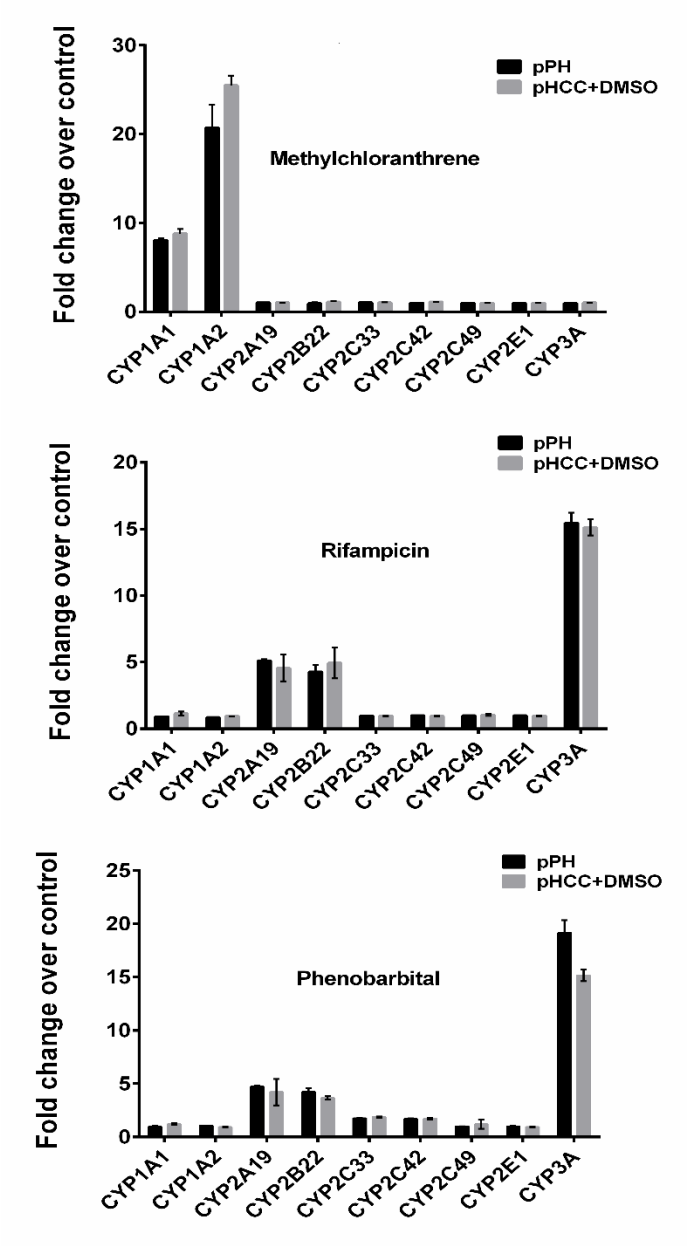

Figure 5.11. Effect of selective CYP modulators on P450 enzyme transcript expression in primary hepatocytes and pHCC (+DMSO) cell lines. (Porcine hepatocytes and pHCC cell lines (8th passage) were exposed to 2 µm 3-methylcholanthrene, 1 mM phenobarbital, or 50 µM rifampicin for 24 hours. The expression levels of major drug-metabolizing porcine P450 enzymes were quantified by quantitative RT-PCR.The values and error bars represent average and standard deviations of three independent set of experiments. One-way analysis of variance (ANOVA) followed by Dunnett post-test was performed to find out significant difference among control and treatments. * denotes p≤0.05; ** denotes p≤0.01; *** denotes p≤0.001; **** denotes p≤0.0001. pPH denotes porcine primary hepatocytes and pHCC denotes porcine hepatocyte cell line.

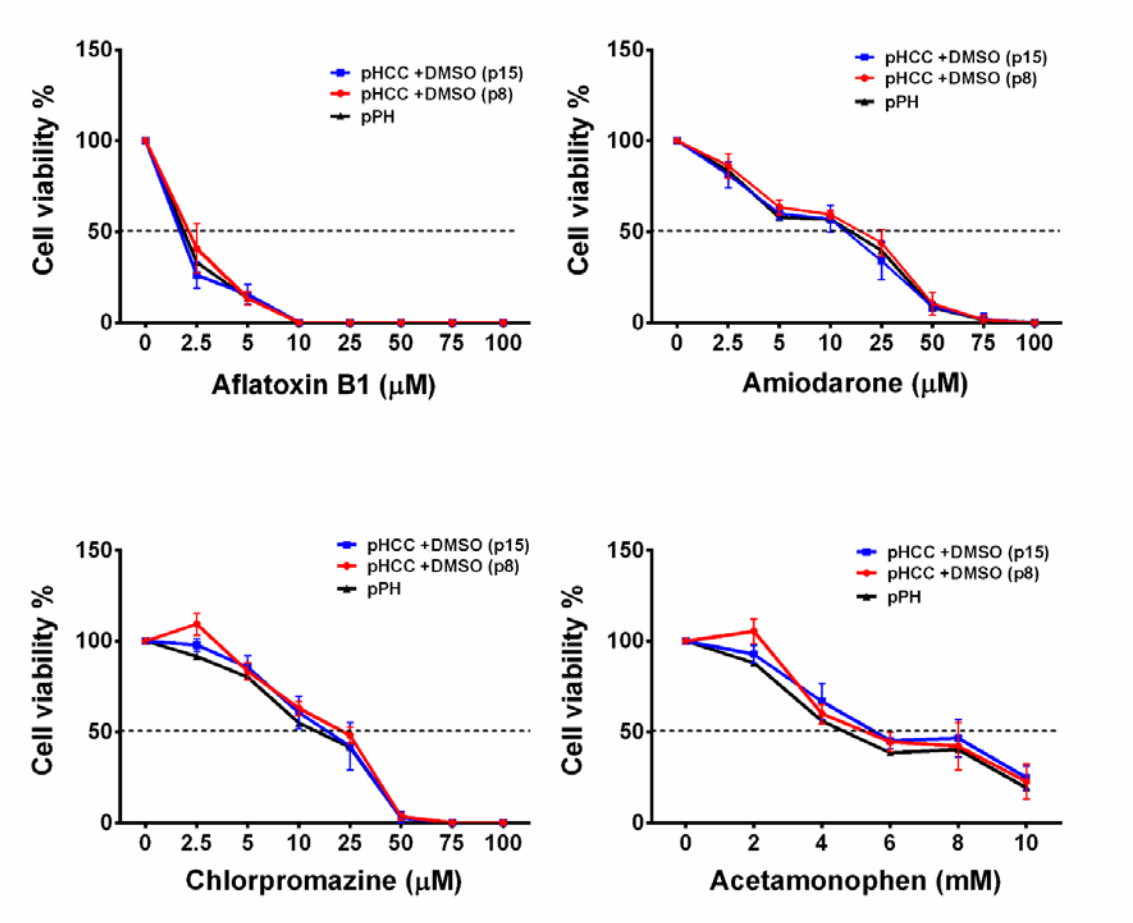

Figure 5.12. Cytotoxic effects of Aflatoxin B1, amiodarone, chlorpromazine, and acetaminophen on pHCC (+DMSO) cell lines. All three pHCC (+DMSO) cells from two different passages (8th and 15th) were exposed to chemicals for 72 h. Cell viability was assessed using standard a MTT test. The results were normalized to untreated cells. All three cell lines recorded similar toxicity response and expressed as means ±S.D. (n=3 cultures)

Table 5.1

Genes	Primers	Sequences (5'-3')	Ta (°C)
CYP1A1	Forward	ATGAGTTCGGGGAGGTGACT	57
	Reverse	TCCGACAGCTGGATATTGGC	
CYP1A2	Forward	AGGAGAATTCCAGCACCAGC	57
	Reverse	TCGGAAGAGCTCCAGGATGA	
CYP2A19	Forward	AAGAAACCGGATGTGGAGGC	58
	Reverse	GAGCCCAGCATAGGGAACAC	
CYP2B22	Forward	TTCGCCTACAGAGATCCCGA	61
	Reverse	CCGGCAAAGAAGAGCGAAAG	
CYP2C33	Forward	CCCTGCGTCTCTTTCCAAGT	61
	Reverse	CCTCAGGGTCATGAGGGAGA	
CYP2C42	Forward	GGTTGTGGTCCTGGTGCTTA	60
	Reverse	ATTCCGCAAGGTCATGAGGG	
CYP2C49	Forward	CCCAACCCAGAGGTGTTTGA	56
	Reverse	CAAAGCCCAGAAGAGGACGA	
CYP2E1	Forward	GCACAAGGACAAAGGGGTCA	58
	Reverse	CTTCCAGGCAGGTAGCGTAG	
CYP3A29	Forward	GACCGTAAGTGGAGCCTGAC	60
	Reverse	CTGATCAGCACCCCGGAAAA	
CYP3A22	Forward	GAGAGGCAAAGAGCAGCACA	
	Reverse	TTCCGCCGATTTGTGAAAGC	
CYP3A39	Forward	CGTGATGATGGTACCGGTTTTC	61
	Reverse	TGAGGAACCAAGCCCAAGTC	
CYP3A46	Forward	AGCTCCCAGGGACTTATCCA	61
	Reverse	TCTGCATGTCTGACCCTCAT	
CYP7A1	Forward	GCCTGTGCTAGACAGTATCATCA	62
	Reverse	GACAGATCGTAGCCCCTGAC	
GSTO1	Forward	GCCTTTGCCTCCTATGCAAC	57
	Reverse	TCAAGGTCATTCAGGTGGGC	
SULT1A3	Forward	TGCAGTGACCACACCATACC	57
	Reverse	GACACTTCTGCAGGTCACCA	
ABCB1	Forward	GGCCACATGGACTTTCAGGA	60
	Reverse	ATGTCTGGTCGAGTGGGGTA	
ABCC2	Forward	GCTTGGACCAGTGACTCTAAA	
	Reverse	CCCAGGAAGCACATAAGCCA	
ABCG2	Forward	CCTGAGATTGGAGCCCTTGG	61
	Reverse	GGGTCCCAGAATGGCATTGA	

Table 5.1. Primer sequences for reverse transcription PCR

Table 5. 2

Gene Name	Primers	Sequences (5'-3')
GAPDH	Forward	GGCAAATTCCACGGCACAGTCA
	Reverse	CTGGCTCCTGGAAGATGGTGAT
ACTB	Forward	GCAAATGCTTCTAGGCGGACTGT
	Reverse	CCAAATAAAGCCATGCCAATCTCA
Porcine Albumin	Forward	TGGTGACTTGGCTGACTGCTG
	Reverse	TGTCGGGGTTATCATTTTTGTGTTG
HNF4A	Forward	AGTCCCAGAGTGGTAGTGGAAAG
	Reverse	CAGATGGTGAAGGGTGGCATTG
G6PC	Forward	ATTGAAAGACGATGACTGTGCCAA
	Reverse	CAAAGGAGGAAGGAGTTCTGAGC
CYP1A1	Forward	AAGAGGCAGAGGTGAAGTGGTGAA
	Reverse	GAGAAGAAGGAAGGCAGTGAAGTGATAG
CYP1A2	Forward	ACACCTTCTCCATTGCCTCAGACC
	Reverse	GCACTCAGCCTCCTTGCTCAC
CYP2A19	Forward	CCGAAGAGTCACCAAGGATACCAAG
	Reverse	ACAGAGCCCAGCATAGGGAACA
CYP2B22	Forward	CAGATGAGTAAACAGAGCCCGAGAA
	Reverse	CGAGAGCCAAGGAGACAGCA
CYP2C33	Forward	TGGAAGAAAAATCACAAGAGGAGAAGG
	Reverse	TTGGAAAGAGACGCAGGGATGT
CYP2C42	Forward	TACAGAGACAACAAGCACCACCA
	Reverse	CTGCCAATCACACGGTCAATC
CYP2C49	Forward	CTTGTGGAGGAGTTGAGAAAAACC
	Reverse	TTGTGGAAAATGATGGAGCAGA
CYP2E1	Forward	ACACCCTGCTGATGGAAATGGA
	Reverse	GTGGTCTCTGTCCCCGCAAA
CYP3A	Forward	TACCTGCCCTTTGGGACTGGAC
	Reverse	AGTTCTGCAGGACTCTGACGA
CYP7A1	Forward	TTCTGCTACCGAGTGATGTTTGAGG
	Reverse	AGGTTGTTTAGGATGAGTGCTTTCTGTG
SULT1A3	Forward	GACCACAGCATCTCAGCCTTCAT
	Reverse	CTGCCATCTTCTCAGCATAGTCG
SULT2A1	Forward	AAATGCTGCAAGAGGTGAGGGAGG
	Reverse	ATCCCCCTTGGAGAGAATCAGGCA
SULT1E1	Forward	GAGAAAGGGGATTGCAGGAGACTG
	Reverse	GTAGACCCCTTCATTTGCTGCTCA
GSTO1	Forward	GAGATTCTGTCCTTTCGCCCAGAG
	Reverse	GATGACTTGATGCCGGATTCCCTT
GSTK1	Forward	GGTACACCATCCACCGTTAGTCTC
	Reverse	CACACAAACACCAGCAAAGACACA
ABCB1	Forward	TGGCAGTGGGACAGGTTAGTTC
	Reverse	CACGGTGCTTGAGCTGTCAATC
ABCB6	Forward	TGTTGTCCCAAGGTGGTGTGTATG
	Reverse	GCTGAAATGGATTTCCCTCCAGGT
ABCC2	Forward	GTGGCTGTTGAGCGAATAAATGAATAC
	Reverse	TGCTGGGCCAACCGTCTG

Table 5.2 (cont.)

Gene Name	Primers	Sequences (5'-3')
ABCC3	Forward	TGATGCAGACGCTGATCTTACACC
	Reverse	ACTCACGTTTGACGGAATTGGTGA
ABCG2	Forward	GATCTTTTCGGGGCTGTTCCTCA
	Reverse	TGAGTCCCGGGCAGAAGTTTTGT
PXR	Forward	GACAACAGTGGGAAAGAGAT
	Reverse	CCCTGAAGTAGGAGATGACT
FXR	Forward	CATTCAACCATCACCACGCAGAGA
	Reverse	GCACATCCCAGACTTCACAGAGA
CAR	Forward	GAAAGCAGGGTTACAGTGGGAGTA
	Reverse	CTTCAGGTGTTGGGATGGTGGTC
LXRA	Forward	TCCAGGTAGAGAGGCTGCAACATA
	Reverse	AGTTTCATTAGCATCCGTGGGAAC
LXRB	Forward	GAGTCTTCCTGAGAGGGGCAGATA
	Reverse	CGTGGTAGGCTTGAGGTGTAAGC
PPARA	Forward	AATAACCCGCCTTTCGTCATACAC
	Reverse	GACCTCCGCCTCCTTGTTCT
PPARG	Forward	CCATGCTGTCATGGGTGAAACTCT
	Reverse	GTCAACCATGGTCACCTCTTGTGA
RXRA	Forward	CCTTCTCGCACCGCTCCATA
	Reverse	CGTCAGCACCCTGTCAAAGATG
RXRG	Forward	CTTCCCGTTCCCCAAACGTGAT
	Reverse	CTTCCAGAAAAGATCCCCAGTCCC

Table 5.2. Primer sequences for real-time PCR

Table 5.3

Gene	pPH1	pPH2	pPH3	hPH
Phase I DME				
CYP1A1	0.00273	0.00288	0.00312	0.0028
CYP1A2	0.02187	0.02305	0.02493	0.0173
CYP2A19[#]	0.00038	0.00043	0.00045	0.0002
CYP2C33[$]	0.05513	0.07583	0.07053	0.0512
CYP2C49[£]	0.07076	0.08120	0.07839	0.0754
CYP2E1	0.01484	0.01153	0.01247	0.0174
CYP3A	0.05668	0.05942	0.04987	0.0115-0.0562
CYP7A1	0.00034	0.00036	0.00039	0.0001
Phase II DME				
SULT1A3	0.01827	0.02032	0.02025	0.0214
SULT1B1	0.03654	0.04064	0.04051	0.0403
SULT2A1	0.03457	0.03791	0.03526	0.0442
SULT1E1	0.00108	0.00118	0.00110	0.0015
GSTO1	0.29733	0.29502	0.29075	0.2539
GSTK1	0.14151	0.12309	0.15677	0.1393
Phase III DME				
ABCB1	0.15931	0.17591	0.16307	0.2388
ABCB6	0.08133	0.14289	0.08153	0.1141
ABCC2	0.38237	0.04976	0.43937	0.4696
ABCC3	0.19119	0.20419	0.19184	0.2403
ABCG2	0.00216	0.00237	0.002204	0.0061

Table 5.3: Relative abundance of drug-metabolizing genes in porcine and human primary hepatocytes

Expression value is a relative number calculated based on the assumption that average expression level of two housekeeping genes GAPDH and ACTB is 1.

Expression values of human primary hepatocytes are reported by Guo et al., 2011

pPH1: Porcine primary hepatocyte 1, pPH2: Porcine primary hepatocyte 2, pPH3: Porcine primary hepatocyte 3, hPH: Human primary hepatocyte

Porcine CYP2A19 is equivalent to human CYP2A13

$ Porcine CYP2C33 is equivalent to human CYP2C9

£ Porcine CYP2C49 is equivalent to human CYP2C18

Table 5.4

Gene	Fold change in different days in culture compared to day '0'			
	Day 3	Day 5	Day 8	Day 15
ALB	-1.35	-1.95	-6.30	-10.62
G6PC	-1.21	-1.84	-4.18	-8.15
CYP1A1	-1.08	-1.18	-1.74	-3.95
CYP1A2	-1.01	-1.23	-2.34	-3.95
CYP2A19	-1.12	-2.01	-2.12	-4.20
CYP2B22	-1.16	-1.80	-6.18	-8.46
CYP2C33	-1.19	-2.61	-4.49	-8.20
CYP2C49	-1.14	-1.48	-4.67	-13.06
CYP2E1	-1.09	-1.35	-2.88	-4.65
CYP3A	-1.14	-2.15	-3.50	-5.30
GSTO1	-1.11	-1.56	-3.42	-4.40
SULT1A3	-1.35	-2.23	-4.71	-5.36
ABCB1	-1.09	-1.20	-1.81	-3.90
ABCC2	-1.14	-1.33	-2.37	-8.35

Table 5.4. Fold change of the hepatocyte specific genes and DMEs in primary hepatocytes in different days of culture**.**

References

1. McKim JM. Building a tiered approach to in vitro predictive toxicity screening: a focus on assays with in vivo relevance. Comb Chem High Throughput Screen. 2010;13: 188–206.

2. Lübberstedt M, Müller-Vieira U, Mayer M, Biemel KM, Knöspel F, Knobeloch D, et al. HepaRG human hepatic cell line utility as a surrogate for primary human hepatocytes in drug metabolism assessment in vitro. J Pharmacol Toxicol Methods. 63: 59–68. doi:10.1016/j.vascn.2010.04.013

3. Tuschl G, Hrach J, Walter Y, Hewitt PG, Mueller SO. Serum-free collagen sandwich cultures of adult rat hepatocytes maintain liver-like properties long term: a valuable model for in vitro toxicity and drug-drug interaction studies. Chem Biol Interact. 2009;181: 124–37. doi:10.1016/j.cbi.2009.05.015

4. Brandon EFA, Raap CD, Meijerman I, Beijnen JH, Schellens JHM. An update on in vitro test methods in human hepatic drug biotransformation research: pros and cons. Toxicol Appl Pharmacol. 2003;189: 233–46. Available: http://www.ncbi.nlm.nih.gov/pubmed/12791308

5. Guillouzo A, Corlu A, Aninat C, Glaise D, Morel F, Guguen-Guillouzo C. The human hepatoma HepaRG cells: a highly differentiated model for studies of liver metabolism and toxicity of xenobiotics. Chem Biol Interact. 2007;168: 66–73. doi:10.1016/j.cbi.2006.12.003

6. Gómez-Lechón MJ, Donato T, Jover R, Rodriguez C, Ponsoda X, Glaise D, et al. Expression and induction of a large set of drug-metabolizing enzymes by the highly

differentiated human hepatoma cell line BC2. Eur J Biochem. 2001;268: 1448–59. Available: http://www.ncbi.nlm.nih.gov/pubmed/11231298

7. Guo L, Dial S, Shi L, Branham W, Liu J, Fang J-L, et al. Similarities and differences in the expression of drug-metabolizing enzymes between human hepatic cell lines and primary human hepatocytes. Drug Metab Dispos. 2011;39: 528–38. doi:10.1124/dmd.110.035873

8. Swanson KS, Mazur MJ, Vashisht K, Rund LA, Beever JE, Counter CM, et al. Genomics and clinical medicine: rationale for creating and effectively evaluating animal models. Exp Biol Med (Maywood). 2004;229: 866–75. Available: http://www.ncbi.nlm.nih.gov/pubmed/15388881

9. Puccinelli E, Gervasi PG, Longo V. Xenobiotic metabolizing cytochrome P450 in pig, a promising animal model. Curr Drug Metab. 2011;12: 507–25. Available: http://www.ncbi.nlm.nih.gov/pubmed/21476973

10. Schook LB, Collares TV, Darfour-Oduro KA, De AK, Rund LA, Schachtschneider KM, et al. Unraveling the swine genome: implications for human health. Annu Rev Anim Biosci. Annual Reviews; 2015;3: 219–44. doi:10.1146/annurev-animal-022114-110815

11. Soucek P, Zuber R, Anzenbacherová E, Anzenbacher P, Guengerich FP. Minipig cytochrome P450 3A, 2A and 2C enzymes have similar properties to human analogs. BMC Pharmacol. 2001;1: 11. Available: http://www.pubmedcentral.nih.gov/articlerender.fcgi?artid=60991&tool=pmcentrez&rendertype=abstract

12. Szotáková B, Baliharová V, Lamka J, Nozinová E, Wsól V, Velík J, et al.

Comparison of in vitro activities of biotransformation enzymes in pig, cattle, goat and sheep. Res Vet Sci. 2004;76: 43–51. Available: http://www.ncbi.nlm.nih.gov/pubmed/14659728

13. Achour B, Barber J, Rostami-Hodjegan A. Cytochrome P450 Pig Liver Pie: Determination of Individual Cytochrome P450 Isoform Contents in Microsomes from Two Pig Livers Using Liquid Chromatography in Conjunction with Mass Spectrometry. Drug Metab Dispos. 2011;39: 2130–2134. doi:10.1124/dmd.111.040618

14. Bogaards JJ, Bertrand M, Jackson P, Oudshoorn MJ, Weaver RJ, van Bladeren PJ, et al. Determining the best animal model for human cytochrome P450 activities: a comparison of mouse, rat, rabbit, dog, micropig, monkey and man. Xenobiotica. 2000;30: 1131–52. doi:10.1080/00498250010021684

15. Nebbia C, Dacasto M, Rossetto Giaccherino A, Giuliano Albo A, Carletti M. Comparative expression of liver cytochrome P450-dependent monooxygenases in the horse and in other agricultural and laboratory species. Vet J. 2003;165: 53–64. Available: http://www.ncbi.nlm.nih.gov/pubmed/12618071

16. Pollock CB, Rogatcheva MB, Schook LB. Comparative genomics of xenobiotic metabolism: a porcine-human PXR gene comparison. Mamm Genome. 2007;18: 210–9. doi:10.1007/s00335-007-9007-7

17. Gray MA, Pollock CB, Schook LB, Squires EJ. Characterization of porcine pregnane X receptor, farnesoid X receptor and their splice variants. Exp Biol Med (Maywood). 2010;235: 718–36. doi:10.1258/ebm.2010.009339

18. Schook LB, Collares T V, Hu W, Liang Y, Rodrigues FM, Rund LA, et al. A Genetic

Porcine Model of Cancer. PLoS One. 2015;10: e0128864. doi:10.1371/journal.pone.0128864

19. Meng FY, Chen ZS, Han M, Hu XP, He XX, Liu Y, et al. Porcine hepatocyte isolation and reversible immortalization mediated by retroviral transfer and site-specific recombination. World J Gastroenterol. 2010;16: 1660–4. Available: http://www.pubmedcentral.nih.gov/articlerender.fcgi?artid=2848376&tool=pmcentrez&rendertype=abstract

20. Yip DK, Auersperg N. The dye-exclusion test for cell viability: Persistence of differential staining following fixation. In Vitro. 1972;7: 323–329. doi:10.1007/BF02661722

21. van Engeland M, Nieland LJ, Ramaekers FC, Schutte B, Reutelingsperger CP. Annexin V-affinity assay: a review on an apoptosis detection system based on phosphatidylserine exposure. Cytometry. 1998;31: 1–9. Available: http://www.ncbi.nlm.nih.gov/pubmed/9450519

22. Andree HA, Reutelingsperger CP, Hauptmann R, Hemker HC, Hermens WT, Willems GM. Binding of vascular anticoagulant alpha (VAC alpha) to planar phospholipid bilayers. J Biol Chem. 1990;265: 4923–8. Available: http://www.jbc.org/content/265/9/4923.abstract

23. Koopman G, Reutelingsperger CP, Kuijten GA, Keehnen RM, Pals ST, van Oers MH. Annexin V for flow cytometric detection of phosphatidylserine expression on B cells undergoing apoptosis. Blood. American Society of Hematology; 1994;84: 1415–20. Available: http://www.bloodjournal.org/content/84/5/1415.abstract

24. Gómez-Lechón MJ, Castell JV, Donato MT. Hepatocytes--the choice to investigate drug metabolism and toxicity in man: in vitro variability as a reflection of in vivo. Chem Biol Interact. 2007;168: 30–50. doi:10.1016/j.cbi.2006.10.013

25. Wilkening S, Stahl F, Bader A. Comparison of primary human hepatocytes and hepatoma cell line Hepg2 with regard to their biotransformation properties. Drug Metab Dispos. 2003;31: 1035–42. doi:10.1124/dmd.31.8.1035

26. Aninat C, Piton A, Glaise D, Le Charpentier T, Langouët S, Morel F, et al. Expression of cytochromes P450, conjugating enzymes and nuclear receptors in human hepatoma HepaRG cells. Drug Metab Dispos. 2006;34: 75–83. doi:10.1124/dmd.105.006759

27. Gómez-Lechón MJ, Donato MT, Castell JV, Jover R. Human hepatocytes in primary culture: the choice to investigate drug metabolism in man. Curr Drug Metab. 2004;5: 443–62. Available: http://www.ncbi.nlm.nih.gov/pubmed/15544436

28. Kistler A, Liechti H, Pichard L, Wolz E, Oesterhelt G, Hayes A, et al. Metabolism and CYP-inducer properties of astaxanthin in man and primary human hepatocytes. Arch Toxicol. 2002;75: 665–75. Available: http://www.ncbi.nlm.nih.gov/pubmed/11876499

29. Dorato MA, Buckley LA. Toxicology testing in drug discovery and development. Curr Protoc Toxicol. 2007;Chapter 19: Unit19.1. doi:10.1002/0471141755.tx1901s31

30. Giezen TJ, Mantel-Teeuwisse AK, Straus SMJM, Schellekens H, Leufkens HGM, Egberts ACG. Safety-related regulatory actions for biologicals approved in the United States and the European Union. JAMA. American Medical Association; 2008;300:

1887–96. doi:10.1001/jama.300.16.1887

31. LeCluyse EL. Human hepatocyte culture systems for the in vitro evaluation of cytochrome P450 expression and regulation. Eur J Pharm Sci. 2001;13: 343–68. Available: http://www.ncbi.nlm.nih.gov/pubmed/11408150

32. Hamilton GA, Jolley SL, Gilbert D, Coon DJ, Barros S, LeCluyse EL. Regulation of cell morphology and cytochrome P450 expression in human hepatocytes by extracellular matrix and cell-cell interactions. Cell Tissue Res. 2001;306: 85–99. Available: http://www.ncbi.nlm.nih.gov/pubmed/11683185

33. Totsugawa T, Yong C, Rivas-Carrillo JD, Soto-Gutierrez A, Navarro-Alvarez N, Noguchi H, et al. Survival of liver failure pigs by transplantation of reversibly immortalized human hepatocytes with Tamoxifen-mediated self-recombination. J Hepatol. 2007;47: 74–82. doi:10.1016/j.jhep.2007.02.019

34. Ogino M, Nagata K, Yamazoe Y. Selective suppressions of human CYP3A forms, CYP3A5 and CYP3A7, by troglitazone in HepG2 cells. Drug Metab Pharmacokinet. 2002;17: 42–6. Available: http://www.ncbi.nlm.nih.gov/pubmed/15618651

35. Lin JH. CYP induction-mediated drug interactions: in vitro assessment and clinical implications. Pharm Res. 2006;23: 1089–116. doi:10.1007/s11095-006-0277-7

36. Kojima M, Morozumi T. Cloning of Six Full-Length cDNAs Encoding Pig Cytochrome P450 Enzymes and Gene Expression of these Enzymes in the Liver and Kidney. J Heal Sci. The Pharmaceutical Society of Japan; 2004;50: 518–529. doi:10.1248/jhs.50.518

37. Gripon P, Rumin S, Urban S, Le Seyec J, Glaise D, Cannie I, et al. Infection of a human hepatoma cell line by hepatitis B virus. Proc Natl Acad Sci U S A. 2002;99: 15655–60. doi:10.1073/pnas.232137699

38. Thörn HA, Lundahl A, Schrickx JA, Dickinson PA, Lennernäs H. Drug metabolism of CYP3A4, CYP2C9 and CYP2D6 substrates in pigs and humans. Eur J Pharm Sci. 2011;43: 89–98. doi:10.1016/j.ejps.2011.03.008

39. Donato MT, Castell JV, Gómez-Lechón MJ. Effect of model inducers on cytochrome P450 activities of human hepatocytes in primary culture. Drug Metab Dispos. 1995;23: 553–8. Available: http://www.ncbi.nlm.nih.gov/pubmed/7587930

40. Madan A, Graham RA, Carroll KM, Mudra DR, Burton LA, Krueger LA, et al. Effects of prototypical microsomal enzyme inducers on cytochrome P450 expression in cultured human hepatocytes. Drug Metab Dispos. 2003;31: 421–31. Available: http://www.ncbi.nlm.nih.gov/pubmed/12642468

41. Soldatow VY, Lecluyse EL, Griffith LG, Rusyn I. In vitro models for liver toxicity testing. Toxicol Res (Camb). 2013;2: 23–39. doi:10.1039/C2TX20051A